Neuroscience Area – PhD course in Cognitive Neuroscience

The Chronometry of Time Processing in Visual and Premotor Cortices

Candidate:
Andrea Solmi

Advisor:
Prof. Domenica Bueti

Academic Year 2019-2020

INDEX

Abstract

Time is the most elusive dimension of everyday experience; we cannot touch nor see time nevertheless time is embedded in any sensory experience of the world and we can surely perceive it. How time is extracted from sensory inputs, how it is processed and represented in the human brain is far from clear. During my PhD I have tried to understand how temporal information in the millisecond range is extracted from visual inputs; i.e. how it is encoded/read-out and perceived. Specifically, I have asked "when", at which stage of temporal information processing (i.e., from sensory drive integration to duration recognition) visual and premotor areas, brain regions known to play a role in temporal computations, are engaged. Focusing on the chronometry of these areas in duration encoding, I tried to better understand the functional role of these areas and at the same time, using stimuli with different sensory load and different durations ranges I have tried to gain insight on the mechanisms underlying duration perception.

To test the chronometry of different areas in duration encoding I used Transcranial Magnetic Stimulation (TMS), that I have applied over visual and premotor areas at different timings from the onset (to the offset) of visual stimuli that had to be judged in duration. In other words, I assumed that TMS applied at different timings after visual stimulus onset would affect duration judgments differently depending on the involvement over time of the target area during the processing of temporal information.

The combination of high temporal resolution (paired-pulse) TMS and duration discrimination tasks allowed me to test: A. the chronometry of primary visual cortex (V1) and extrastriate area V5/MT during the encoding of visual stimuli with different sensory load i.e., empty intervals and filled durations (chapter 2). B. the chronometry of V1 and Supplementary Motor Area (SMA) in duration encoding and reading out of visual temporal information (chapter 4) and C. to test the existence of a topographic representation of time in SMA (chapter 5). Finally, the experimental data of chapters 2 and 4 were modeled using a recently developed leaky integration model (Toso et al.,

2021). This model sees duration perception as a result of the leaking integration of a sensory drive from primary sensory cortex (in Chapter 3 a description of the model with the modelling of chapter 2's data and in Chapter 4, experimental data and modelling).

CHAPTER 1: INTRODUCTION

Time is embedded in many aspects of our sensory experience; sensory events unfold in time and often acquire particular meaning because of their specific temporal structure. The speed of a moving object, the words pronounced by a speaker and the tactile exploration of a texture, are all examples of temporally structured sensory experiences.

Despite the ubiquitousness of the temporal dimension of our sensory experience, the understanding of the neural mechanisms underlying the temporal representation of sensory events, that is the capacity to estimate duration in milliseconds/seconds range, remains a controversial and complex issue.

The controversy relates to the effective involvement of sensory-specific brain regions in the processing of temporal information. The complexity arises from the neurophysiological mechanisms underlying the representation of time in these areas and the functional interplay between sensory-specific and amodal temporal mechanisms (Harrington et al., 2011).

With my PhD work I have tried to shed light into the complexity of the neural mechanisms of duration perception by investigating the involvement of sensory specific and amodal brain regions at different stages of duration processing i.e., from duration encoding to duration recognition/reading out, while using different types of sensory input (empty intervals versus filled durations) and different duration ranges (from 0.2 to 1.5 s).

In this chapter I will first provide a brief theoretical background of the cognitive neuroscience of time, then I will summarize the goals of my PhD work and finally I will introduce the experimental approach used throughout my work.

1.1 State-of-the-art of the neuroscience of time

Time is a fundamental dimension common among sensory modalities. As such, time computation is likely supported by brain structures that are independent of specific sensory modalities. It is well known indeed that many cortical (parietal, premotor, prefrontal and insular cortices) and subcortical (basal ganglia and cerebellum) brain structures have been implicated in the processing of temporal information independently from the sensory modality of the stimuli (Spencer et al., 2003; Coull et al., 2004; Wiener et al., 2010).

In accord with these empirical observations the 'internal clock model' (Treisman, 1963; Meck et al., 2008), the most influential among 'centralized time models', hypothesizes the existence of a single 'universal' 'centralized' and 'amodal' clock (i.e., a neural oscillator and a counter); a temporal mechanism accessible through various sensory modalities, and that is independent from the length of the temporal interval and from the context in which temporal information is used.

Recently, many of empirical observations have challenged the 'internal clock model' by showing that temporal mechanisms are not always modality-independent but can be modality-specific too and that, for example, the representation of temporal properties of visual and auditory environment can be encoded in respectively primary visual and auditory cortices (Bueti et al., 2008a; Bueti et al., 2008b; Bueti et al., 2008c; Bueti & Macaluso, 2010; Bueti et al., 2010; Salvioni et al., 2013).

The results of these studies, which have been supported by other neurophysiological data both in humans (Bosco et al., 2008; Bolognini et al., 2009; Kanai et al., 2011) and animals (Shuler & Bear, 2006; Chubykin et al., 2013), have challenged the 'internal clock' model and prompted a lively debate (Ivry & Schlerf, 2008; Bueti, 2011)

Our understanding of the functional architecture of temporal mechanisms, i.e., how the brain actually discriminates simple intervals or generate timed responses remains unclear. A few interesting theoretical hypotheses have been advanced. 'Intrinsic' timing models for example, describe time as a general and inherent property of neural information processing. A corollary of this assumption is that any area of the brain is

in principle able to encode time i.e., time is *distributed* in the brain and does not require structures dedicated to its computation (Durstewitz, 2003; Buonomano & Maass, 2009).

Temporal computations according to these models rely on inherent temporal properties of neural networks like short-term synaptic plasticity (i.e. State-Dependent networks model-SDNs (Buonomano & Maass, 2009), or arise either from the overall magnitude of neural activity (Eagleman, 2008) or from the linear ramping of neuronal firing rate (Durstewitz, 2003; Reutimann et al., 2004).

An opposite view is that of 'centralized' time models that assume the existence of a 'dedicated', 'centralized' and 'amodal' temporal mechanism (Treisman et al., 1990; Meck et al., 2008)

The 'internal clock model', the most representative of 'centralized' time models, hypothesizes the existence of a pacemaker and an accumulator and assumes that any temporal interval is the result of the integrated activity of these two elements. The pacemaker oscillates at constant frequency and the beats produced are counted by the accumulator. The *neural mechanism* responsible for temporal coding in both 'intrinsic' and 'centralized' models is far from clear. Whether time is encoded through neural oscillators (Meck et al., 2008), ramping activity (Durstewitz, 2003), or state dependent-networks (Buonomano & Maass, 2009) is still an open question.

To summarize from the idea of a single 'universal' and 'amodal' mechanism the field has now moved into that of multiple 'distributed', 'modality-specific' and 'modality-independent' temporal mechanisms. The challenge is now to understand the functional architecture of these different mechanisms (i.e., "how time is represented in these brain regions") and to disclose the functional relationship and the temporal hierarchies between 'modality-specific' and 'amodal' temporal mechanisms (i.e., "what" type of information is processed in these regions and "when" these putative time regions come into play).

1.2 The goal of my PhD work

A way to better understand the functional contribution of sensory specific and amodal putative time areas is to understand:

a) **when**, at which processing stage during duration judgments are these areas engaged?

b) **what** type of duration judgment do these areas support? Are these areas differentially engaged when the sensory load of the duration stimulus change (filled durations versus empty intervals) or when the duration range varies (durations above or below the second)?

In my PhD work I have tried to address the above issues by running a series of Transcranial Magnetic Stimulation (TMS) studies on healthy individuals while they were asked to discriminate the duration of visual stimuli (Chapters 2,4,5). Moreover, thanks to the collaboration with Dr. Alessandro Toso, a former SISSA PhD student and former member of the Tactile Perception and Learning Lab led by Prof. Mathew Diamond, I used a leaky integration model (Toso et al., 2021), a model that sees duration perception as a result of the leaking integration of a sensory drive from primary sensory cortex, to fit my experimental data. By fitting my data with this model, I was able to suggest that a) the encoding of duration from a visual input happens through an integration process whose sensory drive comes from visual areas; b) a distinct contribution of V1 and SMA in providing the sensory drive versus reading out duration information.

In **Chapter 2**. I investigated the role of primary visual cortex (V1) and extrastriate area V5/MT during the duration encoding of different types of stimuli i.e., empty intervals and filled durations. Specifically, we ran 2 distinct experiments in which we stimulated these two areas and the Vertex (as control area) at different timings from stimulus onset (30%, 60% and 90% of the total stimulus's duration) while we asked participants to discriminate the duration of visual stimuli. In experiment 1 (Exp.1) we used empty intervals (time intervals defined by two brief flashes), in experiment 2 we used filled durations (flashes displayed on the screen for a given amount of time). In Exp.1 TMS

worsened the discrimination thresholds when applied over the two areas at 60% and 90% of the of the total interval's duration. This effect was only present for intervals in the range of 0.2 s but not for longer intervals. In Exp.2 the same effects were observed but only when TMS was applied at 30% and 60% of the total stimulus duration. The effects of TMS were present across a wider range of durations (from 0.2 to 0.6 s) Overall, these data show that the chronometry of V1 and V5/MT in duration encoding is stimulus dependent: the stimulus offset is more critical for empty rather than filled stimuli. Moreover, visual cortices seem engaged in temporal processing across a wider range of durations only with filled durations. When filled durations are used, the TMS effects support the idea that V1 and V5/MT encode time via integration/accumulation of sensory input.

In **Chapter 3** I describe a leaky integrator model that was recently developed by Toso and colleagues (Toso et al., 2021). This model is used to explain how the sensory input from rats' barrel cortex is integrated over time to lead to duration perception. We used an adapted version of this model to fit the TMS data of chapter 2 (Experiment 2). The model not only fits well the data but allows to predict a different chronometry between an early visual area (V1) and an amodal premotor region like the supplementary motor area (SMA).

In **Chapter 4** I tested the hypothesis of a functional distinct role of SMA and V1 in duration encoding. In a single experiment I stimulated V1, SMA and the Vertex at different timings from stimulus onset (0%, 60%, 90% and 100% of the total stimulus's duration). Specifically, I predicted that the area where sensory drive comes from i.e., V1, should be maximally affected by TMS stimulation during the stimulus presentation, while an area that simply reads this information should be affected at stimulus offset only. The results confirmed the prediction and also here, the leaking integrator model, compared to other models, best fitted the data.

Finally, in **Chapter 5** to better characterize the functional contribution of SMA during the reading-out of time, in a single experiment I tested the hypothesis that anterior and posterior portions of SMA are preferentially engaged in the representation/reading-out of different durations. Specifically, the anterior portion should prefer the shorter and the posterior part the longer durations of the tested range. In different blocks of trials

TMS was applied over the anterior and posterior SMA while subjects were discriminating visual stimuli of different durations (spanning from 0.2 s to 1.5 s). The results partially confirmed the prediction. The TMS stimulation of the anterior SMA, impaired duration discrimination performance in all tested range, this effect was nevertheless stronger for the shorter durations of the range (0.2-0.4s).

1.3 Methodological approach

1.3.1 The task

To evaluate participants capacity of judging temporal information in milliseconds range I used temporal discrimination tasks in which subjects are asked to compare stimuli of two different durations: a 'standard' and a 'comparison'. Each stimulus can be defined as an empty interval or a filled duration, presented in the visual modality. In filled durations, the visual stimulus is displayed on the screen for a certain amount of time. In empty intervals instead is the time between the onsets of each flash that determines the interval of the stimulus. The duration of the standard stimulus is a fixed value (T) whereas the comparison can be either longer or shorter than the standard (± ΔT). The subject's task is to decide, by pressing one of two response keys, which one of the two stimuli was the longest. A critical component of temporal discrimination tasks relates to how the difference between the standard and comparison duration (ΔT) changes throughout the task. In an *adaptive* ("up-down") procedure this value is adjusted based on the subject's performance (therefore different subjects experience different values and ranges of comparison intervals). In the method of *constant stimuli* ΔT is randomly selected from a fixed set of values at each trial; therefore, all subjects experience the same set of comparison values. Using the adaptive procedure, ΔT is varied in step-wise method that should ultimately converge to a psychophysical threshold (Levitt, 1971), whereas in the method of constant stimuli the percent of correct responses at each value of ΔT is used to fit a psychometric function and calculate the discrimination threshold (difference limen or just-noticeable difference; (Lapid et al., 2008). This threshold is often expressed as half of the value in

milliseconds that spans the range in which subjects get between 25% and 75% of correct responses. In each trial of all experiments there is the sequential presentation of both a comparison and standard stimulus (i.e., 2-AFC two intervals).

1.3.2 Transcranial magnetic stimulation

TMS is widely used in cognitive neuroscience as a non-invasive technique to stimulate the brain and thus modulate neural activity associated with cognitive processes. TMS is based on Faraday's electromagnetic induction principle which states that an electrical current will be induced in a conductor located nearby a changing magnetic field. In the case of TMS, an electrical current flowing through the coil will induce a magnetic field that will in turn cause a change in the polarization of brain tissue laying underneath it. If the polarization change is fast and substantial enough, it will generate an action potential in neurons of the stimulated brain region and it will therefore interfere with their normal activation pattern. Three main ways of delivering TMS are used depending on desired effects. A single pulse (spTMS) protocol is used for stimulation with high temporal and spatial resolution as is the paired-pulse TMS (ppTMS). When two pulses of TMS are delivered within few milliseconds from each other, they summate and increase the effect on the studied cognitive process, ppTMS takes advantage of this property. Repetitive TMS (rTMS) consists in delivering a train of pulses in the target area. With this technique, the effects obtained last longer than the ones observed after sp- and ppTMS but the temporal resolution is lost.

The effects of TMS depend on various factors such as:

- The thickness of the scalp and deepness of the target point (strength of magnetic field rapidly decreases with distance from the coil);
- The cytoarchitectonic organization of the stimulated tissue (magnetic field has to be perpendicular to cell membrane in order to have a maximal depolarizing effect on neurons);
- The intensity of stimulation.

The shape and size of the coil also affects how focal the stimulation is. Two different shapes are mostly used: a circular coil that generates a more distributed magnetic field and a figure of eight coil, that allows for more focal stimulation.

Safety and ethics of this method are well describe in the literature (Rossi et al., 2009).

The most important safety issue is the possible triggering of epileptic seizures, other relatively minor and preventable concerns have to do with tissue heating (estimated to be less than 0.1º C with spTMS) and magnetic forces affecting ferromagnetic and non-ferromagnetic objects (some implants may be moved due to these forces).

By altering a targeted area, TMS allows to unveil a causal implication between that region and a specific cognitive function. Furthermore, spTMS and ppTMS can be used to investigate neural dynamics of cognitive functions by revealing the time at which an area plays a role in a specific process.

Two main approaches try to explain the neural basis underlying the effects of TMS on cognition. The first one is the "virtual lesion" concept that describes the TMS effects as transient and reversible lesion caused by the neural noise TMS induces in a neuronal network (Walsh et al., 1998a; Walsh et al., 1998b; Pascual-Leone et al., 2000)
The second and more recent approach takes into account more subtle behavioral changes induced by TMS. This framework described by Silvanto and colleagues (2008) is based on the fact that TMS has differential effects depending on the initial activation state of a neural population at the time of stimulation and depending on the time point relative to the cognitive process at which TMS is applied. Several studies have shown, for example, that TMS can have not only disruptive and inhibitory effects as predicted by the virtual lesion idea (Vincent Walsh & Cowey, 1998; Pascual-Leone et al., 1999) but it can also facilitate cognition (Töpper et al., 1998).

The simple explanation for these dual effects was demonstrated in a study by (Silvanto et al., 2007) where the authors showed that phosphenes solicited after visual adaptation to a color took on the appearance of that color. This discovery means that TMS preferentially facilitates neuronal networks that are less active at time of stimulation. The disruptive effects on TMS observed when applied during cognitive task, are thus explained by the preferential facilitation of the neuronal populations that are not

engaged in the task and are therefore at a baseline level of activation. This activation decreases the signal-to-noise ratio inducing a general decrease in the behavioral outcome. On the other hand, when TMS is applied shortly before a cognitive process, all neural populations are at baseline levels of activation and they are therefore all equally facilitated by TMS. Of the stimulated populations, the ones solicited during the cognitive process will show a greater sensitivity in comparison to their previous state. Recent developments in the use of neurostimulation approaches are reviewed in (Romei, Thut, & Silvanto, 2016).

CHAPTER 2: THE CHRONOMETRY OF TIME PROCESSING IN VISUAL CORTICES

Abstract

- A few transcranial magnetic stimulation (TMS) studies have shown that primary visual cortex (V1) and extrastriate area V5/MT are necessary to the temporal encoding of visual intervals (Bueti at al., 2008a, Salvioni et al., 2013). However, how duration information is encoded in these brain regions remains unclear.
- Here we test the chronometry of right V1 and right V5/MT in duration processing. Specifically, we asked "when", at which stage of temporal information processing (i.e., from sensory drive integration to duration recognition) these areas are engaged.
- We ran 2 different experiments in which we used paired-pulse TMS (ppTMS) to stimulate the right V1, the right V5/MT and the Vertex (as control area) at different timings from stimulus onset (30%, 60% and 90% of the total interval's duration) while we asked participants to discriminate the duration of different visual durations.
- In different experiments we used stimuli with different sensory load and different duration range (from 0.2 to 0.6 s). In experiment 1 we used empty intervals (i.e., empty time between two brief visual flashes), in experiment 2 we used filled durations (i.e., flashes displayed on the screen for a given amount of time).
- The results showed different chronometries for filled durations and empty intervals, but no differences between V1 and V5/MT stimulation. In both areas

the most effective stimulation timings compared to Vertex were: a) closer to stimulus offset (60% and 90% of the total stimulus duration) for the empty intervals, b) either early or closer to the middle of the stimulus (30% and 60%) for filled durations. c) For empty intervals the TMS effects were present for intervals in the 0.2 s range only. For filled durations the effects were equally present across the different range of tested durations.

The results of the two experiments suggest the existence of a different engagement of visual cortices in duration encoding depending on the type of stimulus used (filled versus empty). When a stimulus is constantly presented on screen its duration can be estimated via integration of a sensory drive. The features of this integration model are better characterized in chapter 3 where the modelling of experiment 2 data is also presented.

2.1 Introduction

Time is embedded in many aspects of our sensory experience; sensory events unfold in time and often acquire particular meaning because of their specific temporal structure. The speed of a moving object, the words pronounced by a speaker and the tactile exploration of a texture, are all examples of temporally structured sensory experiences. Despite the ubiquitousness of the temporal dimension of our sensory experience, the understanding of the neural mechanisms underlying the temporal representation of sensory events, that is the capacity to estimate duration in milliseconds/seconds range, remains unclear.

Over the years, two main framework has been proposed to explain how our brain is able to perceive time: the first hypothesizes the existence of a central and amodal clock capable of timing any type of stimulus (Gibbon et al., 1984), the second posits the existence of a series of distributed clocks, each of them in charge of the encoding of the temporal features of a stimulus early in the stream of processing, namely the

primary sensory cortices, and within the same modality of the presented stimulus. (Merchant et al., 2013a).

More generally, the metaphor of distributed clocks implies the idea that the processing of temporal information can take place thanks to a distributed network whose involvement depends on the sensory modality of the stimuli to be timed and on the requirements of the task at hand (Wiener et al., 2010). Central to these models is therefore the possibility that time encoding can already take place in the primary sensory areas.

More specifically to the visual domain, neurophysiological and behavioral studies carried out in the past years have supported the idea that visual areas are involved in the encoding of temporal information. Shuler and Bear, for example, showed that the firing rate of V1 in rats is modulated by the prediction of the expected time of a reward (Shuler & Bear, 2006); Moreover, selectivity to temporal frequency has been described in monkey and cat visual cortices (Movshon et al., 1978; Foster et al., 1985; Hawken et al., 1996).

Furthermore, behavioral studies have highlighted the link between specific sensory features of the stimuli and alterations in perceived duration (Brown, 1995; Kanai et al., 2006; Benton & Redfern, 2016). For example, the perceived duration of a visual stimulus can be compressed when it is presented shortly before or after a saccade (Morrone et al., 2005). This compression happens only when the stimulus is visual not when it is auditory. These studies, taken together, highlight the importance of visual areas in duration perception at least in the sub-second scale.

In support of this second framework, also TMS evidence over the years has supported the idea of a specific involvement of visual cortices in visual time perception (Bosco et al., 2008, Bueti et al., 2008a, Kanai et al., 2011). Specifically, both the primary visual area (V1) and extrastriate visual area V5/MT have been found to be causally involved in temporal discrimination of visual stimuli.

Although these latest studies have causally demonstrated the role of visual areas in the perception of time, they do not clarify which temporal computation these areas carry out, nor the temporal dynamics of these computation within and between visual

regions. To date, one study tried to shed light over the mechanism that our brain uses to encode time of visual information (Salvioni et al., 2013). In this study, the authors used paired-pulse TMS (ppTMS) over V1 and V5/MT during the encoding of empty temporal intervals. They applied ppTMS at different timings after stimulus onset and found that the most effective stimulation timing was the one closest to the offset (155 ms, first pulse delivered at 60% of the stimulus duration). According to their view, the most effective stimulation was the one closest to the offset because it has been shown that neurons in early visual areas shows an activity that increase monotonically over time, and this increase has been linked to time perception (Ghose & Maunsell, 2002, Shuler & Bear, 2006, Bueti et al., 2010). By disrupting visual activity at later stages of time encoding, the process is influenced when the areas are more involved. It is also worth to notice that their earliest timing of stimulation (50ms, 25% of the 200ms stimulus) was not effective.

What the study by Salvioni et al. left unclear is: whether the most effective TMS stimulation timing depends on a) the length of the temporal interval at hand (Salvioni et al used a single range around 0.2 s) or b) the type of stimulus duration used (i.e., an empty interval where stimulus' duration critically depends on the offset). Moreover, Salvioni and colleagues did not find any difference in chronometry between V1 and V5/MT, and this lack of difference might be due to the poor temporal resolution of the paired-pulse protocol used (inter-pulse interval was 35ms).

To address the issues outlined above we conducted two separate experiments in which, compared to Salvioni and colleagues, we used a) not only empty intervals but also filled durations, b) a wider range of TMS stimulation timings (30%, 60%, 90% of total stimulus duration) c) a wider range of durations (from 0.2 to 0.4 s) and d) a temporally more precise ppTMS protocol (with inter-pulse interval of 12ms).

Before heading into that materials and methods of the first two experiments, I will outline the crucial characteristics of TMS to then clarify some aspects of the methodological approach used.

2.1.1 Transcranial Magnetic Stimulation

Transcranial magnetic stimulation is based on Faraday's principles of electromagnetic induction. A magnetic stimulator consists of a capacitor discharge system to which an external coil is connected. The capacitor generates a pulse of current within the coil and thus a pulse of magnetic field (Barker, 1999). When the coil is placed close to the scalp it induces electrical activity within the superficial layers of the cortex under the coil. The induced pulse can cause a depolarization of a population of neurons and the generation of action potentials when the pulse is of a suitable size, duration, and location (Miniussi et al., 2012) and possibly causing observable effects on behavior.

This method has been used to test a causal relation between some of the aforementioned regions and time perception and time production. TMS effects in temporal tasks have been found in the cerebellum (Théoret et al., 2001, Koch et al., 2007, Del Olmo et al., 2007), the DLPFC (Jones et al., 2004, Méndez et al., 2017), SMA (Méndez et al., 2017), and visual cortices (Bueti et al., 2008a, Salvioni et al., 2013). Differences in results may come from variations of duration ranges (e.g. sub- vs suprasecond durations), tasks (e.g. time perception vs production), and TMS protocols (e.g. differences in stimulation parameters and coils).

2.1.2 Paired-pulse TMS and short-interval cortical inhibition

The behavioral effects that follow the stimulation of TMS depend on the task context and the method of stimulation (Wiener, 2014). Most paradigms investigating the role of different areas in time perception used repetitive TMS (rTMS) which delivers TMS pulses at a certain frequency over a certain period of time. Other approaches to TMS include single pulse TMS and paired pulse TMS (respectively spTMS and ppTMS): these paradigms allow for greater temporal resolution. Specifically, during ppTMS stimulation consists of TMS pulses divided by a short inter-pulse interval (IPI). Paired-pulse TMS (ppTMS) has a larger effect than single-pulse and still allows a reasonable temporal resolution defined by the temporal distance between the two pulses (Pascual-Leone & Walsh, 2001; Silvanto et al., 2005). Historically spTMS and ppTMS have been applied to study the motor system through the stimulation of motor areas to

produce a motor-evoked response (MEP) that can measured through electromyography (Farzan, 2014). The TMS intensity to elicit a response depends on each person's cortical excitability and is called the resting motor threshold (RMT). More specifically, the RTM is defined as the minimum intensity sufficient to be able to observe 7 MEPs over 10 stimulations. Using ppTMS, the RMT can be suppressed or facilitated relative to a spTMS, depending on the interstimulus interval (ISI), i.e. the duration between the two pulses, and the intensity of each pulse (Kujirai et al., 1993; Di Lazzaro et al., 2006).

The mechanisms underlying the facilitation or suppression of neural activity following ppTMS are known as short interval intracortical inhibition (SICI) and short interval intracortical facilitation (SICF).

Inside the motor domain, the motor evoked potential represents a unique opportunity for those who want to use TMS having a relatively handy feedback to get information on the effects that the TMS is causing. Since TMS effects strongly depend on many stimulation parameters (such as intensity and interstimulus interval) and other factors (such as cortical target, TMS coil geometry and pulse waveform), the motor evoked potential can be used to get insights about what effect the TMS will have on behavior and therefore it represents a reliable outcome measure. Other elements that naturally influence the effect of TMS is the intensity, which is commonly defined as a percentage of stimulator's maximum output. In the motor domain, normally the researcher would manipulate stimulation intensity according to the individual RMT, because a sub-threshold intensity for one subject could be suprathreshold for another.

Outside the motor domain and over occipital cortex, one protocol to assess cortical excitability consists of using TMS to induce phosphenes in the participants. Consequently, in this case the threshold is defined as the minimum TMS intensity that leads to a report of perception of phosphenes from the participant. A detailed and rigorous procedure of this method based on a Bayesian adaptive staircase approach has been given by Abrahamyan and colleagues (2011).

Despite this, our aim was not to find the phosphenes threshold, but to be sure that the low-level processing of our participants was not impaired and, therefore, we did not

want them to experience any phosphenes at all. With this goal in mind, we can make a comparison between the motor and the visual domain. In the motor domain it has been shown that to elicit a short-interval cortical inhibition, the optimal ISI is 1-6ms (Reis et al., 2008) and the optimal intensity of the first pulse would be subthreshold (for example 80% of the RMT) followed by a suprathreshold (for example 120% of the RMT) second pulse. In the visual domain the parameters to successfully obtain a SICI are different: it has been shown that cortical inhibition already happens after ppTMS delivered with an intensity of 50% of stimulator's maximum output (Moliadze at al., 2003), and that the switch from enhancement of intracortical inhibition at short ISIs (2–5ms, SICI) to intracortical facilitation at longer ISIs (7–30ms), as demonstrated for human motor cortex, was not evident (Moliadze et al., 2005). It seems therefore that in the visual domain the intensity of stimulation is critical to obtain either facilitation or inhibition, with little involvement of the ISI.

Therefore, we concluded that a stimulation intensity of 55% of the maximum stimulator output was high enough to cause SICI, but not high enough to induce phosphenes. This intensity was sufficiently low to prevent phosphene detection or other kind of visual interferences caused by TMS pulses (Kamitani & Shimojo, 1999, Cowey & Walsh, 2000).

2.2 Materials and methods

2.2.1 Subjects

A total of 25 participants took part in the two experiments (15 and 10 for Exp.1 and Exp.2, respectively), 6 of them participated in both. They were healthy individuals with normal or corrected-to-normal vision (experiment 1: mean age was 24.3, range was 20-30; 4 men, 11 females. Experiment 2: mean age was 23.4, range was 20-30. 3 men, 7 female). All participants gave written informed consent, approved by Ethics Committee of SISSA.

2.2.2 Stimuli and procedure

Both experiments involved a temporal discrimination task (Figure 2.1, Panel A). In both experiments subjects sat in front of a computer (resolution 1920x1080, 144 Hz refreshing rate) and were asked to make a duration discrimination judgment. A white fixation cross was continuously displayed for the entire duration of the trial at the center of the screen (size: 16 px, subtending 0.43° of visual angle at a 60cm viewing distance). Each trial consisted of the sequential presentation of two visual stimuli ("standard duration, S1" and "comparison duration, S2"), separated by the interstimulus interval (ISI), a random value taken from a uniform distribution ranging from 0.9 to 1.2 s (Salvioni et al., 2013).

The duration of the standard duration (S1) in each block was fixed (200, 400 or 600ms). In every trial the standard duration was paired with a comparison duration (S2, Figure 2.1, Panel A). The comparison duration was the standard duration (S1) +/- a ΔS value . For the 200ms S1, S2 was equal to 140, 160, 180, 220, 240, 260ms; for the 400ms S1, S2 was equal to 280, 320, 360, 440, 480, 520ms; for the 600ms S1, S2 was equal to 420, 480, 540, 660, 720, 780ms. In experiment 1 we tested S1 equal to 200 and 400ms. In experiment 2 we tested S1 equal to 200, 400 and 600ms.

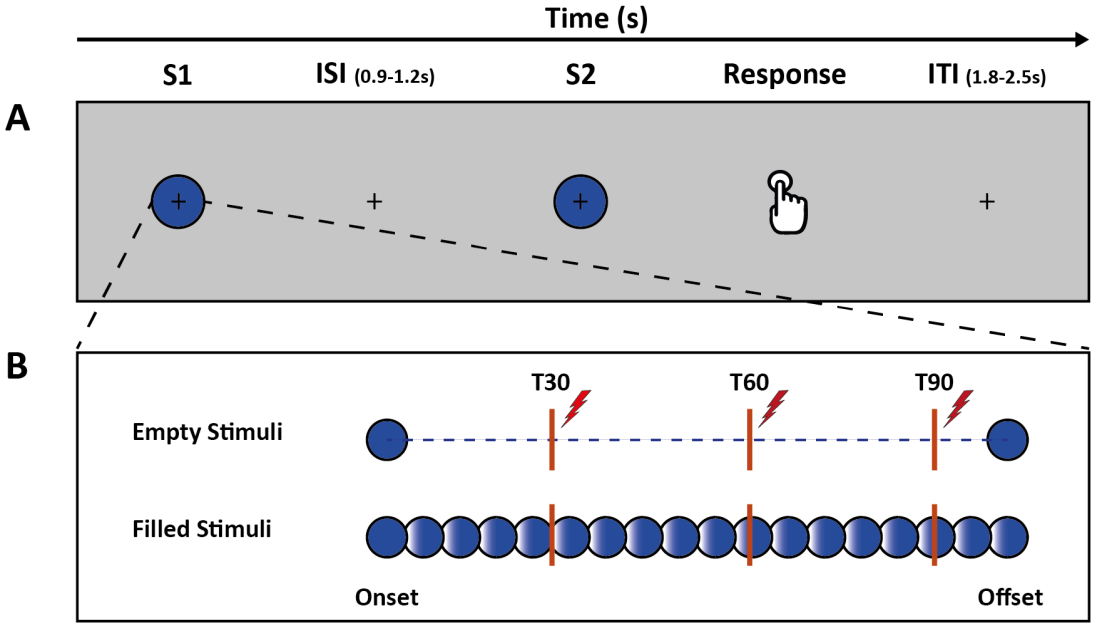

Figure 2.1. A) Schematic representation of the experimental paradigm. After a brief inter trial interval (ITI) lasting between 1.8 and 2.5 seconds, the first stimulus/interval is presented at the centre of the screen. Paired Pulse stimulation is delivered at this stage, in different blocks at different timings. After the first stimulus and after a brief inter stimulus interval (ISI) lasting between 0.9 and 1.2s, the second stimulus/interval is presented. After the end of the second stimulus/interval, the subject responded using the keyboard. In experiment 1 the first stimulus is always the standard duration (S1). In experiment 2 it can be either the standard (S1) or the comparison duration (S2). **B)** ppTMS was delivered at different timings from S1 onset. Unlike Salvioni et al., (2013), in different block we stimulated different S1. The timings of stimulations have therefore been called T30, T60, T90, which corresponds to 30%, 60% and 90% of each S1.

In Experiment 1 we used empty intervals. Participants were shown two sequential brief (7ms) visual flashes. The flashes were light blue disks (rgb: [65 105 225], diameter: 112 px) subtending 3° of visual angle at a 60cm viewing distance and were presented at the center of the screen. A temporal interval was defined as the empty interval between these two successive flashes, and in every trial 2 empty intervals were presented in sequence. Participants had to decide by pressing one of two response keys on the keyboard which one of the two intervals lasted longer.

In each experimental block the 6 possible pairs of S1 and S2 durations were presented 24 times for a total of 144 trials per block. Each block was split in 2 halves of 72 trials each. In 83% of the trials S1 was presented first (120 trials), in 17% of the trials S2 was presented first (24 trials). The two S1 standards (200 and 400 ms) were tested in

separate blocks of trials. In this experiment for the 200ms S1 standard we tested only 2 timings (60 and 90% of the total duration of the stimulus) for 400 ms we tested instead 3 timings (30, 60 and 90% of the total duration of the stimulus). We decided not to stimulate the 200ms empty interval at 30% of its total duration because Salvioni et al. (2013) for the same duration did not find any effect at this timing.

The combinations of 3 stimulation sites (V1, V5/MT and Vertex), 2 S1 standards (200 and 400 ms) and 2/3 stimulation timings (T60 and T90 for S1; T30, T60 and T90 for S2) lead to a total 15 blocks, performed in 2 experimental sessions in different days.

In Experiment 2 we used filled durations. The stimuli were identical to those of experiment 1 (light blue disks). The main difference is that in this experiment they remained on the screen for an entire duration (filled duration). So in Experiment 2 we had the sequential presentation of 2 disks (i.e., S1 - the standard and S2 - the comparison duration). In 50% of the trials S1 was the first stimulus of the pair, and in the other 50% it was the second.

In this experiment we had an unbalanced number of repetitions of the 6 S1-S2 pairs. Specifically, we had 15, 25 and 20 repetitions, for respectively the easiest (Weber fraction 0.3), the intermediate (Weber fraction 0.2) and the most difficult pair to discriminate (Weber fraction 0.1). The total number of trials in a block was 120 trials. Each block was split in 2 halves of 60 trials each. The combination of 3 stimulation sites (V1, V5/MT and Vertex), 3 S1 standards (200, 400, 600 ms) and 3 stimulation timings (30, 60 and 90% of the total length of the stimulus) lead to 27 blocks performed in 3 experimental sessions in different days.

2.2.3 Areas localization

The Vertex was localized by measuring half of the distance between the nasion and the inion and the half the distance between the left and the right ear's tragus. Right V1 and right V5/MT were instead localized through neuronavigation software (Freesurfer to analyze structural MRI scans and BrainSight to locate the areas on the scalp of the subjects). In order to find the region correspondent to the fovea in right V1, we used

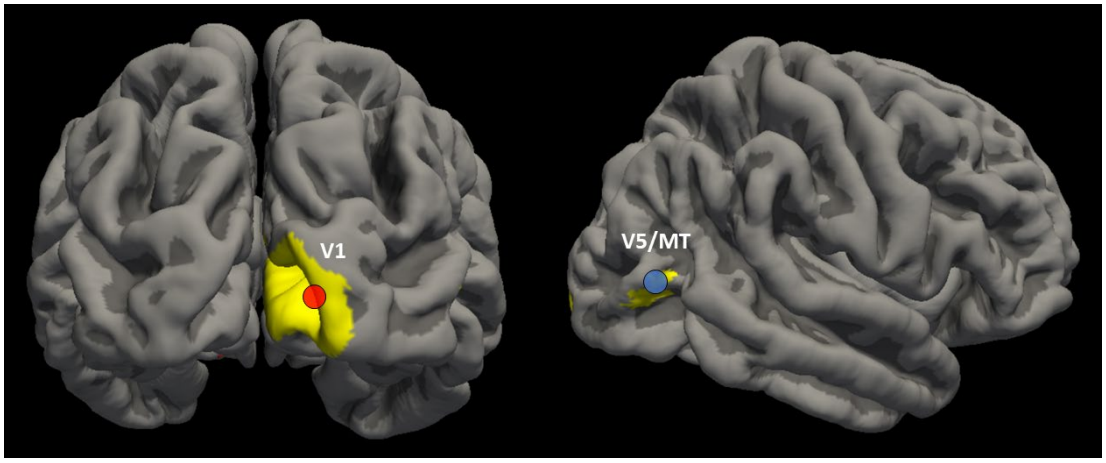

Figure 2.2. Coronal (on the left) view of right V1 (yellow patch) and the target (red dot) as seen with Freeview. Sagittal (on the right) views of right V5/MT (yellow patch) and the target (blue dot) as seen with Freeview. The template displayed is the "Fsaverage" (an "average" brain constructed of MRI scans of 40 subjects).

the algebraical method developed by Benson (Benson et al., 2012) which allows to infer the retinotopic organization of the visual cortex from the structural images of the subject (Figure 2.2).

For all subjects right V5/MT was located using average coordinates in Talairach space determined by Dumoulin (Dumoulin et al., 2000).

2.2.4 TMS protocol

In both experiments we used a Magstim stimulator (Magstim Super Rapid^2 Plus).

Paired-pulse TMS was applied in different blocks over right V1, right V5/MT and on the Vertex as a control area; the order of the blocks was randomized across subjects. We used a 70mm figure-of-eight shaped coil over the Vertex, and a 50mm figure-of-eight shaped coil over right V1 and right V5/MT. Paired-pulse TMS (ppTMS) has a larger effect than single-pulse and still allows a reasonable temporal resolution defined by the temporal distance between the two pulses (Pascual-Leone & Walsh, 2001; Silvanto et al., 2005).

For right V1, we placed the wings of the coil parallel to the midline with the current flowing lateral-medial leftwards (handle on the right). For right V5/MT, we placed the coil with the handle on the left, with the current flowing posterior to anterior.

Relatively to the visual domain, ppTMS has been shown to lower visual cortex excitability as measured by phosphene threshold when applied using an interpulse interval (IPI) ranging from 2 to 100ms (Ray et al., 1998, Gerwig et al., 2005, Kammer & Baumann, 2010). Since one of the challenges of these experiments is to maximize the temporal resolution of our stimulation, we decided to use the lowest IPI possible given the stimulator namely 12.5ms.

The intensity of TMS was set to 55% of the maximum stimulator output for both pulses.

Moreover, other studies have successfully used ppTMS to disrupt visual information processing with the two pulses at the same intensity. Silvanto et al. (2005) used ppTMS to disrupt visual motion detection when they applied TMS over V1 and V5/MT at 60% of the maximum stimulator output with an interpulse interval of 20ms. Salvioni et al. (2013) have successfully used ppTMS at 55% of the maximum stimulator output with an interpulse interval of 35ms to disrupt time encoding of visual stimuli when applied over V1 and V5/MT.

When choosing the parameter of the TMS stimulation, it is worth to stress that our aim was to disrupt the normal function of right V1 and right V5/MT by increasing neural noise (Walsh and Pascual-Leone, 2003).

One way to describe the functional impact of TMS is in fact that it introduces random noise in neural processing shifting the brain activity from its optimal functioning. For example if a target area is accumulating information regarding a stimulus that has to be timed, the TMS may induce neural activity uncorrelated with the task at hand (Harris et al., 2008). It is worth mentioning that feeding noise to an integrator decreases its performance for the duration of the noise (Miller & Wang, 2006).

In each trial ppTMS was applied during the presentation of the first stimulus of the pair, in order to impair purely the encoding process. Applying TMS during the

presentation of the second stimulus would mean interfering also with working memory and decision processes. The pulses were applied at different delays from stimulus onset (30%, 60% and 90% of the total stimulus's duration; these timings of stimulation are named T30, T60 and T90; Figure 2.1, Panel B). For example, for the standard duration of 200ms we stimulated in one block at 60-82ms (30%, T30), 120-132ms (60%, T60) and 180-192 (80%, T90) ms from interval onset (offset of the first flash). A microsecond-precision trigger-box allowed for an accurate delivery of the TMS stimulation.

In experiment 1 we stimulated at T60 and T90 for the 200ms S1 and at T30, T60 and T90 for the 400ms S1 empty interval. In experiment 2 we stimulated all standard durations (200, 400 and 600ms) at T30, T60 and T90, because nobody had ever applied ppTMS at different timings in an experiment involving filled durations. It is also important to stress here that in this experiment, since in 50% of the trials the order of S1 and S2 presentation was reversed, in half of the trials the TMS was applied on the comparison duration.

2.2.5 Block design and additional information

In summary, there were 15 blocks in experiment 1. Three sites (right V1, right V5/MT and the Vertex) by two different standard durations (200ms and 400ms); one standard duration (200ms) by two different timings of stimulation (T60, T90), the other standard duration (400ms) by three different timings of stimulation (T30, T60, T90).

In experiment 2, we had 27 blocks. Three sites (right V1, right V5/MT, and the Vertex) by three different standard duration (200ms, 400ms and 600ms) by three different timing of stimulation (T30, T60, T90). It should be noted that in our design the vertex stimulation is not the only control condition. In fact, the comparison between TMS blocks on the same area but at different timings allowed us to be sure of the specificity of the effects found and to exclude unspecific TMS artifacts.

Finally, a potential bias for the duration perception in our experiment was given by the acoustic noise produced by the TMS apparatus during pulses delivery. In fact, it has

been shown that playing an acoustic stimulus regularly before the presentation of a visual cue, can bias the perceived duration of a visual stimulus (Treisman et al., 1990). In order to prevent this effect, we recorded the TMS sound and played it through headphones that the participants were wearing, during both the first and the second interval. The timings of the fake TMS pulses were synchronized with the TMS delays.

2.2.6 Data analysis

In this context, the subject performance can be described by two main parameters, bias (the "point of subject equality", PSE) and sensitivity (the "just noticeable difference", JND).

For each block of all participants, we fitted the psychometric curves using the MATLAB function FitPsycheCurveLogit, which uses general linear model with a logit link function (Experiment 1=Figure 2.3 Panel A; Experiment 2=Figure 2.3 Panel B). The JND was calculated as the difference between 25% and 75% correct "longer" answers divided by two, while the PSE was calculated as the duration value that was associated with 50% of performance.

As for the study of Salvioni and colleagues (2013), we expected the TMS to have an effect on the JND rather than the PSE.

For both experiments the JND and the PSE were obtained for every block. To make the different durations comparable the individual JND and PSE values were normalized to the appropriate S1 duration (e.g., PSE_{200} /200 ms).

In both experiments we first conducted a repeated-measures analysis of variance (ANOVA) on both the JND and the PSE, with area, timing, and duration as within-subject factor. Once the ANOVA revealed a significant difference between visual areas (V1/V5) and the Vertex, then we proceeded to normalize the individual JND and PSE obtained in each V1 and V5/MT blocks to the Vertex stimulation (site-vertex)/vertex. We performed ANOVA also on these normalized data to the vertex. T-tests were then used for *post-hoc* comparisons. Alpha level was set to 0.05.

Additionally, as for Salvioni et al. (2013), we decided to control if the effect that TMS may have caused are correlated between V1 and V5/MT.

Finally, participants whose JNDs exceeded 2 or more interquartile ranges in any TMS conditions were marked as outliers and removed from the dataset. In experiment 1 three subjects were excluded using this method, whereas in experiment 2 one subject was excluded.

2.3 Results

In experiments 1 and 2, healthy participants have been asked to discriminate the duration of two visual stimuli S1 and S2 while we applied TMS over V1, V5/MT and the Vertex (as control site) at different timings from the onset of the first stimulus (I stimulated at T30, T60 and T90 of the total stimulus's duration). In experiment 1 we used empty intervals (time intervals defined by two brief flashes), in experiment 2 filled durations (flashes displayed on the screen for a given amount of time).

Experiment 1. A repeated-measures analysis of variance (ANOVA) was performed on the JND with area (V1, V5/MT, Vertex), timing (T60, T90) and duration (200ms, 400ms) as a within-subject factor.

The ANOVA revealed a significant interaction between Area and Duration ($F(2, 22) = 7.963$, $p=0.003$). Specifically, compared with vertex stimulation, discrimination thresholds were significantly higher following TMS in both V1 ($t(23)=3.2$, $p= 0.0037$) and V5/MT ($t(23)=5.4$, $p<0.0001$), but only when the S1 involved was 200ms. The ANOVA did not show a main effect of timing ($F(1, 11) = 3.532$, $p=0.087$), nor a main effect of area ($F(2, 22) = 2.392$, $p=0.114$).

The ANOVA conducted on the normalized data with the same factors confirmed that the effect of TMS on the JND was significantly higher when S1 was 200ms when compared to the JND of 400ms (Main effect of Duration, ($F(1,11)=17,797$, $p=0.001$).

Experiment 2. A repeated-measures analysis of variance (ANOVA) was conducted on the JND with area (V1, V5/MT, Vertex), timing (T30, T60, T90) and duration (200ms, 400ms, 600ms) as a within-subject factor.

The ANOVA revealed a significant main effect of the Area ($F(2,16)=5.469$, $p=0.015$). T-tests revealed that, compared to vertex stimulation, the JNDs were significantly higher when we stimulated V1 ($t(80)=-3.5$, $p<0.001$) and V5/MT ($t(80)=4.9$, $p<0.001$).

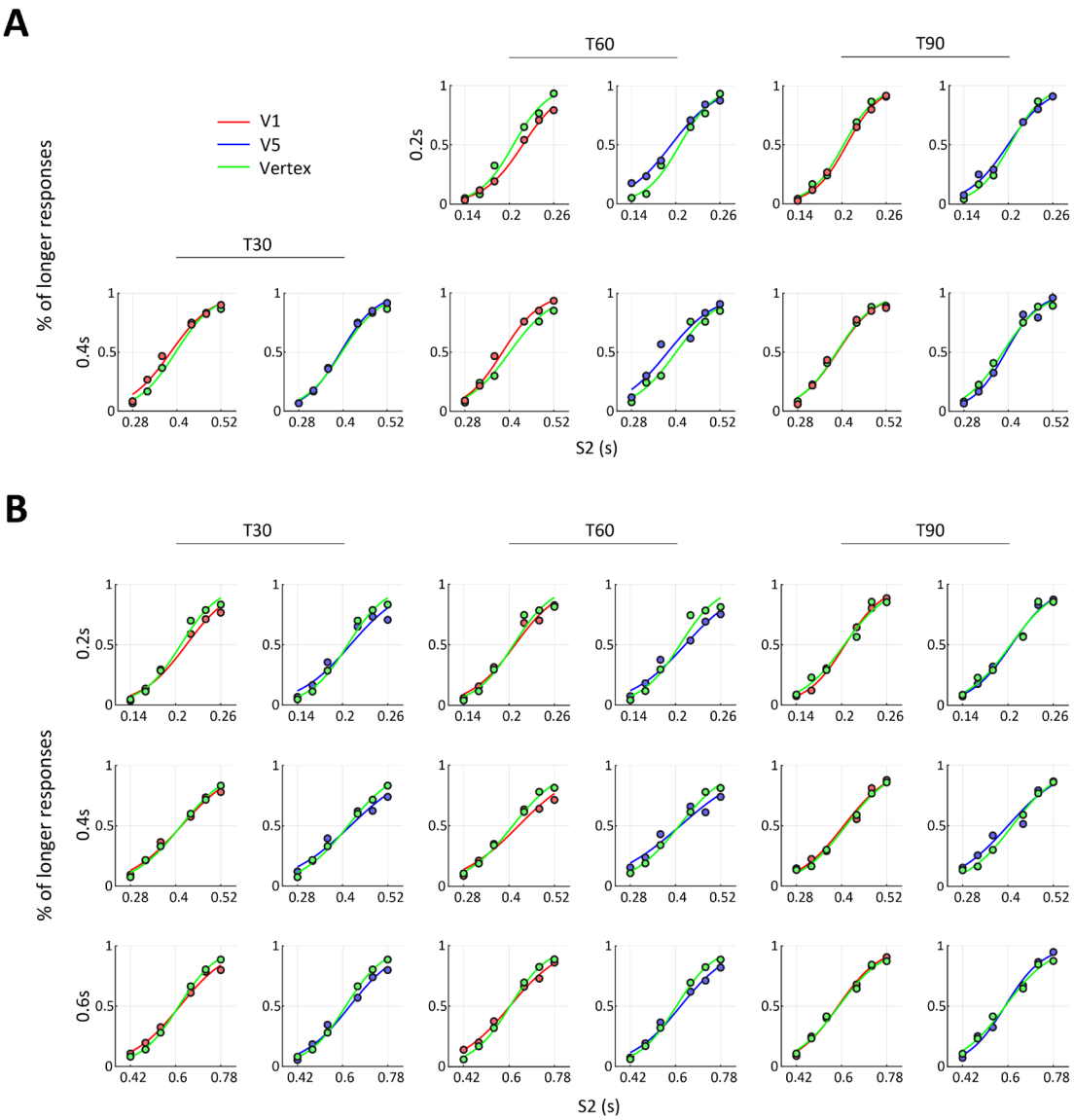

Figure 2.3. **A) Exp 1:** Psychometric curves (average) of the group of participants (N=12) in experiment 1. On the x axis the duration of S2, while on the y axis is the % of time the S2 has been judged longer than S1. The red line is V1 performance, the blue line V5/MT performance, the green line is the vertex performance. The curves are coupled (V1 and the Vertex, V5/MT and the Vertex). In the upper part there is the condition with S1=0.2s and in the lower part the conditions S2=0.4s. On the horizontal plane, the plots are organized according to the three timing of stimulation. It can be noted that the upper left plots are missing since we have decided not to test the T30 condition with S1 = 0.2s. **B) Exp 2:** Psychometric curves (average) of the group of participants (N=9) in experiment 2. The organization of the plots is similar to experiment 1. On the vertical plane the plots are organized according to the three different S1 (0.2, 0.4 and 0.6s), while on the horizontal plane they are organized according to the three timing of stimulation (T30, T60 and T90).

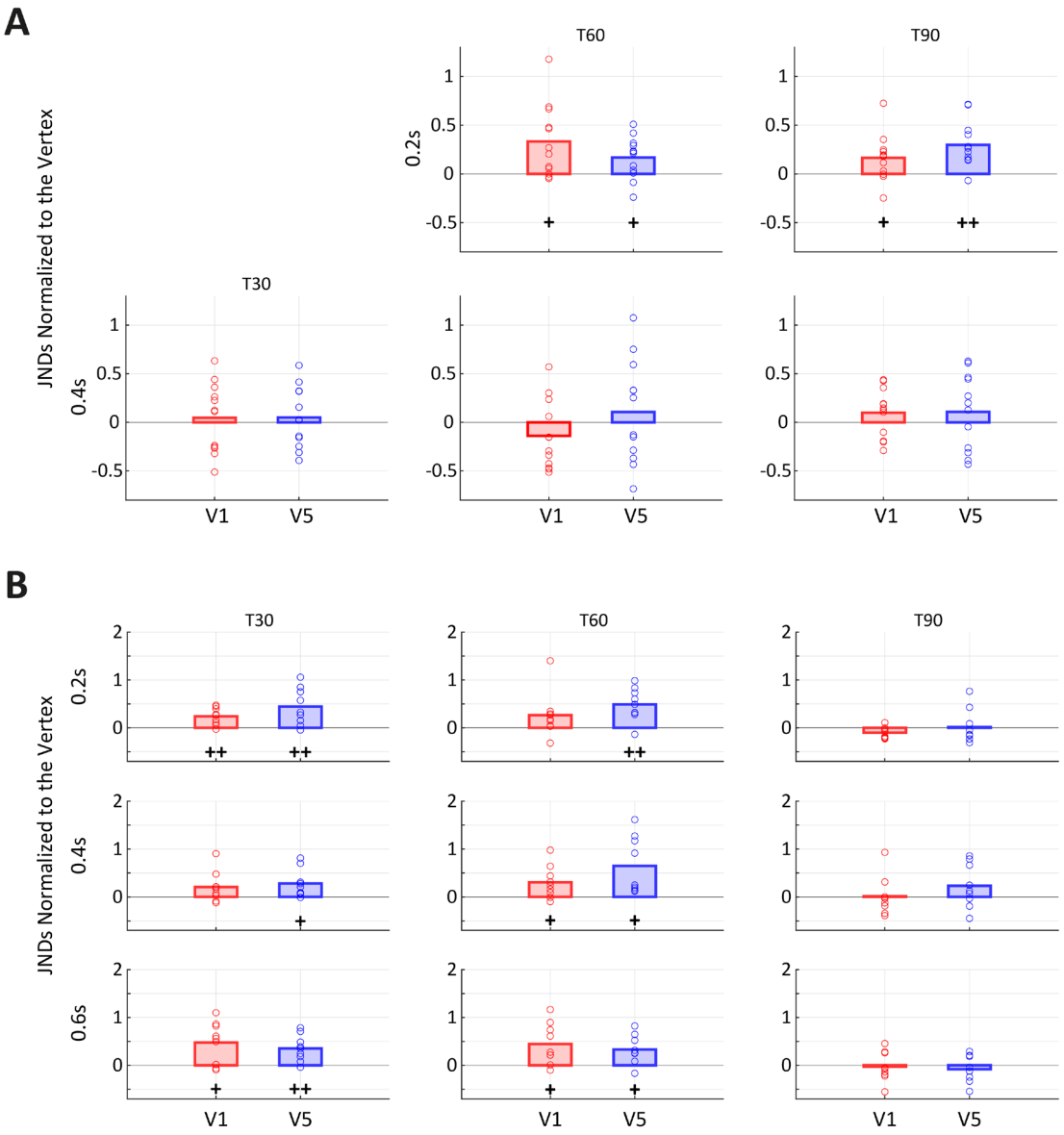

Figure 2.4. **A) Exp 1:** JND (group average) of V1 and V5/MT normalized to the Vertex for experiment 1. We normalized these JND as follows: (site-vertex)/vertex. By doing this, now the data can be seen as a percentage difference from the vertex. Therefore, in these plots the 0 is the vertex. Plus symbols represent the results of the one-sample *t* tests significant at + $p < 0.05$ and ++ $p < 0.01$; in this dataset a one-sample t test highlights a difference with the significant with the vertex. In the vertical plane plots are again organized according to the S1 involved, while on the horizontal plane, the plots are organized according to the two timing of stimulation. **B) Exp 2:** JND (group average) of V1 and V5/MT normalized to the Vertex for experiment 2. The organization of the plots is again similar to that of experiment 1.

	Paired t-test								
	T30			T60			T90		
	V1	V5	VX	V1	V5	VX	V1	V5	VX
V1	-	0.78	<0.001***	-	0.15	<0.001***	-	0.17	0.13
V5	0.78	-	<0.001***	0.15	-	<0.001***	0.17	-	0.87

Table 2.1. T values of and two-sample t test computed on JNDs normalized to the vertex stimulation for experiment 2. Asterisks symbols represent the results of the two-sample *t* tests significant at *** $p < 0.001$.

This time, the ANOVA showed also a significant main effect of timing ($F(2, 16)=13.281$, $p<0.001$) and a significant interaction between timing and area ($F(4,32)=7.159$, $p<0.001$). Specifically, t-tests revealed higher JND when stimulating T30 and T60 compared to T90 (T30vsT90, $t(80)=3.0$, $p=0.0038$. T60vsT90, $t(80)=4.0$, $p<0.001$), showing that the TMS at T30 and T60 is more effective. This finding is confirmed by the significant interaction of timing and area: the t-tests show that the effect of TMS is significantly higher when stimulating V1 and V5/MT compared to the vertex stimulation, but only when stimulating at T30 and T60 (Table 2.1).

The repeated-measures analysis of variance performed on the normalized data with the same factors showed a significant main effect of timing ($F(2, 16)=32.217$, $p<0.001$), and – again – the pattern of results is similar to the one described above. In fact, t-tests showed higher JND when stimulating at T30 and T60 compared to T90 (T30vsT60, $t(53)=-5.0$, $p<0.001$. T30vsT90, $t(53)=5.0$, $p<0.001$; T60vsT90, $t(53)=7.1$, $p<0.001$).

PSE. Unexpectedly, a repeated-measures analysis of variance (ANOVA) conducted on the PSE with area (V1, V5/MT, Vertex), timing (T30, T60, T90) and duration (200ms, 400ms, 600ms) as a within-subject factor, showed a significant main effect of timing in experiment 2 ($F(2,16)= 14,932$, $p<0.001$). T-tests revealed that, regardless of the area stimulated, the PSE were significantly lower when we stimulated at T90 if compared to T30 ($t(80)=5.2$, $p<0.001$) and T60 ($t(80)=3.6$, $p<0.001$) (Figure 2.5).

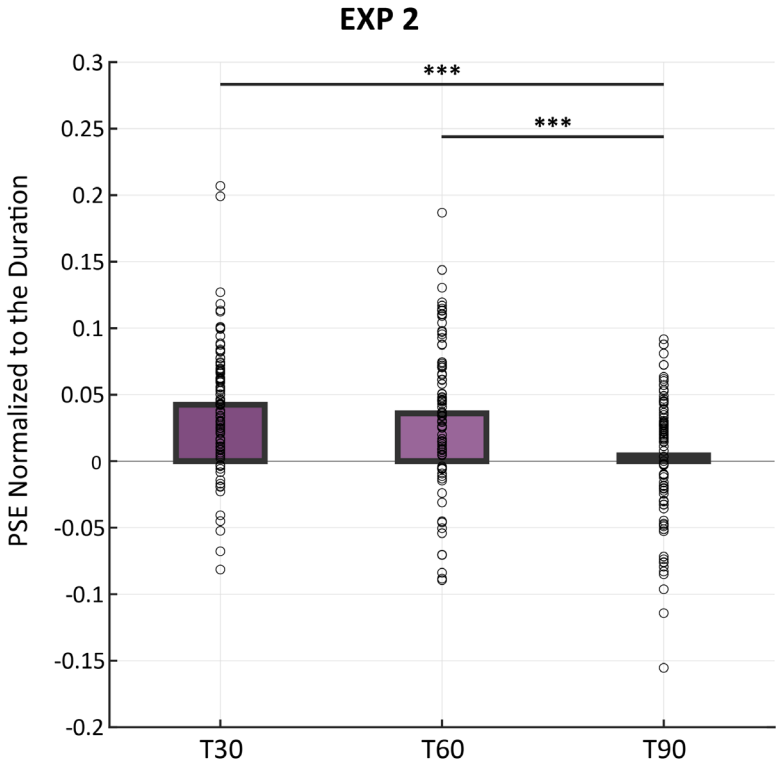

Figure 2.5. Group average of the PSE values across V1, V5/MT and vertex (average of the group e distribution) plotted for the 3 timings of stimulations in experiment 2. The PSE are averaged across the stimulation sites since there is no difference between them. Asterisks symbols represent the results of the two-sample *t* tests significant at *** $p < 0.001$.

2.4 Discussion

With this experiment, we aimed to investigate the chronometry of time encoding in visual cortices.

For both experiment 1 and 2, the initial ANOVAs on the non-normalized JND data showed that the TMS stimulation had a significant effect when applied to the right V1 and the right V5/MT compared to the Vertex stimulation. This result is compatible with previous studies, showing the involvement of visual areas in time encoding.

However, when empty intervals are involved, this does not appear to be true for durations greater than 200ms. In the 400ms condition, there was no significant difference between TMS stimulation of V1 and V5/MT.

On the other hand, when filled durations were involved, the critical difference between V1,V5/MT and the Vertex was not present when we stimulated at T90.

If in experiment 1 seems that the duration is critical for finding TMS effects (significant effects only with short durations, 200ms), in experiment 2 the timing seems to be critical (significant effects only with early stimulation, T30 and T60).

This initial consideration confirms one of our initial ideas. The effect of TMS strictly depends on which stimulus the brain is encoding.

The subsequent analysis carried out on the normalized data in experiment 1 confirms that the effects are isolated to the shortest duration irrespectively of the stimulated area (V1 or V5/MT) or timing (T60 or T90). We replicated the results of Salvioni and colleagues at T60 and we introduced the finding that also T90 is an effective timing of stimulation – as we had hypothesized – but the two timings of stimulation essentially are not different. Also, regarding the areas, we hoped to find different chronometry, but this was not the case.

On the contrary, in the second experiment the TMS was effective when applied over V1 and V5/MT in all tested durations (therefore up to 600ms) if compared with the Vertex performance, but only when we were stimulating at T30 and T60.

This is confirmed from the analysis carried out on the normalized data. In this case, the ANOVA highlighted only a significant main effect of timing. In other words it does not matter if we stimulate V1 or V5/MT, the crucial aspect is that the stimulation is critical at T30 and T60, but not at T90.

Overall, the results of the 1° experiment support some of our initial hypothesis. As suggested by Salvioni and colleagues (2013), a timing of stimulation closest to the offset was indeed effective, but not significantly more effective if compared with the timing of stimulation closest to the middle of the stimulus. What is interesting is that all effects disappear when a longer stimulus was involved. This is particularly interesting because it is linked to one of our initial hypotheses. We hypothesized that the effectiveness of a stimulation timing depended on the duration of the stimulus at hand. In our specific case, the stimulation at T60 of V1 and V5/MT during the stimulus of 200ms is in absolute terms comparable with the stimulation at T30 during the stimulus of 400ms, since in both cases the stimulation was delivered after 120ms. Therefore, the fact that the two conditions have a different effect confirms the idea that when it comes to time, the stimulation timing must be linked to the duration of the stimulus at hand.

This is especially true of the second experiment. The stimulation is effective when delivered at T30 and T60 regardless of the duration of the stimulus. It is important to note, for example, that for a 400ms stimulus, T90 is 360ms, while for a 600ms stimulus, 360ms is equivalent to a T60 stimulation. That said, although the absolute

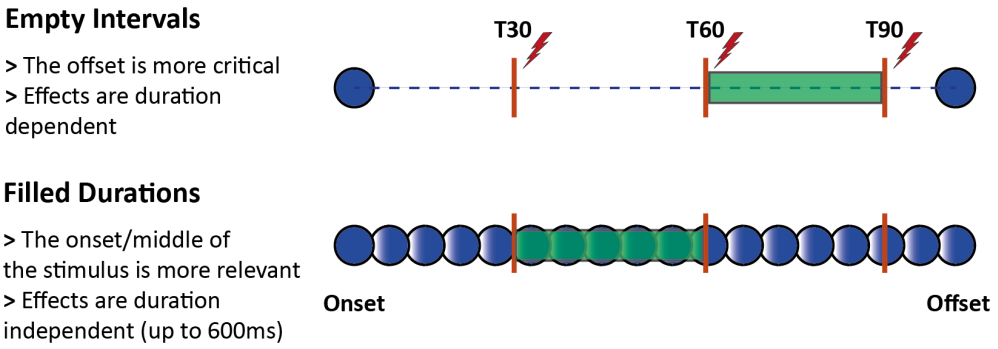

Figure 2.6. Figure depicting the summary of our results. For empty intervals, stimulations were found to be effective when delivered at T60 and T90, but only in the condition with the shortest stimulus (200ms). We can then hypothesize that effective stimulations could be delivered in a time window between T60 and T90. For filled durations, stimulations were effective when delivered at T30 and T60 in all tested durations. We can then hypothesize that effective stimulations could be delivered in a time window between T30 and T60.

timing is the same, in the case of a stimulus of 600ms the stimulation is effective, while in the case of a stimulus of 300ms - being at T90 - it is not.

Regarding the PSE, we found that the PSE at T90 shows significantly lower values than at T30 and T60. Since this effect does not depend on the stimulated area, our interpretation is that it depends on some factor related to the TMS per se. Although we tried to control the presence of the TMS sound by applying a similar sound on the second stimulus, we could not control the tactile sensation that a TMS pulse produces.

2.4.1 Conclusions

The results of the first two experiment suggests that our brain encode time information from empty and filled stimuli using probably different mechanisms (Figure 2.6).

Regarding the 1° experiment, our results are compatible with our initial hypothesis, even if only when short stimuli are involved (<400 ms). The offset seems to be critical, and the effects are duration dependent.

Regarding the 2° experiment, it seems that the onset/middle of the stimulus is more critical, and that the effects seem to be duration independent (at least up to 600ms).

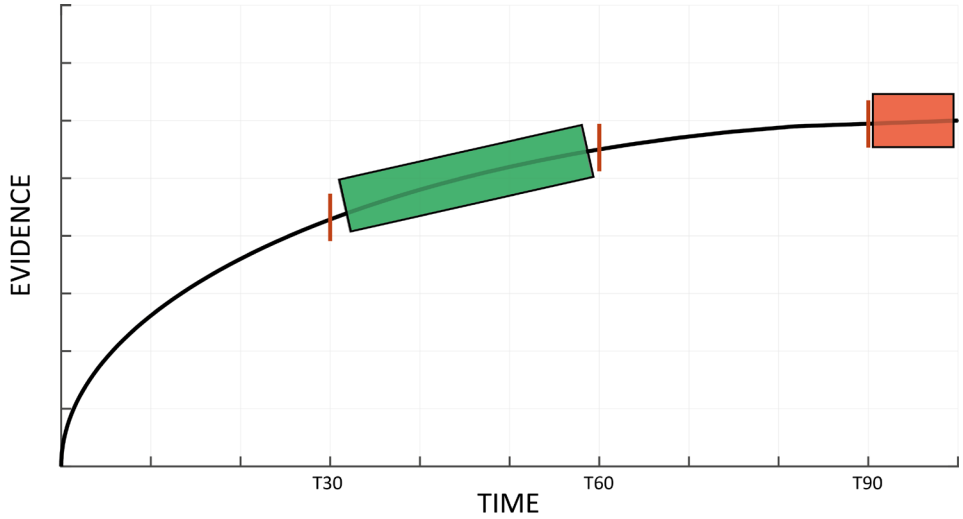

Figure 2.7. Figure depicting our hypothesis. In green is the time window that we believe can be effective if a TMS stimulus is given. In red the time window that we believe is not critical if a TMS stimulus is given. This is true only for the filled durations of experiment 2.

For filled durations the T90 stimulation is less effective than the T60.

If we think that the activity of visual areas represents the drive of an accumulator, we can try to speculate on the reasons leading to the observed TMS effects.

Previously we said that if we inject noise into a system that is integrating sensory inputs, the performance of the system will be lower the longer the period in which the noise is injected. With this in mind, we can therefore imagine that at T90 the induced noise of the TMS stimulation had not enough time to be accumulated to cause a drop in performance. On the other hand, a stimulation given at the core of the process would lead to a greater decrease in performance because there is more time for this noise to be accumulated (Figure 2.7).

In the next chapter I will try to prove this idea by using a leaky integrator model of duration perception (Toso et al. 2021) to simulate our empirical data.

CHAPTER 3: A LEAKY INTEGRATOR MODEL OF VISUAL DURATION ENCODING

Abstract

- In the previous chapter, we showed that the stimulation of V1 and V5/MT in the right hemisphere, impaired the duration discrimination of visual filled durations when applied early after stimulus onset or right in the middle of the duration to be timed (30% and 60% of the total stimulus's duration). This result seems to suggest that the duration of a visual sensory event can be estimated via integration/accumulation of a sensory drive. If this integration over time is perturbated because the sensory drive or the integration process itself is perturbated by TMS then the perception becomes noisier (less precise).

- This possibility is tested by fitting the V1 and V5/MT TMS data of Experiment 2 of the previous chapter with a leaky integrator model (Toso, et al., 2021). This model was originally used to explain how the sensory input from rats' barrel cortex is integrated over time to lead to duration perception. We adapt the original leaky integrator model to the TMS data. TMS was modeled as a parameter increasing the noise of the sensory drive (i.e., the standard deviation of the neural noise). According to our model an area that provides the sensory drive, like V1, should be greatly affected by the TMS noise only if this noise is applied early after stimulus onset and at middle trial time.

- The leaky integrator model fits well the experimental data.

3.1 Introduction

In the past years, brain stimulation studies have shown that the primary visual cortex (V1) and the extrastriate visual area V5/MT are causally engaged in the duration discrimination of visual stimuli (Bosco et al., 2008, Bueti et al., 2008a, Kanai et al., 2011, Salvioni et al., 2013). However, these studies fail to clarify the kind of computations the visual areas perform during time encoding and the temporal unfolding of these computations within each region.

By acquiring information on the time course of visual encoding of time information we tried to understand what kind of computations these areas are implementing. To do so, we stimulated right V1, right V5/MT and the Vertex (as control area) at different timings from stimulus onset (30%, 60% and 90% of the total stimulus's duration) while we asked participants to discriminate the duration of visual stimuli. Our results showed that the most effective timing of stimulation to impair participants' performance when stimuli were filled durations were 30% and 60% of the total stimulus's duration.

This result seems to suggest that duration encoding takes place as an accumulation process that can be greatly affected in its unfolding but not at its end. The role visual areas play in this process is difficult to access with the original experiment. One possibility is that visual cortices, specifically V1 and V5/MT, represent the sensory drive of an integration process that may take place in the visual cortex itself or elsewhere in the brain. The possibility that a sensory area provides the sensory drive to an integration process leading to duration perception has been recently proposed by Toso and colleagues (2021). In this work the authors combine human and rat psychophysics with sensory cortical neuronal firing to construct a computational model of the perception of time embedded within sense of touch. In this work, subjects are asked to judge the duration of a vibration applied to the fingertip (human) or whiskers (rat), while the duration and the intensity of the stimulation was simultaneously varied. Increasing stimulus intensity led to increasing perceived duration. Symmetrically, increasing vibration duration led to increasing perceived intensity. The authors modelled the real spike trains recorded from vibrissae

somatosensory cortex as input to dual leaky integrators–an intensity integrator with short time constant and a duration integrator with long time constant–generating neuromeric functions that replicated the actual psychophysical functions of rats. These results highlight the role of accumulation of sensory drive from sensory cortex as possible mechanism for duration perception.

I collaborated with Dr. Alessandro Toso, a former SISSA PhD student, a former member of the Tactile Perception and Learning Lab led by Prof. Mathew Diamond and the first author of the aforementioned paper. In this chapter we used a modified version of the leaky integrator model formalized in Toso and colleagues (2021) to model the data of experiment 2 of the previous chapter. This modelling would allow us to strengthen the interpretation of the role of visual cortices in duration perception.

3.2 Methods

Following Toso and colleagues (2021), we tried to model our data on the assumption that time encoding is mediated by visual areas and that these areas provide the drive to an integrator that nonlinearly accumulate sensory signal over time during the encoding of the stimulus.

The leaky integration is a model of accumulation of perceptual information (Usher & McClelland, 2001).If the accumulation would not be leaky, the process of information accumulation would proceed indefinitely without loss or decay of information. In this case, the accuracy would increase without bound: as long as there is any difference among the stimuli, accuracy will be perfect. But this does not reflect one of the fundamental properties of the just noticeable difference (JND). We know that the smallest the difference between two stimuli, the poorer the performance; moreover, The JND is proportional to the initial stimulus duration.

As in the original model by Toso and colleagues, we posit that the duration perception of a visual event results from the accumulation of sensory signal over time (Toso et al., 2021). Leaky integration of sensory input can be formulated as:

$$C\frac{d\Upsilon}{dt} = -\lambda\Upsilon + f(L_t, t) \quad (1)$$

where Υ is the percept, $f(L_t, t)$ is the external drive to the integrator, λ is the leak rate and $\frac{C}{\lambda} = \tau$ specifies a time constant of integration.

We assume that the external drive to the integrator is made up of the visual input L plus noise. We further assume the sensory signal follows a power law with luminance input raised to exponent α. Furthermore, we assume additive normally distributed noise, ξ, that is independent from the stimulus and might even originate through a different sensory modality. Thus, external drive can be specified as:

$$f(L_t, t) = L_t^{\alpha} + \xi \quad (2)$$

Based on previous TMS results on duration discrimination tasks (results of Salvioni et al., (2013) and of experiment 2 in chapter 2, where TMS affected sensitivity rather than inducing a systematic bias, we posit that the TMS may increase the variance of the noise at the level of the input. Feeding noise into an integrator causes a decrease in performance proportional to the duration of noise (Miller & Wang, 2006).

The model assumes that the TMS stimulation is affecting the variance σ_b^2 of the normally distributed noise ξ in Equation 2. More specifically, TMS activation is increasing σ_b^2 by a multiplicative free parameter k, that was called Gain. Based on previous literature on the physiological consequences of ppTMS on visual cortex, we assumed that the duration of the TMS effect is 150 ms (Moliadze et al., 2003). Alternatively, if the TMS had an effect on the bias (PSE), we would have had a change in the noise mean. We will explore the possibility of different competing models in Chapter 4.

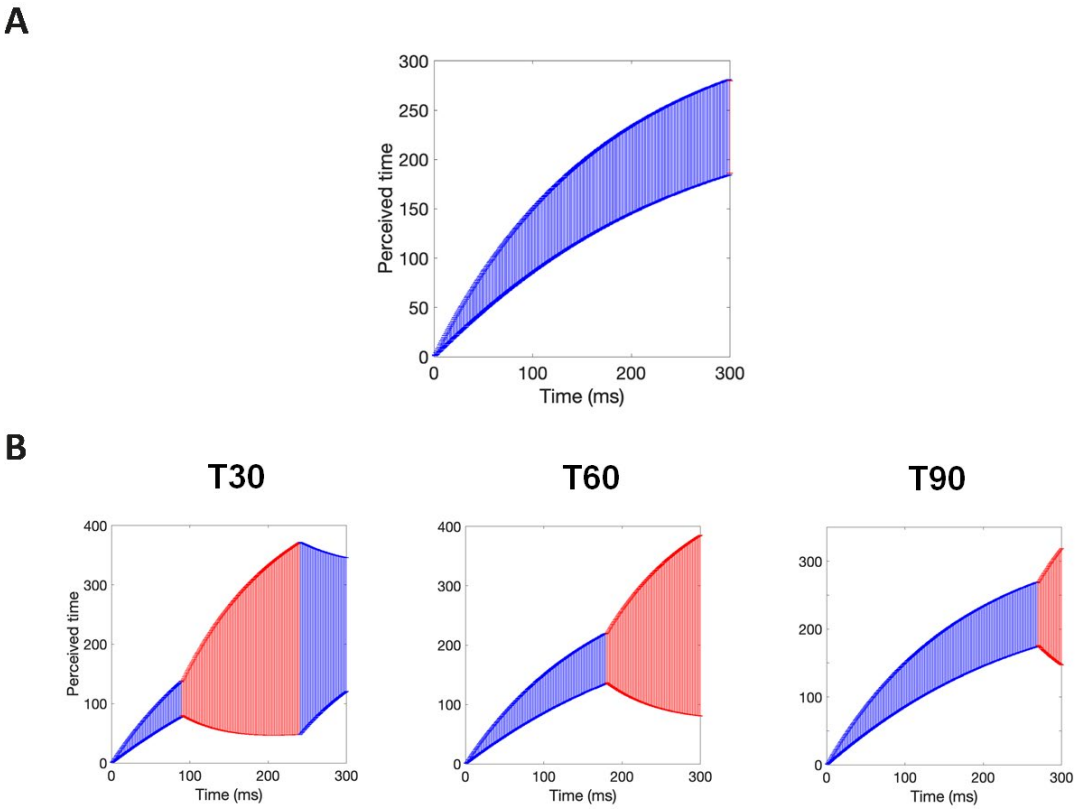

Figure 3.1. **A)** Accumulation of sensory drive over time. The accumulator integrates information over time, but also loses some information over time. Because of that, the variance of the perceived duration increases with longer stimuli. The variance of the perceived duration at the offset reflects the sensitivity of the system and the overall accuracy. **B)** When TMS is delivered, the variance of the noise increases. For a time window of 150ms (i.e., the hypothetical duration of ppTMS in visual cortex) , the accumulator integrates additional noise, leading to a further increase in the variance of the response, therefore to a lowering of performance.

The behavior of the accumulator under no TMS and with the TMS delivered at T30, T60 and T90 can be seen in figure 3.1. We obtained this graphical representation of the accumulator behavior by running the model on a stimulus of 300ms duration for 500 times. At the top of the figure 3.1 it possible to appreciate the behavior of the model in the condition without TMS. The variance of the perceived time increases with increasing time, and the final variance represents an indicator of the performance of the accumulator. In the lower panel of the figure are shown the effects of the TMS pulse at three different timings of stimulation. The accumulator accumulates the input with increasing noise, due to the TMS. 150 ms after TMS onset, the accumulator begins to "forget" the noise of the TMS, and the speed with which this occurs is

inversely proportional to the magnitude of τ.

From a visual inspection it is already possible to appreciate how the model output mimics our results. When TMS is delivered at T30, the integrator begins to accumulate noise. When the effect of the TMS ends, the accumulator begins to "forget" the noise of the TMS. The variance of the perceived duration is greater at T60 precisely because the accumulator has no time to "forget" the noise of the TMS. At T90, on the other hand, the accumulator does not have enough time to accumulate the noise of the TMS for the variance of the perceived duration to be affected.

In the duration discrimination experiment, we assume that subjects compare the percepts of the two stimuli, $Y_1(T1)$ and $Y_2(T2)$ respectively. The probability that $Y_2(T2) > Y_1(T1)$ can be calculated, given that both percepts are normally distributed, and their mean and variance are known. Thus

$$P\big(Y_2(T_2) > Y_1(T_1)\big) = \int_{-\infty}^{+\infty}\int_{Y_1}^{+\infty} P(Y_2, Y_1)\mathrm{d}Y_2\,\mathrm{d}Y_1 = \frac{1}{2} + \frac{1}{2}\mathrm{erf}(d') \tag{3}$$

$$d' = \frac{\mathrm{E}[Y_2(T_2)] - \mathrm{E}[Y_1(T_1)]}{\sqrt{2(\mathrm{Var}[Y_2(T_2)] + \mathrm{Var}[Y_1(T_1)])}} \tag{4}$$

where $\mathrm{erf}(x)$ is the normal error function. Given that on some trials, the subject may lapse (that is, make a non-sensory error), we assume that the probability of reporting that the second percept is larger than the first is:

$$P\big(\mathrm{choice}(2 > 1)\big) = \mathrm{p_{low}} + \big(1 - \mathrm{p_{low}} - \mathrm{p_{high}}\big)\left[\frac{1}{2} + \frac{1}{2}\mathrm{erf}(d')\right] \tag{5}$$

Where $\mathrm{p_{high}}$ ($\mathrm{p_{low}}$) is the probability of making an incorrect decision due to a lapse at a trial with large positive (negative) mean $Y(T)$ difference.

Parameter name	Fitting range
τ	$[0, 5000]$ms
σ_b^2	$[0, 10^5]$
$\mathrm{p_{high}}$	$[0, 0.5]$
$\mathrm{p_{low}}$	$[0, 0.5]$

Table 3.1. Parameters and fitting range. We fitted these parameters using the Vertex Condition.

Each percept evolves through time following equation 1, with different parameters values which were fitted to the experimental data through the procedure described below.

We fitted the behavioral data from each individual subject in the Vertex condition with 4 free parameters (Table 3.1), so that the least squared difference between the observed fraction of choices Stimulus 2 > Stimulus1 and the model predicted choice probability was minimized.

We assumed that $\mathrm{Var}[Y(0)]$ and μ_b are always equal to zero, the target function that guides the parameter fits was the least squared difference between the observed fraction of choices Stimulus 2 > Stimulus1 and the model predicted choice probability (Equation 5) for each T1 and T2 pair.

The reported fitted parameters values were obtained by using lsqcurvefit MATLAB function. We then fixed the values of σ_b^2, τ, $\mathrm{p_{high}}$ and $\mathrm{p_{low}}$, and fitted the behavioral data from the three stimulation conditions (T30, T60 and T90) in parallel using the MATLAB fmincon function, with a single free parameter *k*. The target function that

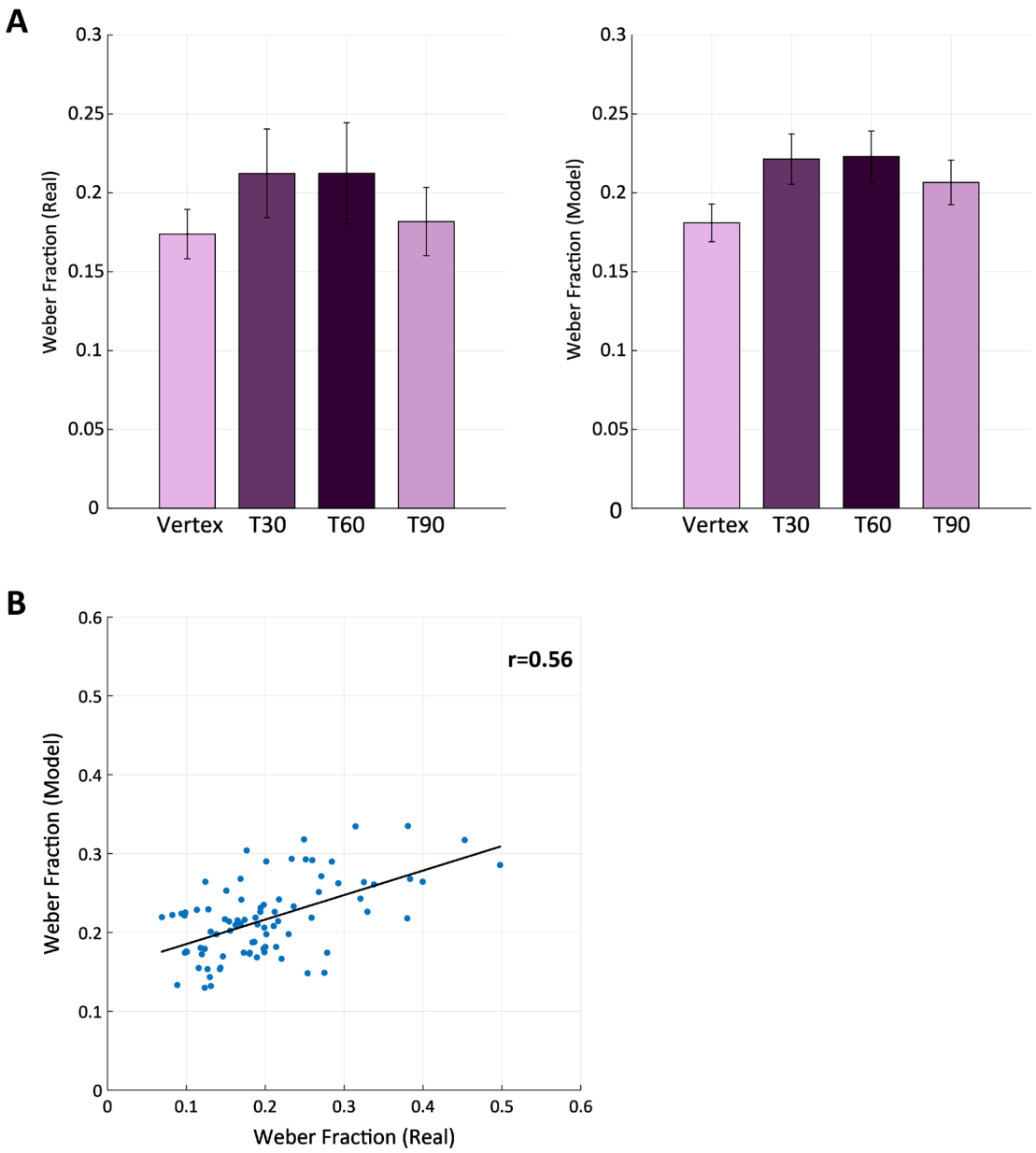

Figure 3.2. **A)** weber Fraction from experiment 2 on the right, and on the left the weber fraction obtained from the model. **B)** Correlations across subjects between experimental weber fraction and the output of the model.

guides the parameter fits was the least squared difference between the observed fraction of choices Stimulus 2 > Stimulus1 and the model predicted choice probability (Equation 5) for each T1 and T2 pair.

3.3 Results

We posit that during time encoding the visual areas provide the sensory drive to an integrator accumulating sensory signal in a leaky fashion. In addition to accumulating sensory signal, our model also accumulates a certain amount of intrinsic signal noise. In our model TMS increases the variance of the noise from TMS onset until 150 ms after it. We fitted the parameters we needed to predict the behavior from the condition of the Vertex. Once we obtained the parameters, we fitted our model with k as the only free parameter.

Figure 3.2A shows the results of the model fit in all TMS conditions (T30, T60, T90) in V1 and V5/MT. On the right the real data as observed in V1 and V5/MT (see chapter 2, Experiment 2), on the left the fitted data averaged across subjects. The figure clearly shows a close similarity between fitted and real data. In both cases, the TMS stimulation at T90 is the closest to the Vertex baseline. According to the model at T90 does not have enough time for the accumulator to accumulate noise.

Moreover, the experimental weber fractions and the output of the model are positively correlated across subjects ($r=0.56$, $p<0.001$) (Figure 3.2, Panel B). This is an indication that the model mimics the real data well.

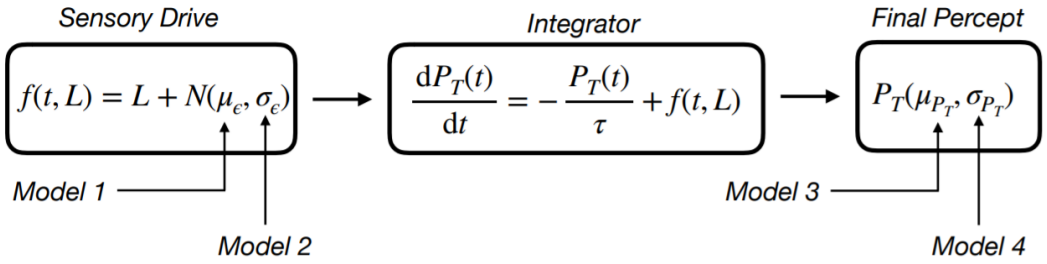

Figure 3.3. Our model consists of three instances: the sensory drive, the accumulator, and the final percept. The 4 different models assume that the TMS affects different parts of the model.

3.4 Limitations

A great limitation of what we have done so far is not having considered alternative models to fit our data. We modeled the effect of TMS as an increase in the variance of incoming noise by a multiplicative free parameter k. There are two key assumptions we made in the tested model: 1) that the TMS affects the variance of the noise; 2) and that the TMS noise affects the level of the sensory drive.

However there are alternative possibilities to seeing TMS as uniquely affecting the sensory drive. It could also be that TMS affects the final percept. Figure 3.3, show possible alternative models. In Model 1 and 2 TMS have an effect respectively on the mean and on the variance of the sensory drive. Model 1 predicts that TMS causes a bias in the perception of stimulus duration, while Model 2 predicts that TMS affects duration sensitivity without creating a bias. Model 2 has been tested in this chapter.

Model 3 and Model 4 instead are models in which TMS affects the final percept without affecting the sensory input. In both these models the change in perception is due to a change in integration of a fixed amount of sensory drive. Model 3 changes the percept mean, Model 4 changes the variance.

The predictions of the models that sees TMS affecting the final percept are presented in Figure 3.4.

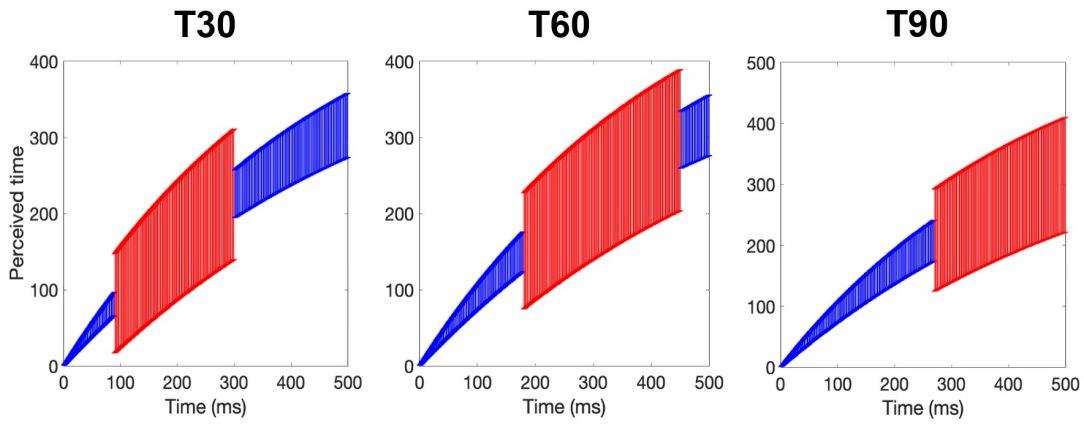

Figure 3.4. Prediction of the effects of TMS given at different timings at the level of the final percept. In this case the reference model is model 4. The TMS increases the noise of the final percept, and this increases the variability of the response. Since the accumulator is not affected, the increase in variance does not increase over time.

As shown in Figure 3.4, the variance of the perceived duration increases during the time window of the TMS effect, but this induced noise does not increase over time since the integrator is accumulating without interference. Moreover, according to these models the TMS stimulation timing that best produces an effect in performance is at T90. This prediction is clearly against what the TMS results showed for visual areas (chapter 2, experiment 2).

Now since TMS affects visual cortex early after stimulus onset and at middle trial time, as model 2 predicted, we are more inclined to believe that visual areas provide the drive to the integrator. We also hypothesize that a different upstream area reads out the output of the integrator. A possible candidate for the read-out is the supplementary motor area (SMA). In humans, the role of SMA in temporal perception has been extensively documented (Macar et al., 2002; Ferrandez et al., 2003; Macar et al., 2006). SMA has been implicated in a variety of timing tasks (Coull et al., 2004; Bueti et al., 2008c; Bueti & Macaluso, 2010) with a range of durations spanning from a few hundreds of milliseconds to a few seconds (Morillon et al., 2009; Lewis & Miall, 2003) and with stimuli of different sensory modalities (Rao, 1997; Coull et al., 2008; Pastor et al., 2004). It is therefore likely that this area represents a high-level stage of temporal processing. SMA is also the area where a topographic representation of time has been recently described (Protopapa et al. 2019). In the next chapter I will describe a TMS

experiment in which we tested the possibility that SMA reads out the output of a hypothetical integrator. In the same experiment we applied TMS over SMA and V1 at different timings from stimulus onset (T0, T60, T90, T100) while asking participants to discriminated visual millisecond range visual durations.

According to the hypothesis of the different functional role of V1 and SMA in duration encoding, we expect the greatest impairment on duration discrimination (i.e., higher JND) after V1 TMS at T60 and after SMA TMS at T90 and T100.

CHAPTER 4: CHRONOMETRY OF TIME PROCESSING IN VISUAL AND PREMOTOR AREAS

Abstract

- The leaky integrator model presented in the previous chapter posit that the duration perception of a sensory event depends on the integration over time of a sensory drive coming from a sensory region.
- In this chapter, I will present a TMS experiment in which I tested the hypothesis that left V1 and left SMA play a distinct role in visual duration encoding. Specifically, within the leaky integrator framework I expect V1 to feed a hypothetical integrator with its sensory input and the supplementary motor area (SMA) to read-out the integrator's output. In the same experiment we applied TMS over SMA and V1 at different timings from stimulus onset (T0, T60, T90, T100) while asking participants to discriminate millisecond range visual durations. According to the hypothesis of the different functional roles of V1 and SMA in duration encoding, I expect the greatest impairment on duration discrimination (i.e., higher JND) after V1 TMS at T60 and after SMA TMS at T90 and T100.
- The TMS results confirmed the predictions and the data were modeled with 4 different versions of the leaky integrator model. The four models differed in the target of the TMS noise i.e., noise either at the input or at the percept level and affecting either the mean or the variance of the neural noise. The model best fitting V1 data, was again the one assuming an effect of TMS on the variance of the neural noise at the input level. Whereas the model best fitting the SMA data was the one assuming a TMS effect on the variance of the noise at the level of the percept. Overall these data suggest a different functional role of V1 and SMA in duration encoding. If the duration perception of a visual

event is the result of an integration processes of a sensory input, V1 provides the input to the integrator whereas SMA reads-out the output of the integrator.

4.1 Introduction

TMS evidence over the years has supported the idea of a specific involvement of visual cortices in time perception (Bosco et al., 2008, Bueti et al., 2008a, Kanai et al., 2011, Salvioni et al. 2013). In particular, it has been shown that the primary visual cortex (V1) and the extrastriate visual area V5/MT are causally involved in the encoding stage of a visual duration discrimination task. However, these studies fail to clarify the type of computations visual areas perform during duration encoding.

In previous chapter (chapter 2) I have presented two experiments in which I have tried to find out whether the engagement of V1 and V5/MT during the encoding of visual durations depends on the sensory load of the stimuli (filled versus empty) and on the range of durations at hands (from 0.2 to 0.6 s). The two previous experiments have shown that chronometry of V1 and V5/MT in duration encoding is identical (no difference between V1 and V5/MT) and depends on the stimuli used. When the stimuli were empty intervals and the visual input serves as onset and the offset markers, the most effective timing of TMS stimulation was the one closest to the interval offset. Moreover, TMS disrupted the discrimination of temporal intervals in the shortest range only (i.e., around 0.2s). On the other hand when durations were defined with a stimulus continuously displayed on screen for a given amount of time, the chronometry of V1 and V5/MT changed and the most effective timings of stimulations were those close to middle of the duration (i.e., 30-60% of the total stimulus duration). Moreover, TMS was effective across a wider range of durations (0.2 to 0.6 s).

These results seem to suggest the existence of different mechanisms for the encoding of empty intervals and filled durations. Filled duration seems to require a greater involvement of visual regions while the stimulus unfolds over time. Our hypothesis, using a model formalized and described by Toso and colleagues (2021) is that the duration perception of a visual event requires the leaky integration over time of a

sensory input. This input comes from visual cortex if the event is visual. We tested this hypothesis by fitting a leaky integrator model to our experimental data. By assuming that the TMS noise affects the variance of the neural noise at the level of the sensory input we were able to successfully fit the behavioral data obtain after V1 stimulation. Now, if V1 represents the input level of this model which brain area reads its output? A region that reads the output of the integrator should be affected by TMS only after the integration process has taken place, so towards the offset of the to be timed stimulus. Continuing the collaboration with Dr. Alessandro Toso, we chose as a candidate read-out area the supplementary motor area and we decided to stimulate in the same experiments V1 and SMA at different timing from stimulus onset (T0, T60, T90, T100) while asking participants to discriminated visual millisecond range visual durations (filled durations).

In humans, the role of SMA in temporal perception has been extensively documented (Macar et al., 2002; Ferrandez et al., 2003; Macar et al., 2006). SMA has been implicated in a variety of timing tasks used (Coull et al., 2004; Bueti et al., 2008c; Bueti & Macaluso, 2010) with a range of durations spanning from a few hundreds of milliseconds to a few seconds (Morillon et al., 2009; Lewis & Miall, 2003) and with stimuli of different sensory modalities (Rao, 1997; Coull et al., 2008; Pastor et al., 2004). It is therefore likely that this area represents a high-level stage of temporal processing. SMA is also the area where a topographic representation of time has been recently described (Protopapa et al. 2019).

According to the hypothesis of the different functional role of V1 and SMA in duration encoding, we expected the greatest impairment on duration discrimination (i.e., higher JND) after V1 TMS at T60 and after SMA TMS at T90 and T100.

4.1.1 SMA as possible time “read out”

A possible candidate for the read-out role is the supplementary motor area (SMA).

The involvement of SMA in time perception tasks have been shown extensively, in studies using very different neuroscientific methods, e.g. single cell recording in

monkeys (Mita et al., 2009; Merchant, et al., 2013b), fMRI (Ferrandez et al., 2003; Morillon et al., 2009; Protopapa et al., 2019) and TMS (Méndez et al., 2017).

SMA activity has been shown to correlate with the processing of temporal information regardless of the task being used (Coull et al., 2004; Bueti et al., 2008c; Bueti & Macaluso, 2010) or the sensory modality involved (Rao, 1997; Coull et al., 2008; Pastor et al., 2004), and with a range of durations spanning from a few hundreds of milliseconds to a few seconds (Morillon et al., 2009; Lewis & Miall, 2003).

Moreover, SMA receive temporal signals coming from different regions of the brain (Buonomano & Maass, 2009, Wiener et al., 2012; Salvioni et al., 2013), and it has been shown that SMA is the main projection site of the straito-frontal motor loop and is believed to recruit timing information from the basal ganglia (Alexander et al., 1991).

Because of this, it has been proposed that the activation of SMA in time tasks may reflect an active reconstruction of temporal signals coming from different regions of the brain (Protopapa et al., 2019).

In a recent fMRI study, Protopapa et al. (2019), showed that in SMA neuronal units preferring a certain stimulus duration are organized topographically within the area. More specifically, the anterior portion of SMA showed a higher number of voxels that showed a preference for short stimuli, whereas the posterior portion showed a higher number of voxels that showed a preference for long stimuli. This high level of functional organization reflects a high level of processing, maybe close to duration judgments stage.

Interestingly, chronomaps in SMA were observed at the offset, and this is consistent with the predictions of our model.

These finding suggesting the centrality of SMA in time processing suggests us that SMA could read-out time information collected from a number of areas.

It is therefore possible that this area constitutes an “amodal” and “high-level” core of a timing network in which duration is represented in an abstract form independent of specific sensory modality or motor behavior.

4.1.2 SMA and TMS

A number of TMS studies probed the involvement of SMA in timing tasks with contradictory results. While some of them did show no significant change of timing behavior after stimulating the SMA (Jones et al., 2004; Koch et al., 2004; Giovannelli et al., 2014) others showed an involvement of SMA (Méndez et al., 2017) or connected areas (Wiener et al., 2012). Importantly, those studies used a variety of different protocols, including different tasks, stimuli coming from different modalities and most importantly different TMS setups.

One of the previously cited studies used TMS and visual stimuli (Jones et al., 2004). In this study, the authors showed an effect of TMS in time reproduction after stimulating the dorso-lateral prefrontal cortex (DLPFC), but not SMA. More specifically they applied rTMS over DLPFC and SMA at the onset of a short (0.5s) and a long (0.2s) interval that the participants had to encode in order to successfully reproduced it. In this experiment, the intervals were empty intervals defined by flashes that lasted 100ms and the rTMS were applied four times starting from stimulus onset at a rate of 20 Hz. They did not find any significant effect after stimulating SMA.

Interestingly our model predicts a significant effect of TMS with a different experimental design: the stimuli must be full intervals and the TMS must be given towards the end of the stimulus.

4.2 Materials and methods

4.2.1 Subjects

15 healthy participants with normal or corrected-to-normal vision (mean age was 26.7, range was 21-36; 6 men, 9 females) took part in the experiment. All participants gave written informed consent, approved by Ethics Committee of SISSA.

4.2.2 Stimuli and procedure

Participants were involved in a temporal discrimination task (Figure 4.1, Panel A).

Subjects sat in front of a computer (resolution 1920x1080, 144 Hz refreshing rate) and were asked to make a duration discrimination judgment. A white fixation cross was continuously displayed for the entire duration of the trial at the center of the screen (size: 16 px, subtending 0.43° of visual angle at a 60cm viewing distance). Each trial consisted of the sequential presentation of two visual stimuli ("standard duration, S1" and "comparison duration, S2"), separated by the interstimulus interval (ISI), a random value taken from a uniform distribution ranging from 0.9 to 1.2 s (Salvioni et al., 2013). The duration of the standard duration (S1) in each block was fixed (400ms). In every trial the standard duration was paired with a comparison duration (S2, Figure 4.1). The comparison duration was the standard duration (S1) +/- a ΔS value, which was equal to 260, 300, 340, 460, 500 and 540ms. In half of the trials S1was the first element of the pair, in the other half it was the seconds.

We used filled durations. The filled durations were light blue disks (rgb: [65 105 225], diameter: 80 px) subtending 2.14° of visual angle at a 60cm viewing distance and were presented at the center of the screen. Participants had to judge which one, S1 or S2, was presented for longer time and answer on the keyboard by pressing the left arrow if the first stimulus was longer or the right arrow if the second stimulus was judged longer. Subject were instructed to respond in half of the block (60 trials) with the right

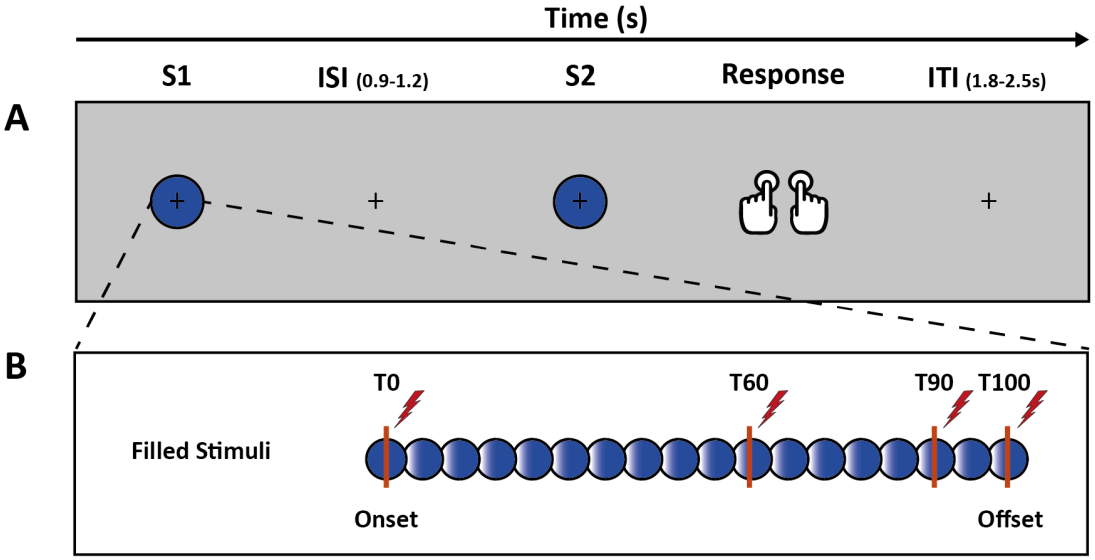

Figure 4.1. **A)** Schematic representation of the experimental paradigm. After a brief inter trial interval (ITI) lasting between 1.8 and 2.5 seconds, the first stimulus is presented at the centre of the screen. Paired Pulse stimulation is delivered at this stage, in different blocks at different stimulation timings. After the first stimulus and after a brief inter stimulus interval (ISI) lasting between 0.9 and 1.2s, the second stimulus is presented. After the end of the second stimulus, the subject responds using the keyboard. the subject is instructed to answer half block (60 trials) with the right hand and the other half with the left hand. **B)** ppTMS was delivered during S1. The timings of stimulations for this experiment are T0, T60, T90 and T100.

hand and in the second half with the left hand. The left/right order of response was counterbalanced across subjects.

In this experiment we had an unbalanced number of repetitions of the six S1-S2 pairs. Specifically, we had 15, 25 and 20 repetitions, for respectively the easiest (Weber fraction 0.35), the intermediate (Weber fraction 0.25) and the most difficult pair to discriminate (Weber fraction 0.15). The total number of trials in a block was 120 trials. Each block was split in 2 halves of 60 trials each. The combination of 3 stimulation sites (left V1, left SMA and Vertex), and 4 stimulation timings (0, 60, 90 and 100% of the total length of the stimulus) lead to 12 blocks performed in 2 experimental sessions conducted in separate days.

4.2.3 TMS protocol

ppTMS was delivered with a Magstim Bistim stimulator (Magstim BiStim²).

Paired-pulse TMS was applied in different blocks over left V1, left SMA and on the Vertex as a control area; the order of the blocks was randomized and counterbalanced across subjects. We used a 50mm figure-of-eight shaped coil over the three areas.

For left tV1, we placed the wings of the coil parallel to the midline with the current flowing lateral-medial rightwards (handle on the left). For left SMA the wings of the coil were parallel to the midline with the current flowing lateral-medial rightwards.

To both areas we applied a ppTMS protocol used in the motor cortex to induce cortical inhibition. We delivered 2 pulses 2 ms apart, the first delivered at 80% and the second at 120% of the resting motor threshold (RMT, (Reis et al., 2008). We chose this protocol because its physiological effects have been extensively studies (Ray et al., 1998, Ziemann et al., 1998; Gerwig et al., 2005, Kammer & Baumann, 2010), and because both intensity of stimulation and inter-pulse interval were compatible with analogous inhibitory effects observed in the visual domain (Moliadze at al., 2003).

All pulses were given in each trial during the presentation of the first stimulus of the pair, in order to impair purely the encoding process. The pulses were applied at different delays from stimulus onset (0%, 60%, 90% and 100% of the total stimulus's duration; these timings of stimulation are named T0, T60, T90 and T100; Figure 4.1, Panel B). Concerning the onset stimulation (T0) we gave the first pulse concurrently with the first frame of the stimulus. Regarding the offset stimulation (T100), we anticipated the stimulation of 2ms to avoid to deliver the second pulse during the inter-stimulus interval. Consequently, with a standard duration of 400ms, we stimulated at 1-3ms (0%, T0), 240-242ms (60%, T60), 360-362 (90%, T90) and 398-400 (100%, T100). A microsecond-precision trigger-box allowed for an accurate delivery of the TMS stimulation. Since in 50% of the trials the S1-S2 order of the stimuli was reversed, in half of the trials the TMS was applied on S2.

4.2.4 Block design and additional information

In summary, there were 12 blocks. Three sites (left V1, left SMA and the Vertex) by four different timings of stimulation (T0, T60, T90 and T100).

Finally, a potential bias for the duration perception in our experiment was given by the acoustic noise produced by the TMS apparatus during pulses delivery. In fact, it has been shown that playing an acoustic stimulus regularly before the presentation of a visual cue, can bias the perceived duration of a visual stimulus (Treisman et al., 1990). In order to prevent this effect, we recorded the TMS sound and played it through headphones that the participants were wearing, during both the first and the second interval. The timings of the fake TMS pulses were synchronized with the TMS delays.

4.2.5 Resting motor threshold

Single-pulse TMS delivered over the primary motor cortex (M1) elicits a muscle response. The excitability of the stimulated area can be measured with the motor evoked potential (MEP) which is recorded with electromyography (EMG) and used to determine the resting motor threshold (RMT) of each individual participant. Finding the RMT, i.e. the excitability of the stimulated muscle at rest, was essential for the TMS protocol we used. To elicit a SICI (short latency intracortical inhibition) the conditioning stimulus needed to be lower than the RMT, the test stimulus higher.

For the MEP acquisition the coil was placed over the subject's hand area at a 45° angle from the midsagittal line, perpendicular to the central sulcus (Brasil-Neto et al., 1992). Once we found a point on the scalp eliciting an MEP, the RMT was defined as the lowest stimulus intensity (given as percentage of MSO, i.e. maximal stimulator output) that is required to induce a MEP with a peak-to-peak amplitude of 50 μV in 5 out of 10 trials. The Electromyography (EMG) was recorded using a BIOPAC MP150 system. Three electrodes were used: two Ag-AgCl surface electrodes, placed over the belly of the first dorsal interosseous (FDI) muscle of the right hand and over the head of the radius bone and one ground electrode (metallic surface electrode) placed on the right forearm. The mean MEP was 57.41% (+/- 5.17%) of the MSO.

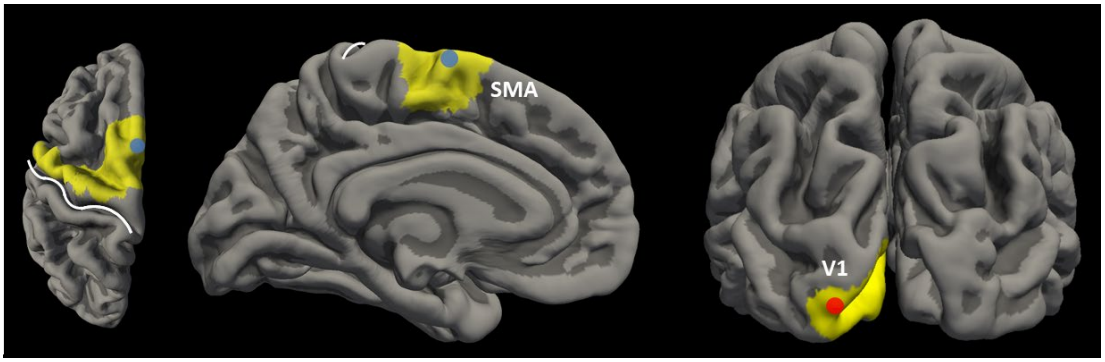

Figure 4.2 Axial (on the left) and sagittal (in the centre) views of the BA6 (yellow patch) as seen with Freeview. In both figures the central sulcus is highlighted with a white line. Coronal (on the right) view of left V1 (yellow patch) and the target (red dot) as seen with Freeview. The template displayed is the "Fsaverage" (an "average" brain constructed of MRI scans of 40 subjects). We localized the posterior part of SMA as the most anterior part of the prefrontal gyrus, and the for the anterior part (blue dot) we moved 1.5cm anteriorly from the posterior part.

4.2.6 Areas localization

As for the previous experiments, we tested participants that had already participated to a fMRI experiments and therefore possessed an MRI scan. The vertex was localized by measuring half of the distance between the nasion and the inion and the one between the left and the right ear. Instead left V1 was localized through neuronavigation software (Freesurfer to analyze the structural MRI scans and Brainsight to co-register the MRI scan with external landmarks on the subject's head). In order to find the region correspondent to the foveal input in V1, we used the algebraical method developed by Benson (Benson et al., 2012) which allows to infer the retinotopic organization of the visual cortex from the structural images of the subject. In order to localize left SMA we overlaid on each individual T1-weighted image the Freesurfer label image (lh.BA6.exvivo.thresh.label) corresponding to Brodman area 6 (Figure 4.2). The SMA target was the anterior SMA, that we identified moving 1.5 cm away from the most anterior part of the prefrontal gyrus. Each subject's anatomical MRI scan was co-registered with visible landmarks on the subject's head using the Brainsight frameless stereotaxy system together with the Polaris infra-red tracking camera and sensors (Northern Digital, Waterloo, Canada). The Polaris system allowed us to constantly track the coil position with respect to the target area thorough the experiment.

4.2.7 Data Analysis

In this context, the subject performance can be described by two main parameters, bias (the "point of subject equality", PSE) and sensitivity (the "just noticeable difference", JND).

In all individual subjects, we fitted the psychometric curves using the MATLAB function FitPsycheCurveLogit, which uses general linear model with a logit link function (Figure 4.4). The JND was calculated as the difference between 25% and 75% correct "longer" answers divided by two, while the PSE was calculated as the duration value that was associated with 50% of performance accuracy.

According to our previous result, we expect TMS to have an effect on the JND rather than on the PSE.

We first conducted a repeated-measures analysis of variance (ANOVA) on both the JND and the PSE, with area (Vertex, SMA, V1) and timing (T0, T60, T90 and T100) as within-subject factor. T-tests were then used for *post-hoc* comparison. Alpha level was set to 0.05. Finally, participants whose JNDs exceeded 2 or more interquartile ranges in any TMS conditions were marked as outliers and removed from the dataset. One subject was excluded using this method (Figure 4.3).

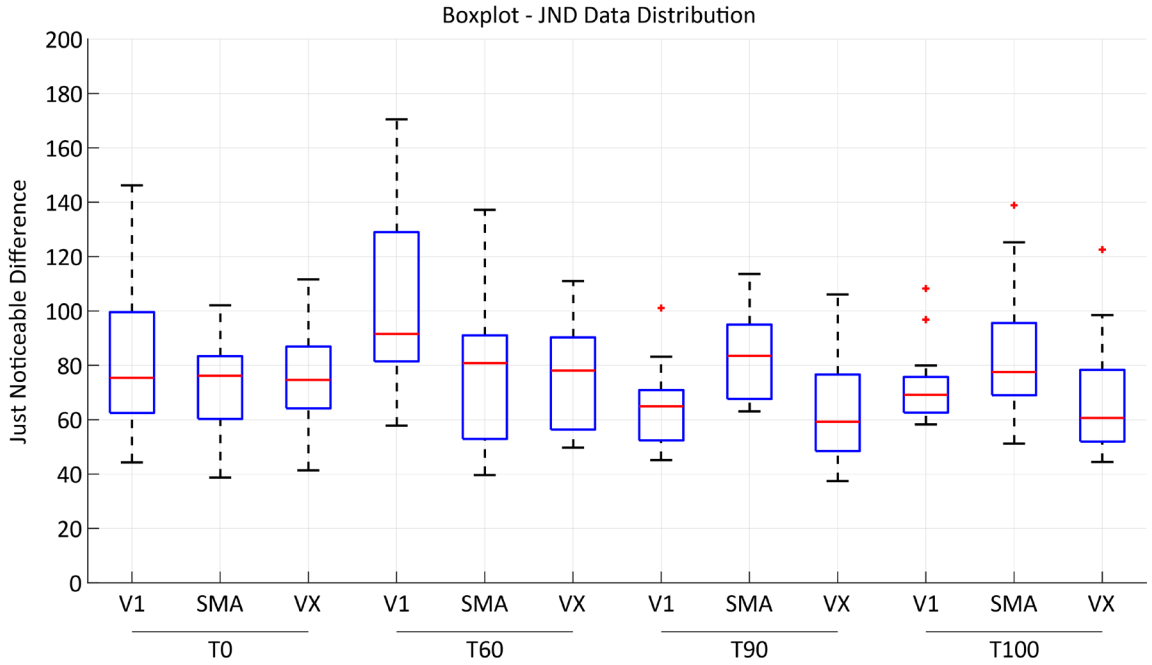

Figure 4.3. Data distribution of the JNDs for every condition. Participants whose JNDs exceeded 2 or more interquartile ranges in any TMS conditions were marked as outliers and removed from the dataset. One subject was excluded using this method.

4.3 Results

In experiments 3, 15 healthy participants were asked to discriminate the duration of two visual stimuli S1 and S2 while we applied TMS over V1, SMA and the Vertex (as control site) at different timings from the S1 onset (I stimulated at T0, T60, T90 and T100 of the total stimulus's duration).

4.3.1 Just noticeable difference

A repeated-measures analysis of variance (ANOVA) was conducted on the JNDs with area (V1, SMA, Vertex) and timing (T0, T60, T90 and T100) as a within-subject factor.

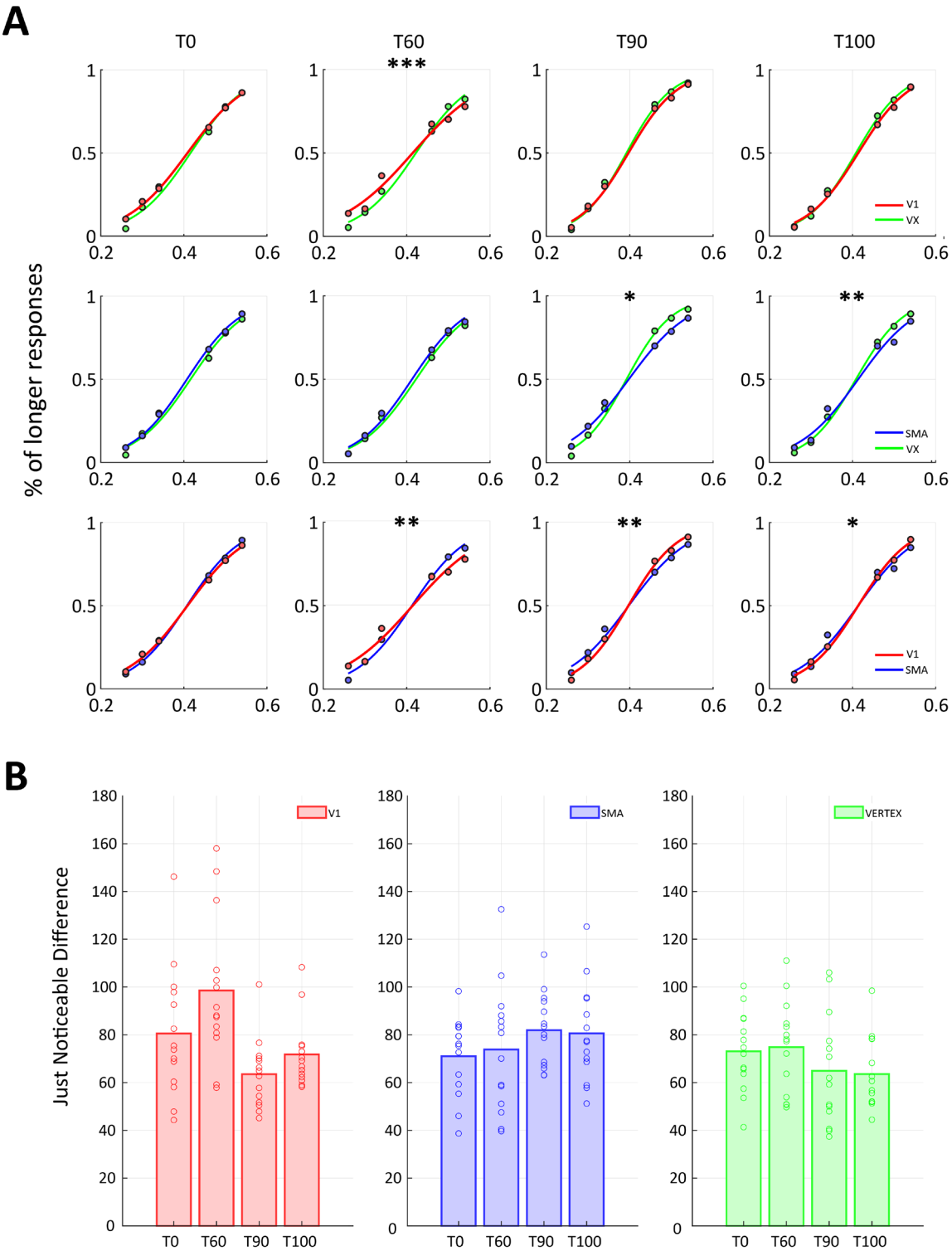

Figure 4.4. A) Group average (N=14) of the psychometric curves . On the x axis are S2 durations , while on the y axis the % of time the S2 has been judged longer than S1. The red line is V1 performance, the blue line SMA performance, the green line is the vertex performance. The plots are organized according to the four timings of stimulation and according to the target area. In the top row there are V1 and the Vertex, in the middle section SMA and the Vertex, and in the bottom row V1 and SMA. **B)** Group average of the Just Noticeable Differences (JND). Single points are single subjects. The plots are organized according to the three different areas, and within a single plot are organized according to the four timings of stimulation.

A	V1 vs SMA	V1 vs VX	SMA vs VX
T0	p=0.1716	p=0.3717	p=0.6367
T60	**p=0.0015****	**p<0.001*****	p=0.8282
T90	**p=0.0015****	p=0.7986	**p=0.0110***
T100	**p=0.0308***	p=0.0551	**p=0.0021****

Table 4.1. T values of paired-sample t test computed on JNDs of different areas (V1, SMA and Vertex (VX)) at the same timing of stimulation. Asterisks symbols represent the results of the paired-sample *t* tests significant at * $p < 0.05$, and ** $p < 0.01$, and *** $p < 0.001$.

The ANOVA revealed a significant main effect of the area ($F(2, 26) = 4.743$, $p=0.018$). Specifically, compared to vertex stimulation, discrimination thresholds were significantly higher following TMS in both V1 ($t(55)= 3.0848$, $p=0.0032$), and SMA ($t(55)= 2.9207$, $p=0.0051$) (V1 mean 78.6019, standard deviation 25.7321 – SMA mean 76.8481, standard deviation 20.1201 – Vertex mean 69.1148, standard deviation 18.8112).

We also observed a significant interaction between area and timing ($F(6, 78) = 8.305$, $p<0.001$). As shown in table 4.1 there was a significant difference between V1, SMA and vertex at specific timings. Specifically, at T60, after V1 TMS (mean 98.5361, standard deviation 30.3300) JNDs were significantly higher compared to SMA (mean 73.8238, standard deviation 26.5561) and Vertex (mean 74.8633, standard deviation 16.4846). At T90, after SMA TMS (mean 81.9072, standard deviation 15.3370) JNDs were significantly higher compared to V1 (mean 63.5427, standard deviation 14.4956) and Vertex (mean 64.9328, standard deviation 22.8264). At T100 after SMA TMS (mean 80.5921, standard deviation 20.3238) JNDs were significantly higher compared to V1 (mean 71.7798, standard deviation 14.3910) and Vertex (mean 63.5742, standard deviation 15.0933).

To better visualize the differences between the different stimulation timings within each area we decided to normalize V1 and SMA JNDs to T0 (Figure 4.5), a stimulation timing where no differences were observed between V1, SMA and the vertex.

As shown in Figure 4.5 leftwards panel, V1 JNDs are worst at T60 compared to all other timings (T60vsT0: $t(13)=2.7$, $p=0.0188$; T60vsT90: $t(13)=6.0$, $p<0.001$; T60vsT100: $t(13)=3.2$, $p=0.0073$). Regarding SMA, JNDs at T90 and T100 are significantly different from T0 (T0vsT90: $t(13)=1.9$, $p=0.0437$; T0vsT100: $t(13)=1.9$, $p=0.0374$). From the visual inspection of Figure 4.5 we can see that most of the subjects show higher JNDs at the timings closer to the offset (T90, T100).

To better visualize the comparisons between SMA and V1 at different timings we decided to normalize the JND of V1 to those of the SMA (Figure 4.6).

In figure 4.6, a positive value indicates a higher JND in V1 than in SMA at a specific timing. A negative value indicates a higher JND in SMA. As before also here we can see that differences between SMA and V1 are at timings T60, T90 and T100 (T60: $t(13)=3.3$, $p=0.0057$; T90: $t(13)=-3.9$, $p=0.0018$; T100: $t(13)=-2.15$, $p=0.0255$).

4.3.2 Point of subjective equality

As for experiment 2, a repeated-measures analysis of variance (ANOVA) conducted on the PSE with area (V1, SMA, Vertex) and timing (T0, T60, T90 and T00) as a within-subject factor showed a significant main effect of timing ($F(3,42)= 8,398$, $p<0.001$). T-tests revealed that, regardless of the area stimulated, the PSE were significantly lower when we stimulated at T90 (mean -0.0069, standard deviation 0.0373) if compared to T0 (mean 0.0259, standard deviation 0.0478), T60 (mean 0.0442, standard deviation 0.0528) and T100 (mean 0.0328, standard deviation 0.0424) (T0vsT60: $t(41)= -3.6699$, $p<0.0001$; T90vsT60: $t(41)= -5.1216$, $p<0.0001$; T0vsT100: $t(41)= -4.6974$, $p<0.0001$). Moreover, PSE were also significantly lower at T0 compared to T60 ($t(41)= -2.4019$, $p= 0.0209$) (Figure 4.7).

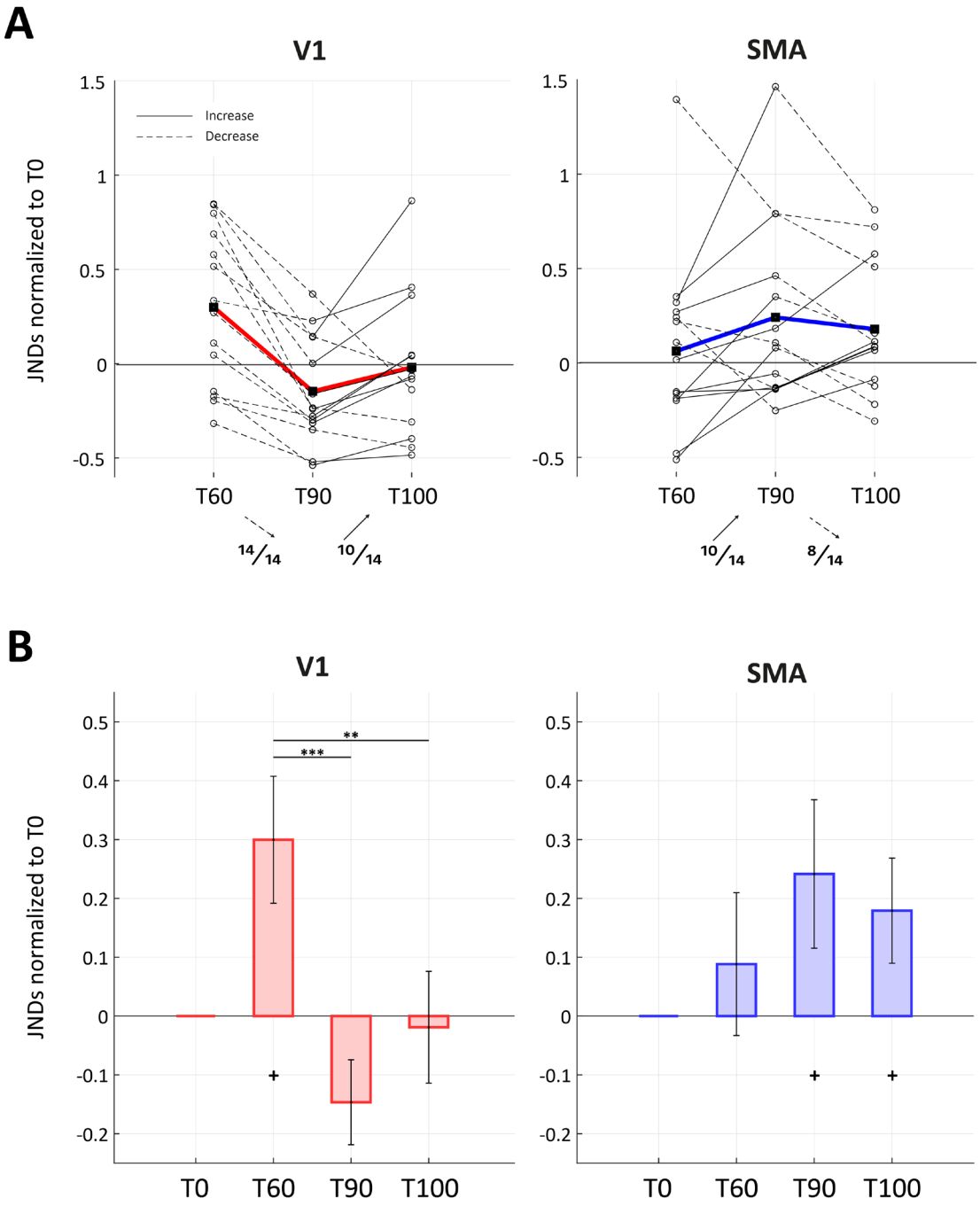

Figure 4.5. **A)** Individual JNDs in left V1 (leftward panel) and in left SMA (rightward panel) normalized to T0. The thinner lines are individual subjects, the thick line is the group average. To better visualize the trend, we used a solid line to identify an increase between two timings and a dashed line to indicate a decrease between two timings. Below the x-axis are summarized the number of subjects (total n = 14) who had an increase or a decrease in JND **B)** Bar plots with the group average JNDs normalized to T0 organized by the two areas and the four different timings. Errorbars are the standard error of the mean. Asterisks symbols represent the results of the paired-sample *t* tests significant at * $p < 0.05$, and ** $p < 0.01$, and *** $p < 0.001$. Plus symbols represent the results of the one-sample *t* tests significant at + $p < 0.05$ – these comparisons represent the difference from T0.

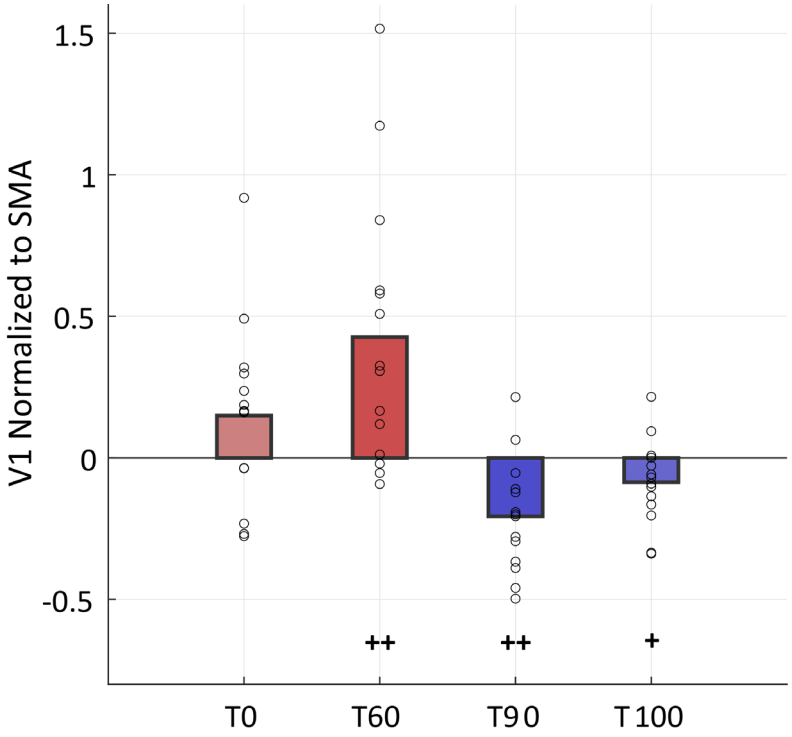

Figure 4.6. JNDs of left V1 normalized to the JNDs of SMA in the same condition (the different circles are individual subjects). In this plot is possible to appreciate that most of the value at T0 and T60 are positive (meaning greater JNDS for V1), while the values at T90 and T100 are mostly negative (meaning greater JNDs for the SMA). Plus symbols represent the results of the one-sample *t* tests significant at + $p < 0.05$ and ++ $p < 0.01$.

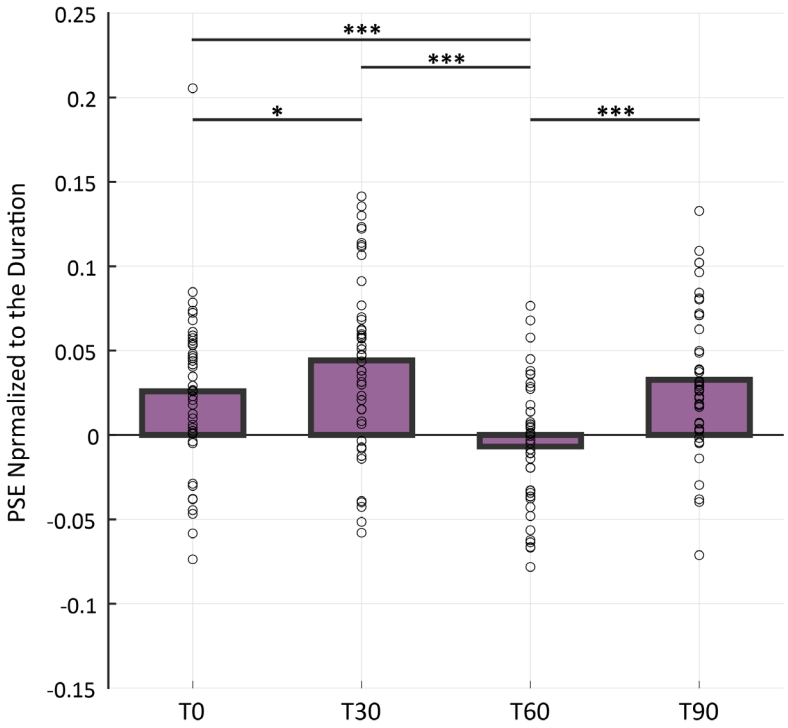

Figure 4.7. Significant effect of TMS timings on PSE. The values of the PSE here are normalized to S1. The PSE are averaged across the stimulation sites (V1, SMA and Vertex) since there is no difference between them. Asterisks symbols represent the results of the paired-sample *t* tests significant at * $p < 0.05$, and ** $p < 0.01$, and *** $p < 0.001$.

4.4 The leaky integrator model

4.4.1 Introduction

As reported in Chapter 3, we hypothesized that the duration perception of a sensory event depends on the integration over time of a sensory drive coming from a sensory region. In formal terms as illustrated in Figure 4.8, our model consists of three instances. The sensory drive, which is a function of time and luminance, the integrator which nonlinearly accumulate the sensory drive over time (the non-linearity is due to τ), and the final percept. Both the sensory drive and the final percept are characterized by a mean (μ) and a variance (σ). At the level of the sensory drive μ and σ depends on the characteristic of the stimulus, while at the level of the final percept they depend on the accumulation process that has taken place.

In an attempt to find the best way to model the effects of TMS, we thought of 4 alternative models; each of these can affect the μ or σ at the level of the sensory drive or final percept. Verifying which of the four competing models best explains the experimental data of V1 and SMA will allow us to answer two fundamental questions.

1. The role of V1 or SMA could alternatively be assimilated to the sensory drive or the final percept. Our hypothesis is that V1 constitutes the sensory drive of the accumulator and that SMA, reading the accumulated value, places itself at the level of the final percept.
2. When we observe significant effects of TMS, we can better describe these effects. Does the TMS affect the mean or the variance? Does the TMS affect the sensory drive or on the final percept?

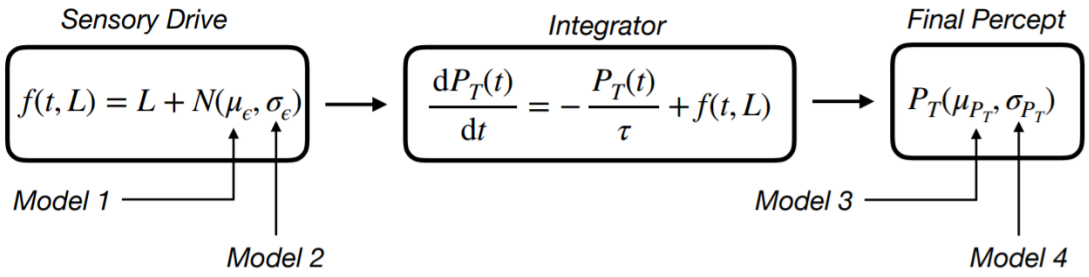

Figure 4.8. Our model consists of three instances: the sensory drive, the accumulator, and the final percept. The 4 different models predict that the TMS affects different parts of the model.

4.4.2 The four competing models

The four competing models can be seen in image 4.7. The four models can initially be grouped according to whether they act on the sensory drive or on the final percept. Regarding the sensory drive:

1 Model 1 posits that the TMS is changing the μ. In other words the μ can increase or decrease thanks to a parameter (positive or negative) that we have called Gain, which is the parameter of the TMS. From a neural point of view, if this model proved to be the best in explaining our data, it would mean that TMS had an excitatory or inhibitory effect on neural activity - leading to effects on the PSE. Since the paradigm we used was inhibitory, we would expect such an effect. In any case, at this point we do not make any assumptions that could influence the process of selecting the winning model.

2 Model 2 posits that the TMS is changing the σ. In other words the σ is multiplied by the Gain, which is the parameter of the TMS. The TMS in this scenario would increase the noise of the signal and would be seen as an injection of noise into the system. This would affect JND.

Regarding the final percept:

3 Model 3 posits that the TMS is changing the μ. TMS is not influencing the accumulator process but the mean of the values that has been accumulated. Again, this model would lead to effects on the PSE.

4 Model 4 posits that the TMS is changing the σ. TMS is not influencing the accumulator process but the variance of the values that has been accumulated. Again, this model would lead to effects on the JND.

We simulated the effects of the TMS of the 4 different models similarly to Chapter 3 to better visualize what effects each stimulation would have at the 4 different timings.

We obtained this graphical representation of the accumulator behavior by running the model on a stimulus of 300ms for 500 times. These simulations can be seen in Picture 4.8. In this image it possible to appreciate how over time the accumulator accumulates the values coming from the sensory drive (blue color). Again, the variance of the final percept increases over time, and the variance at the offset of the stimulus represents and indicator for the performance of the model. When TMS is delivered this process changes according to the model at hand (red color). It is important now to stress that we have set the duration of the effects of TMS at 150ms, based on a electrophysiology study (Moliadze et al., 2005). This is an important assumption and it will be discussed later. I will now describe the behavior of the TMS effects at the four timings according to the model considered. As we said earlier, Model 1 posits an increase or decrease in the sensory drive μ. In the simulation it was rendered with an increase in the μ. This, as can be seen from the Figure 4.9., results in an increase in the slope of the curve. In other words, when the effect of the TMS is present, the overall perceived time grows over time and this increase is reflected on the greater slope of the integrator. The effect of TMS would be the opposite with a negative Gain. Model 2 posits an increase in the sensory drive σ. As it possible to

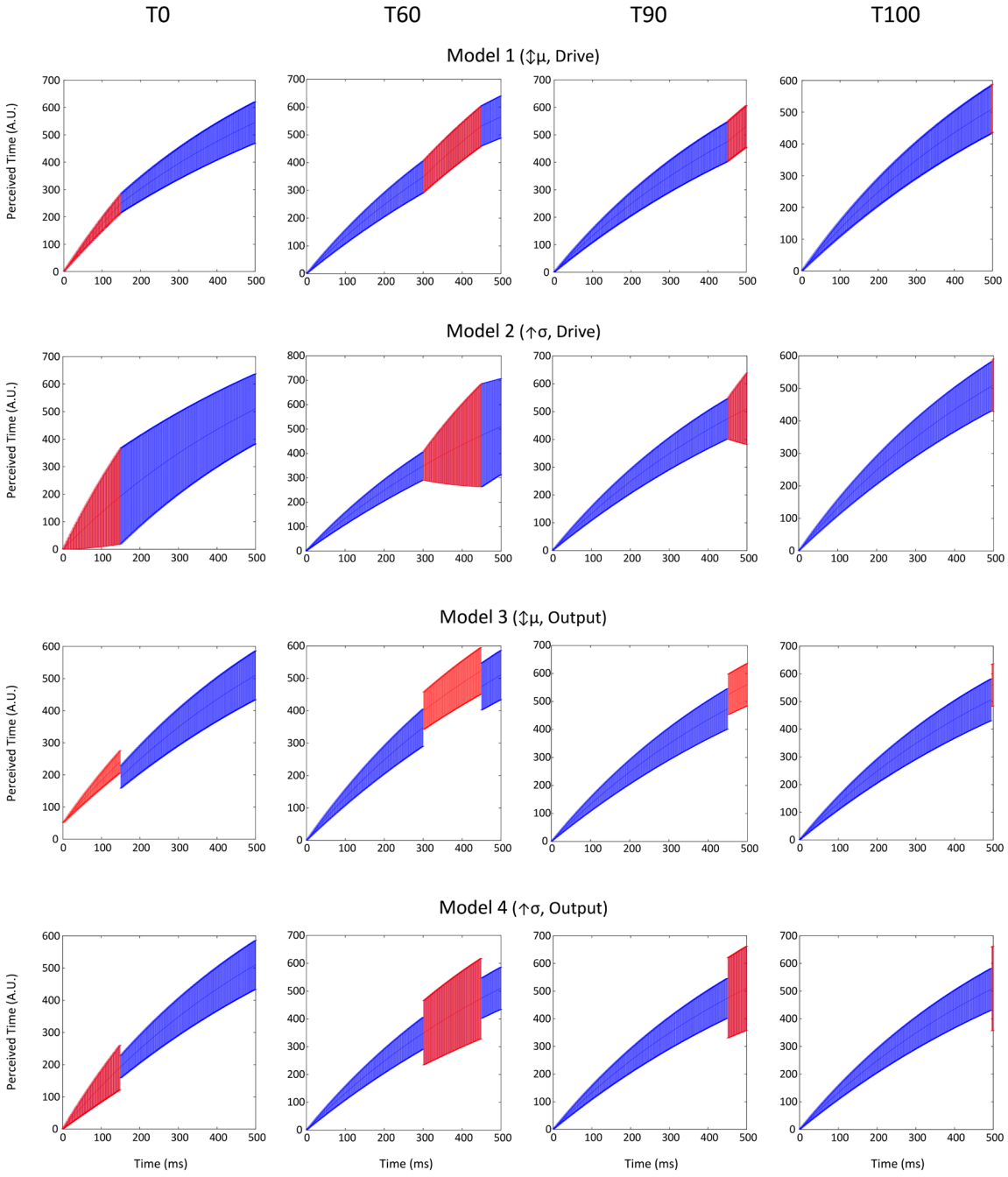

Figure 4.9. Simulations of the 4 possible models at the four possible timings. The blue part represents the normal accumulation, the red part the time window where the effect of the TMS is present.

appreciate from Figure 4.9, when the effect of the TMS is on the accumulator accumulate the incremented noise

from the input, and this led to an overall increase of the variability of the perceived time. The interesting part is that after the 150ms effect of the TMS, the overall variability tends

to decrease, and how quickly the variability returns to baseline depends on τ. The lower the τ, the faster the system "forgets" the noise of the TMS. On the contrary, the higher the τ, the more the system tends to maintain the noise of the TMS (see fitting part, later). This characteristic of the model lead to interesting effects: as it is possible to see from Figure 4.9, the variability at the offset is greater for T60 than T0, and that is because when the TMS is delivered at T0 the model has more time to forget the increased noise that was accumulated. On the other hand, T60 variability at the offset is also greater than the variability at T90, and that is because the model at this point has no time to accumulate the increase noise. The same idea can be applied to T100, when there is literally no time left to accumulate the noise. Overall, in model 2 the timing that led to the larger increase on the variability of the final percept results T60.

Model 3 posits an increase or decrease in the final percept μ. At this point we switch from the models that act on the sensory drive on the models that act on the final percept. The interesting feature of this pair of models is that it is not crucial what happened during the accumulation process, because at the level of the final percept the TMS is not changing the integration, but what has already been integrated. Also the non-linearities given by the μ disappears. What is really crucial is that the effect of the TMS (again, lasting 150ms) “survives” until the offset of the stimulus. Back to Model 3, it is possible to see that the TMS increase the mean of the curve but, since this change is not accumulated, it goes back to baseline as soon the TMS effect is over. Again it is necessary to stress in this model the Gain can increase or decrease the μ of the final percept, even if in the simulation we posit an increase of the μ. Again, the only thing that seems to be important is that the TMS effect is on at the offset. From a more practical point of view, the TMS effect has to be present when the read-out at the offset happens.

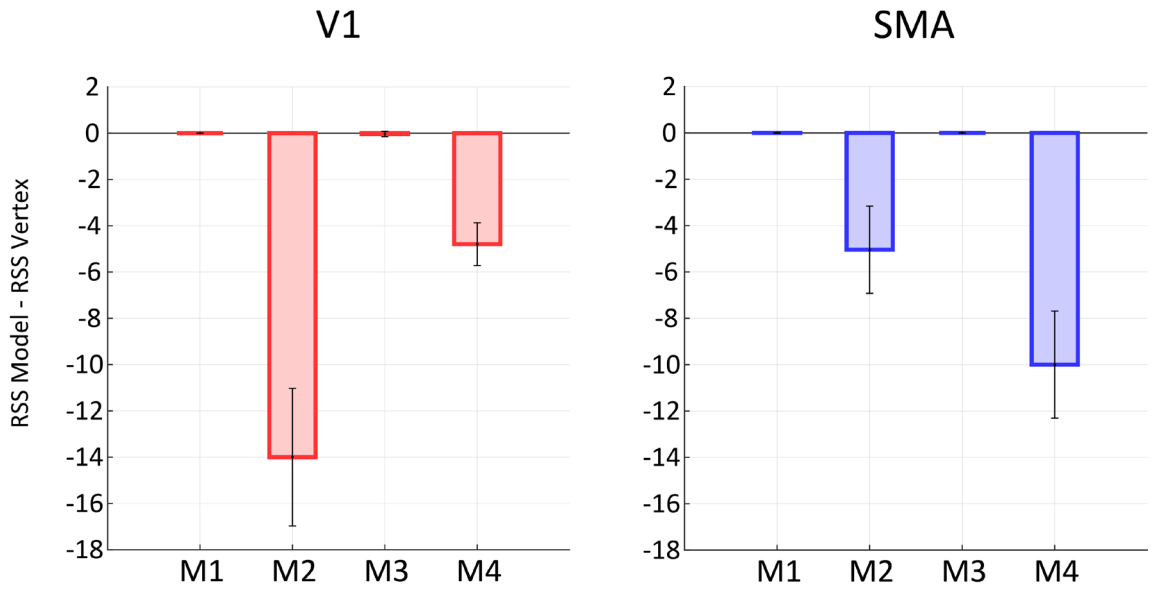

Figure 4.10. Plot of the residuals in the 4 models (M) for both V1 and SMA. The best model for V1 is model 2, the best one for SMA is model 4. The successful models are those that posit an increase of the variance (σ) of the neural noise (M2 and M4)

The same logic applies to Model 4, which posit an increase of the final percept σ. Here the gain changes the variance of the final percept.

For the Model 3 and 4 it is important to stress that another assumption that we are making is that the offset matches the supposed read-out. Another assumption that follows this is that after the offset the integration is over. As we will discuss later, this could not be the case.

4.4.3 Fitting procedure

Similarly to chapter 2, we fitted the parameters from the Vertex condition. Fitting the parameters from a dataset other than the experimental one allows us to avoid overfitting. So we considered the vertex as a condition with no effects of TMS. For every trial we can calculate the expected perceived time for S1 and S2 and its variance. From this we can calculate the probability of having the subjected reporting T2>T1, therefore we can fit psychometric curves. From this procedure we obtained the best parameters that matched our data in the Vertex condition. The parameters are the

lapses, the τ, and the σ noise (baseline noise), considering the μ noise in the absence of TMS as equal to 0.

In other words, we assumed that $\mathrm{Var}[\Upsilon(0)]$ and μ_b are always equal to zero, the target function that guides the parameter fits was the least squared difference between the observed fraction of choices Stimulus 2 > Stimulus1 and the model predicted choice probability for each T1 and T2 pair.

The reported fitted parameters values were obtained by using lsqcurvefit MATLAB function. We then fixed the values of σ_b^2, τ, α, $\mathrm{p_{high}}$ and $\mathrm{p_{low}}$, and fitted the behavioral data from the three stimulation conditions (T0, T60, T90 and T100) in parallel using the MATLAB fmincon function, with a single free parameter k. The target function that guides the parameter fits was the least squared difference between the observed fraction of choices Stimulus 2 > Stimulus1 and the model predicted choice probability (Equation 17) for each T1 and T2 pair.

It is important to note at this point that the only free parameter used to fit the V1 and SMA curves is the TMS gain.

4.4.4 Models selection

We fitted all the possible models separately for V1 and SMA. We evaluated every model quantifying the square residuals from the model minus the square residual from the condition where we supposed there are no TMS effects (the vertex). In other words, we are quantifying how much the residuals of adding the gain parameters decrease compared to the vertex condition. In Figure 4.10 the more negative is the value, the more the model is better in explained the TMS effects compared to the vertex.

As it is possible to notice, Model 2 and Model 4 are the one that better explained the data. Both the models are the one that posit an increase of the variance (σ), the first at the level of the sensory drive, the latter at the level of the final percept.

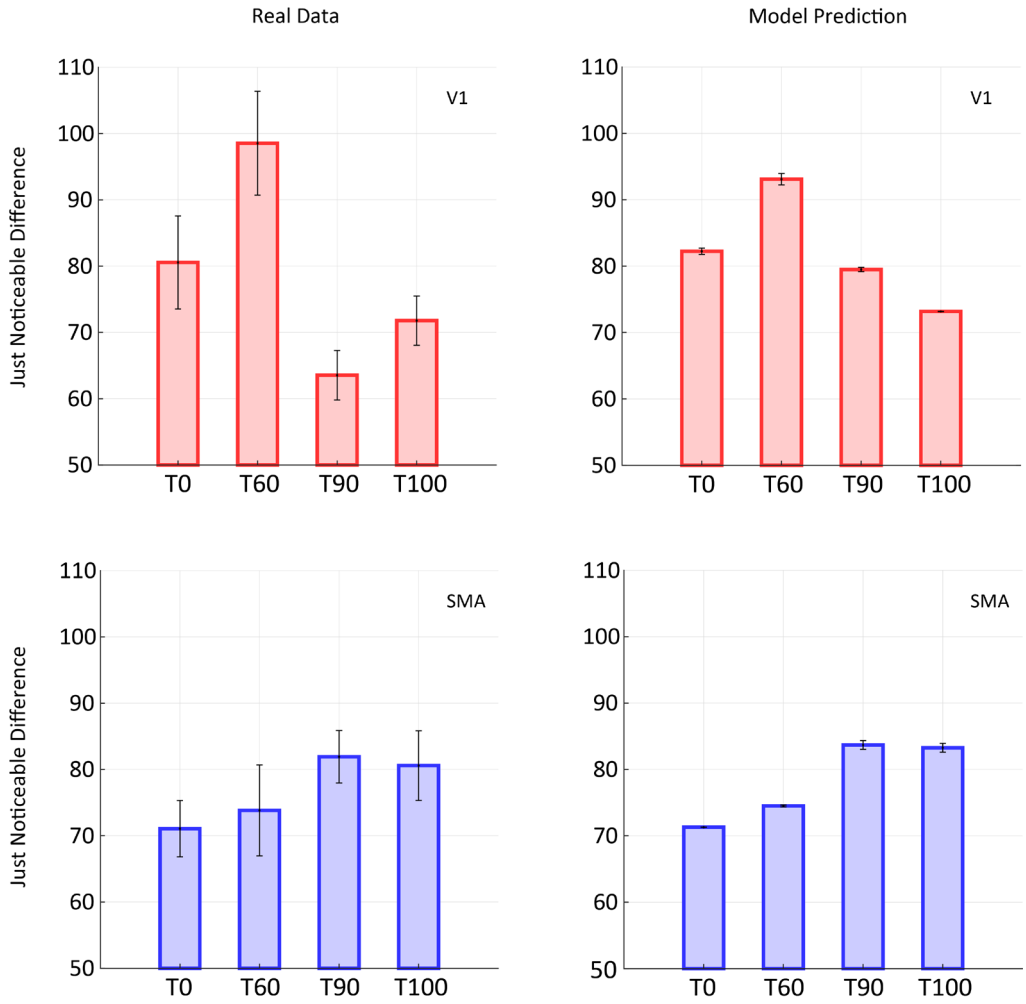

Figure 4.11. JNDs of real data and model predictions for V1 (upper plots) and SMA (lower plots) organized by the four different timings of stimulation.

More specifically, V1 data seems to be better explained by Model 2 (increase of σ at the level of the sensory drive), while SMA data seems to be better explained by Model 4 (increase of σ at the level of the final percept). I will present the output of the models of these 2 models.

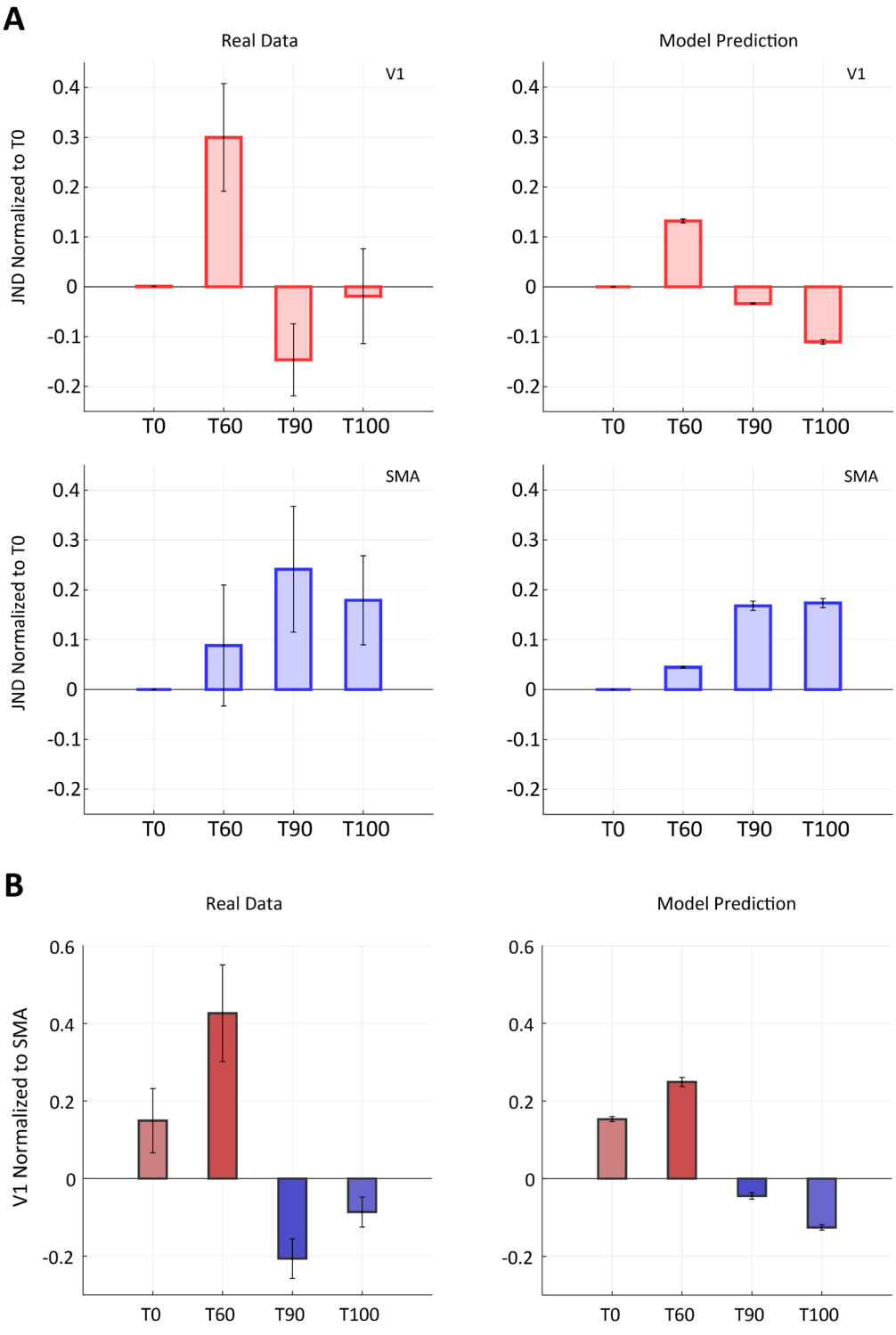

Figure 4.12. **Panel A**. JND normalized to T0 for V1 (upper part) and SMA (lover part) both for the real data (left part) and the model prediction (right part). **Panel B**. V1 JND normalized to SMA. The bars are colour coded. Red for V1 (positive bars) or blue for SMA (negative bars).

4.5 Discussion

Our data showed that TMS delivered on both V1 and SMA had a significant effect compared to the vertex stimulation. This is the lowest level of evidence we can find, but nevertheless it is an important control. It indicates that V1 and SMA are – somehow – involved in the encoding of the duration of a stimulus.

Furthermore, we have shown that the effects of TMS on V1 and SMA compared with the vertex are isolated only at specific timings of stimulation. Speaking of V1, the effects are isolated at T60, while for SMA they are isolated at T90 and T100.

This is a slightly higher level of evidence than the previous one. Not only is it important *where* we stimulate (V1 and V5/MT, but not the Vertex), but also *when* we stimulate (specific timings). For an experiment that aims to study chronometry, this is an essential control.

The next level of analysis is represented by the comparison between the different timings within the same area. This is an important control because, again, it tells even if we are stimulating the same area (either V1 or SMA), the different timings of stimulations lead to different effects. As for V1, the most effective stimulation is again T60. Regarding SMA, the T90 and T100 timing of stimulation lead to greater JND if compared to T0.

Finally, the most important evidence is given by the comparison between the two experimental areas (V1 and SMA) at the same timing of stimulation - and this represents the most important control because it can tell us that the two areas really show a different chronometry. The two areas are significantly different at T60 and T90, with higher JND for V1 at T60 and higher JND for SMA at T90.

These results already suggest that our hypothesis may be correct. V1 shows relatively early effects (at T60). Nevertheless, we replicated the results of Experiment 2. At the same time SMA, whose chronometry had never been tested, shows late effects, consistent with the view that this area may be involved in a higher level in the hierarchy.

Despite this, we tried to go further by trying to model these data. As I said earlier, the two outstanding questions we can try to answer by applying the model designed by Toso et al. (2021) adapted for my experiment are:

1. Are the effects observed on V1 compatible with the view that V1 constitutes the drive of an accumulator? Are the effects observed on SMA compatible with the view that SMA constitutes the read-out?
2. What kind of effect the TMS had?

We tried to answer these questions by considering four different models. As we have seen, the model that best explains the data of V1 is model 2 (increase of σ at the sensory drive level), while the model that best explains the SMA data is model 4 (increase of σ at the level of perception the final).

As we can see from Figure 4.12 (Panel A), the behavior of the experimental data seems similar to the one of the models. The only difference that can be appreciated is that V1 at T90 is supposed to have slighter higher JND that at T100, according to the model – while in our data the pattern is the opposite. This difference can be explained in two ways.

1 Experimental data are noisy. We did not expect a perfect match between real data and the output of the model. More specifically, the timing of stimulation at T90 and T100 are really close (40ms apart), and maybe in our experiment we were not able to obtain clear differential effects for these two very close timing of stimulation.
2 We assume that only one mechanism is in place (the one described by the model), but since the offset is special, perhaps some other mechanism is in place (perhaps a rebound top-down effect from higher level areas to V1 at the offset).

Despite this the experimental data correspond well with the model output. This can also be observed in Figure 4.12, where we presented the JNDs normalized to T0 (Panel A), and the JNDs of V1 normalized to that of SMA (Panel B). These figures help visualize the effects at the individual subject level. Again, we can appreciate that the

effects are similar, despite an overestimation of the real data from V1 to T60 (or an underestimation of the model).

Overall, these results suggests that the effects observed on V1 are compatible with the effects we would observe if we would interfere with the drive of the accumulator, while the effects we observed on SMA are compatible with the effects we would observe if we would interfere with an area responsible of the read out.

Moreover, both effects are compatible with the idea that TMS increases the neural noise (either at the level of the sensory drive or at the final percept level). This is confirmed at the experimental level by the fact that our main finding is on the JNDs. The effect on the PSE is we found do not depend on the stimulated area (V1, SMA or the Vertex) – similarly to experiment 2 these effects are probably caused by some feature of the TMS stimulation, even if at this point we are not able to explain which. The fact that the TMS at critical timings influence the variance and not the mean is further interesting. Although we had chosen an inhibitory paradigm, the observed effect was not of this nature.

Finally, it is good practice to consider some limitations of our model, assuming that more work may be needed.

First and foremost, the idea that following the delivery of TMS pulses, the effects are constant for 150ms, is an approximation from an electrophysiological point of view. A further step that perhaps can be considered is the idea of modeling the effects of TMS within the 150ms time window based on electrophysiology data from Moliadze et al., (2005), or from other relevant literature.

Furthermore, the offset is also a problem. First of all because, in order to explain the encoding phase, we have assumed that the model stops at the offset. This is due to the assumption that the time reading (the read-out) occurs exactly at the offset. Obviously, this is also a strong assumption. If the read-out occurs with some delay with respect to the stimulus offset, this cannot be explained by my experiment or by the model we have adapted.

Finally, although not strictly a limitation of the model, if the effects of V1 are attributable to the effects on the sensory drive of the accumulator, further research, both animal and human, is necessary to explain where this accumulator may be.

Now that we have demonstrated that V1 and SMA have different chronometry when encoding durations, in the next chapter I will try to further characterize the functional organization of SMA during this process, assuming that this area acts as a read-out.

CHAPTER 5: THE CAUSAL CONTRIBUTION OF SUPPLEMENTARY MOTOR AREA IN THE REPRESENTATION OF DIFFERENT DURATIONS

Abstract

- The precise estimation of time is critical for our everyday life activities. Appreciating and playing music, for example, requires the very rapid processing of multiple durations. How the human brain represents multiple durations is unclear (Paton & Buonomano, 2018). A very recent study shows that visual durations ranging from a few hundreds of milliseconds to a few seconds are represented in the human supplementary motor area (SMA) and this representation is topographically organized i.e., stimuli that have similar durations engage the activity of neighboring locations on the cortical surface (Protopapa et al., 2019). Shorter durations are represented in the anterior SMA, longer durations in its posterior part.
- In the current study, we applied paired-pulse transcranial magnetic stimulation (ppTMS) to the left SMA to investigate the causal contribution of this area in durations representation and to prove the existence of chronomaps.
- 20 healthy volunteers were asked to perform a temporal discrimination task of visual stimuli of different durations (ranging from 0.2 to 1.5 s) while TMS was applied to either the anterior or the posterior left SMA. If a chronomap exists in SMA and it has an anterior to posterior orientation for short to long duration

respectively, we expected a worsening of performance accuracy in the shorter durations range after stimulation of the anterior SMA and of the longer durations after TMS of the posterior SMA.

- Results show that SMA is causally involved in the temporal discrimination task as participants performed significantly worse in TMS blocks compared to the non-TMS condition. Unexpectedly, we found that independently from the tested durations, participants' performance was worse after the stimulation of the anterior SMA compared to the stimulation of posterior part. However, after TMS of the anterior SMA the discrimination accuracy was worst for the shortest compared to the longest durations of the range.
- Overall our results suggest that the posterior edge of SMA is less involved in the processing of short durations compared to the anterior part. These findings partially support the existence of a duration map in SMA.

5.1 Introduction

We live in a dynamic world in which we must adapt to quickly changing events or anticipate them. Within this ever-changing perceptual world, a fundamental part of information is given by the temporal structure of sensory events that our brain has to process and understand.

To achieve this, the brain has evolved functions that operate across a wide range of temporal scales. In higher part of the duration spectrum, our brain can deploy various time tracking systems: from the circadian system in the brain's suprachiasmatic nuclei (SCN) that uses the daily variations in light to calibrate our circadian clock to the subsidiary clocks contained in nearly every body cell and that are influenced by the SCN via neuronal and humoral cues, our nervous system can be seen as a timekeeper machine (Dibneret al., 2009).

On the other side of the spectrum – within the seconds/milliseconds range, our brain is a timekeeper for example, it is able to localize sound sources by detecting the

microsecond difference between the time of arrival of the sound to the left or the right ear (Zwislocki & Feldman, 1956, Brand et al., 2002). More generally, our brain is able to make sense from sensory events which differ by only a few tens of milliseconds while it continuously generate complex temporal patters to perceive the passage of time (Paton & Buonomano, 2018).

In this sense, most of our everyday behavior needs a precise timing in the scale of hundreds of milliseconds to a few seconds, such as performing any kind of sports (Merchant & Georgopoulos, 2006), communication (Diehl et al., 2004) and playing an instrument or appreciating music (Janata & Grafton, 2003). While there are dedicated biological systems for seeing, hearing, and tasting, there is no specific organ that senses time and it is less clear which brain areas or circuits are involved in perceiving, estimating, or reproducing durations in the range of hundreds of milliseconds to few seconds.

Various theoretical models have been proposed to account for the brain's ability to keep track of time. At one extreme there is the "pacemaker accumulator model" which hypothesizes the existence of a dedicated, clock-like neural mechanism to explain our perception of time (Treisman, 1963; Gibbon et al., 1984; Ivry & Schlerf, 2008).

At the other extreme, the "State Dependent Network model" proposes that neural circuits encode time intrinsically, without the need for a specialized system, suggesting a distributed representation of time in terms of neural-network states (Karmarkar & Buonomano, 2007). In other words, this model posits that time computations can be performed locally by neurons and cortical circuits have timing ability in the hundreds of milliseconds.

Finally, Merchant and colleagues (Merchant et al., 2013a) have put forward an intermediate hypothesis which suggests a partially distributed timing mechanism; time processing would begin in each sensory domain, and later it would be integrated by core structures such as the cortico-thalamic-basal ganglia (CTBG), the dorsolateral prefrontal cortex (dlPFC), the supplementary motor area (SMA) and the cerebellum (Bueti et al., 2008c; Coull et al., 2011; Merchant et al., 2013a).

Multiple brain areas have been associated to temporal computations. Some of those areas play a content-free and supramodal role in time perception, e.g. basal ganglia and cerebellum (Coull et al., 2011). Others are involved in more specific timing tasks, e.g. the parietal cortex in perceptual and motor timing (Bueti et al., 2008c). Furthermore, while the activity in some of these areas seems to depend on the presented duration time (millisecond- vs second-long intervals), others are less specific (Lewis & Miall, 2003, Hayashi et al., 2014).

These findings suggest that core structures of coordinated neural timing networks are flexibly involved in different timing tasks (Wiener et al., 2011; Merchant et al., 2013a). Still, the neuronal mechanisms and computations underlying our capacity to perceive time remain largely unknown.

5.1.1 Duration tuned neurons

During dancing, motor activity is synchronized with auditory information (Janata & Grafton, 2003). This phenomenon has been studied in the laboratory using the synchronization-continuation task (SCT), in which subjects have to press a button in time with stimuli presented at a fixed interstimulus interval. Subjects then have to maintain the same button press interval but without stimulus presentation (Repp & Su, 2013). Using this task during single-cell recordings in monkeys, Merchant et al., (2013b) found a large population of cells in medial premotor areas that is tuned to different durations, i.e. they respond preferentially to a specific interval duration, covering the whole range of intervals in the hundreds of milliseconds domain.

Duration-selective cells have also been found in cats' early visual and auditory cortices (Duysens et al., 1996) and in monkeys' cortico-basal ganglia circuits (Jin, Fujii, & Graybiel, 2009).

In humans, it is more difficult to analyze the behavior of single neurons. Nevertheless, psychophysical studies suggest a duration-tuning behavior analogous to the orientation selective cells in V1 also in the human brain (Becker & Rasmussen, 2007, Roach et al., 2011).

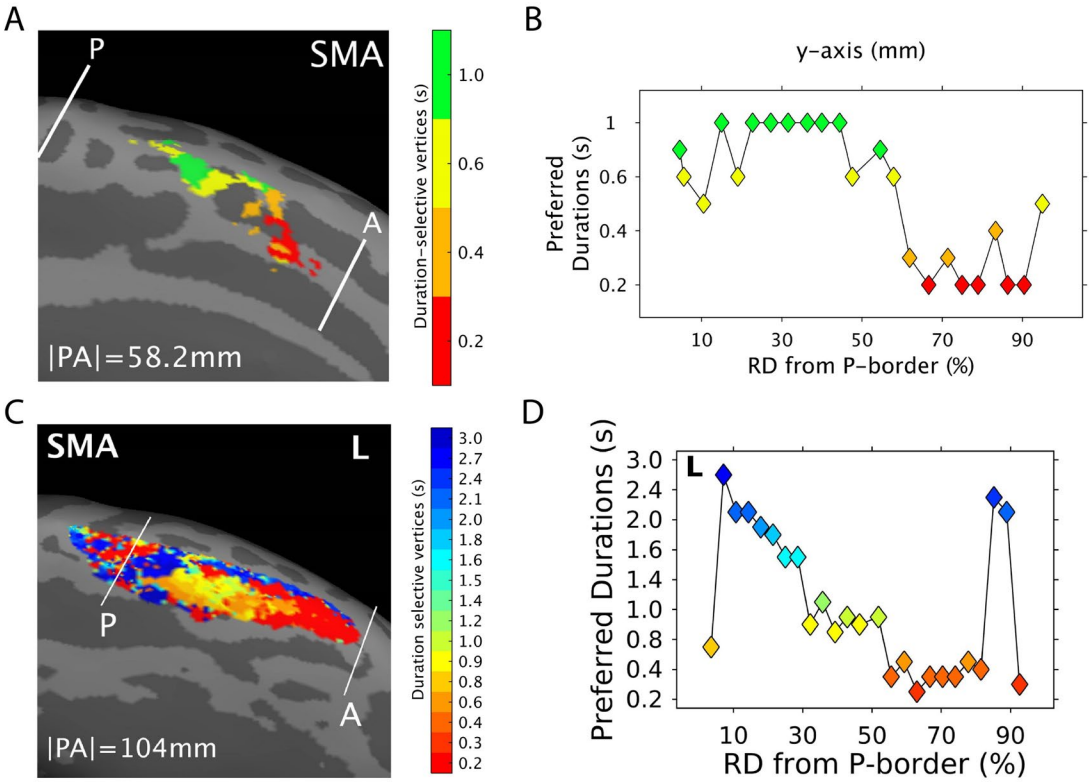

Figure 5.1. Chronomaps in the SMA. A) Vertices (voxels projected onto the cortical surface) that were responsive to the different durations in Experiment 1 (A) and Experiment 2 (C) of the original Protopapa et al. 2019 study. Warmer colors are shorter durations, colder colors longer durations of the tested range, B-D preferred durations of different clusters of voxels laying at different distances from the posterior (P) border. In both experiments the clusters closer to the posterior border prefer longer durations. Reproduced from Protopapa et al., 2019.

In previous psychophysical studies it has been shown that the repeated presentation of auditory or visual events of a given duration (adaptation) influences the perceived duration of a subsequent stimulus. Those so-called after-effects are stronger if the durations of adapting and test stimuli have an optimal temporal distance and decay if adapting and test stimuli are sufficiently different, suggesting a temporal tuning profile (Roach et al., 2011). Hayashi et al. (2015) tried to identify brain areas that show an explicit representation of different stimulus durations by using functional magnetic resonance imaging (fMRI) adaptation. An identical stimulus feature shown multiple times (adaptation) decreases the BOLD signal of the neural population coding this repeated stimulus feature because cortical neurons tend to reduce their activity upon stimulus repetition (Krekelberg et al., 2006, Grill-Spector et al., 2006, Malach, 2012)

The authors hypothesize that the human inferior parietal lobule (IPL) hosts duration-tuned neurons responsive to specific preferred time intervals of a few hundreds of milliseconds.

5.1.2 The chronomap in SMA

Neurons tuned to specific features are commonly topographically organized in the sensory cortices of the brain (Hubel & Wiesel, 1962, DeCharms & Zador, 2000).

A recent fMRI study investigated whether neurons that prefer a certain stimulus duration are represented chronotopically (Protopapa et al., 2019).

Neurons represented in a chronomap, as Protopapa et al. (2019) call it, show a correlation between their spatial progression in SMA (anterior to posterior) and their duration preferences (short vs long). In this experiment, participants performed a temporal discrimination task: two Gabor patches were presented sequentially with varying duration and participants judged which of the two was presented for longer time. Voxels showing a preference for longer durations were located in posterior SMA and those sensitive to shorter durations in the anterior part (see Fig 2a, c). The activity in duration selective voxels was enhanced for the preferred duration and decayed for durations far from the preferred one, showing neural tuning. Chronomaps were identified in two different datasets with different standard durations (0.2-1 s and 0.2-3 s). The size of the map increased with a larger duration range (Figure 5.1, Panel C) s (Protopapa et al., 2019).

The authors concluded that the SMA plays a functional role in temporal processing: they hypothesized that temporal information is first encoded by low-level sensory regions, then organized in an intermediate stage in parietal regions (e.g., IPL) and finally passed to the SMA where the temporal signals is recognized/read-out. At this later stage of duration encoding the information about the whole duration becomes available.

5.1.3 Aim of the study

Duration-tuned cells in the premotor areas have been reported in monkeys (Merchant et al., 2013b). These findings have now been extended to humans. Protopapa et al. (2019) demonstrated a chronotopic arrangement for the first time in the human SMA and showed duration-selective cells that are organized along the anterior-to-posterior axis and that are active in a temporal perceptual task. Using functional brain imaging they found evidence for changes in neural activity in SMA while the participants encoded different durations. However, neuroimaging or single-cell recordings are correlative approaches from which we can infer associations between the visualized neural activity and behavioral or cognitive functions (Sack et al., 2006).

In the current study, we want to extend Protopapa's findings with the use of transcranial magnetic stimulation (TMS) over SMA. This non-invasive brain stimulation technique allows for a controlled manipulation of a brain region's activity which results in a changed performance (e.g., worsening of accuracy). If the interferences have an impact on the participant's behavior, we can conclude that the stimulated brain region is causally involved in, or functionally relevant for, the measured behavior or a particular cognitive function (Walsh & Cowey, 2000, Paus, 2005, Ridding & Rothwell, 2007). TMS is a useful method for our experiment due to its high spatial and temporal resolution which depend on several parameters. As explained below, the TMS protocol used in the experiment is suitable for the aim of our experiment: revealing a causal relationship between duration-tuned neurons and the behavior in judging the durations of stimuli.

5.1.4 Spatial resolution of TMS

The spatial resolution of TMS depends on several parameters, including the size, shape and orientation of the coil, the stimulation intensity and frequency, the physical properties of the targeted region and a probable interaction of those factors (Hartwigsen et al., 2010, Miniussi et al., 2012). The most commonly used coil in cognitive neuroscience studies is the figure-of-eight coil which consists of two round coils placed next to each other with current flow in opposite direction (Ueno et al.,

1988). The induced electrical field is more focal compared to a round coil and it peaks directly underneath the intersection of the two wings of the figure-of-eight coil (Vincent Walsh & Cowey, 2000). Still, the strength of the induced electric field of single-pulse TMS decreases exponentially with increasing distance from the 'hot spot' (Meister et al., 2003).

Some studies report differences in focality (e.g. 1-2 cm^2 on cortical surface; (Thielscher & Kammer, 2004) (Hartwigsen et al., 2010), and depth (e.g. 2-6 cm; Hartwigsen et al., 2010)) of the induced electric fields which can be explained by the differences in the experimental setup. A stimulation study compared 50 coil designs and concluded that the figure-of-eight coils set the best depth-focality tradeoff (Deng et al., 2014). Coils with smaller dimensions generate an electric field that is more focal but also more superficial (Klomjai et al., 2015; Deng et al., 2013).

Furthermore, inter-subject variability in TMS-induced responses correlates to differences in coil-to-cortex distance (McConnell et al., 2001). This is one of the reasons why the stimulation intensity used in our study is personalized to each subject. The distance between the pre-SMA which was covered by the chronomap (Protopapa et al., 2019) and the scalp was measured as 10.9 (+-4.8) mm. Thus, the coil used in our experiment reaches deep enough to stimulate the SMA effectively. Studies successfully stimulated scalp sites 1.5 (Schluter et al., 1998) or even 1 cm (Brasil-Neto et al., 1992). In our experiment, we stimulated two points lying 1.5 cm apart with a figure-of-eight coil of 40mm of diameter.

In summary, the spatial and temporal resolution of TMS is precise enough to enable the investigation of fundamental questions in cognitive neuroscience.

5.1.5 Paired-pulse TMS and short-interval cortical inhibition

The behavioral effects that follow TMS stimulation depend on the task context and the method of stimulation (Wiener, 2014). Most paradigms investigating the role of different areas in time perception used repetitive TMS (rTMS) which delivers TMS pulses in a certain frequency over a certain period of time. In our task, we need a high temporal resolution and a strong inhibiting effect. Paired-pulse TMS (ppTMS) has a

larger effect than single-pulse and still allows a reasonable temporal resolution defined by the temporal distance between the two pulses (Pascual-Leone & Walsh, 2001; Silvanto et al., 2005). At rest a single-pulse stimulation over the primary motor area (M1) evokes a contraction of the stimulated muscle. The intensity needed to elicit a response depends on each person's cortical excitability and is called the resting motor threshold (RMT). In a ppTMS paradigm two pulses are delivered at the same cortical location. The RMT can be suppressed or facilitated relative to a single-pulse stimulation, depending on the interstimulus interval (ISI), i.e. the duration between the two pulses, and the intensity of each pulse (Kujirai et al., 1993; Di Lazzaro et al., 2006). Inhibition happens when the conditioning stimulus (CS, i.e., the first pulse of the pair) has an intensity lower than RMT is followed by a supra threshold test stimulus (TS) (Ziemann et al., 1998). The subthreshold CS inhibits the descending corticospinal activity evoked by the TS but is too low to evoke volleys when delivered alone (Di Lazzaro et al., 1998). This procedure leads to a short-interval intracortical inhibition (SICI) which is needed in our experiment. Similar to Protopapa et al. (2019) our subjects performed a temporal discrimination task with five different standard durations (0.2, 0.4, 0.75, 1.1, 1.5 s) and had to judge whether the standard duration or its comparison was longer. The details of the task will be presented later in the Chapter. We wanted to stimulate the SMA exactly at the offset of the standard duration because this was the moment when the whole duration became available to participants (Protopapa et al., 2019) and because the timings of stimulation close to the offset were revealed to be effective based on the results of Experiment 3. With the procedure of SICI we wanted to inhibit the anterior or the posterior part of the SMA, i.e., the edges of the chronomap. We hypothesized a drop of the participant's performance in identifying longer durations when the posterior SMA was stimulated. Stimulating the anterior SMA should lead to an impaired accuracy for shorter durations.

5.2 Materials and methods

5.2.1 Subjects

20 volunteers (10 females, mean age: 25.6 years, range: 19-45 years) participated in the study. All participants had normal or corrected-to-normal vision with no history of neurological or psychiatric disorders. All participants gave written informed consent. The experimental protocol was approved by Ethics Committee of SISSA.

5.2.2 Stimuli and experimental procedure

All participants had to perform two temporal discrimination tasks. Subjects were asked to discriminate a standard (of fixed duration) from a comparison stimulus (varying in duration) The tasks differed in the way comparison duration was chosen. In the first task, we used an *adaptive procedure* to identify for each individual subject, the value of the comparison duration leading to 79% accuracy (individual Weber fraction, WB). In the second task, we used the method of the constant stimuli, in which the constant steps used to generate the comparison durations were chosen based on individual WB. The latter was the main task of the study. In both tasks participants had to judge which one of two stimuli lasted longer (first or second). The stimuli were light blue disks (rgb: [65 105 225], diameter: 112 px, subtending 3° of visual angle at a 60cm) presented at the center of the screen (resolution: 1680 x 1050 px, refresh rate: 120 Hz). A white fixation cross was continuously displayed for the entire duration of the trial (size: 16 px, subtending 0.43° of visual angle at a 60cm viewing distance). Each trial consisted of two stimuli (standard and comparison duration), separated by the interstimulus interval (ISI), a random value taken from a uniform distribution ranging from 0.9 to 1.2 s (Salvioni et al., 2013).

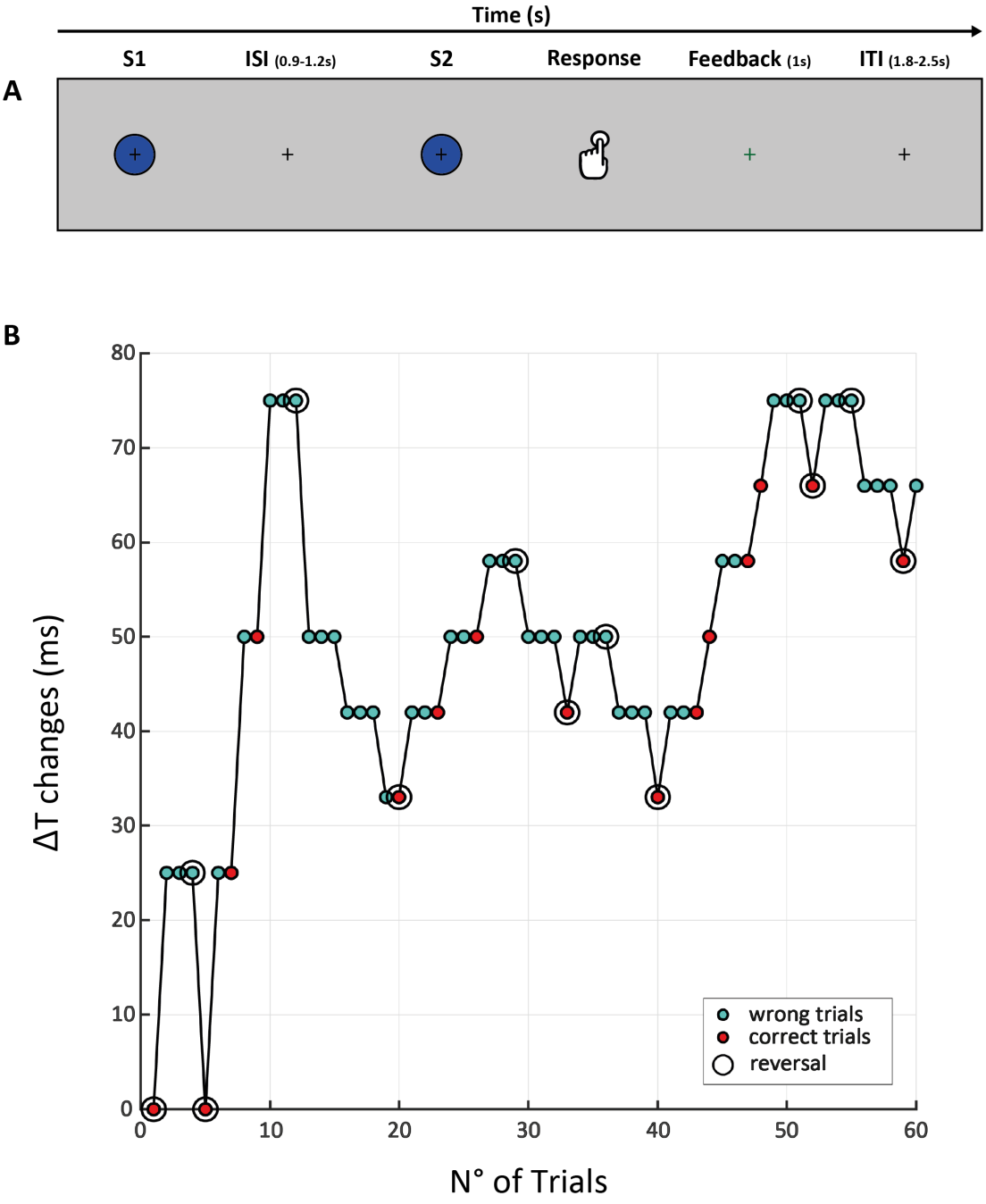

Figure 5.2. Adaptive Procedure. **A)** Schematic representation of a trial in the adaptive procedure. **B)** Representation of the ΔT changes during a block of the adaptive procedure following a transformed up-down staircase. The Weber Fraction was calculated as the mean of the reversals. The first 4 reversals were excluded because participants tend to become more stable after a few trials. Up to the 4th reversal the stimulus changed with a bigger step size (25 ms), afterwards with a step size of 8 ms.

5.2.3 Adaptive procedure

Each participant performed at least twice the adaptive procedure (Fig 5.2) with 60 trials each, after a training with 20 trials. The "standard duration" (S1) was fixed to 300 ms while the "comparison duration" (S2) was the standard plus a positive ΔT value that was changing based on the participant's response (S2 = S1 + ΔT). Standard and comparison stimuli presentation was randomized and counterbalanced across trials, i.e. in half of the trials the standard was presented first, in the other half the comparison. After the participant pressed one of two keys on the keyboard, indicating which stimulus lasted longer (1 or 2), a visual feedback was provided after each trial: the fixation cross turned green if the response was correct and red if the response was incorrect. The duration of the feedback was set to 1 s. Other studies suggested that feedback helps participants to set an internal discrimination criterion and influences the discrimination accuracy (Droit-Volet & Izaute, 2005; Salvioni et al., 2013)

The intertrial interval (ITI), i.e. the time between the feedback offset and the presentation of the next stimulus, was a random value taken from the interval 1.8 - 2.5 s (Salvioni et al., 2013)

The Weber fraction (WF) is a psychophysical estimate of subjective discriminability of two stimuli which is proportional to the physical stimulus. In time perception, this means that the subjective duration and its variability increase linearly with the duration of the interval. In this experiment, the WF was calculated as the ratio between the mean of the ΔTs after the 4th reversal and T (Figure 5.2). During this adaptive procedure, the comparison duration (T + ΔT) was adjusted across trials, to obtain a Weber fraction leading to 79% of correct discrimination. After three consecutive correct responses the ΔT decreased and increased after each incorrect response. Until the fourth reversal the trials were not counted and ΔT was changed in steps of 25 ms (3 screen refreshes). After the fourth reversal the step size decreased to 8.3 ms (1 screen refresh). The point of 79% correct responses on the psychometric curve was estimated by taking the average value of the remaining reversals divided by T (Bueti et al., 2012).

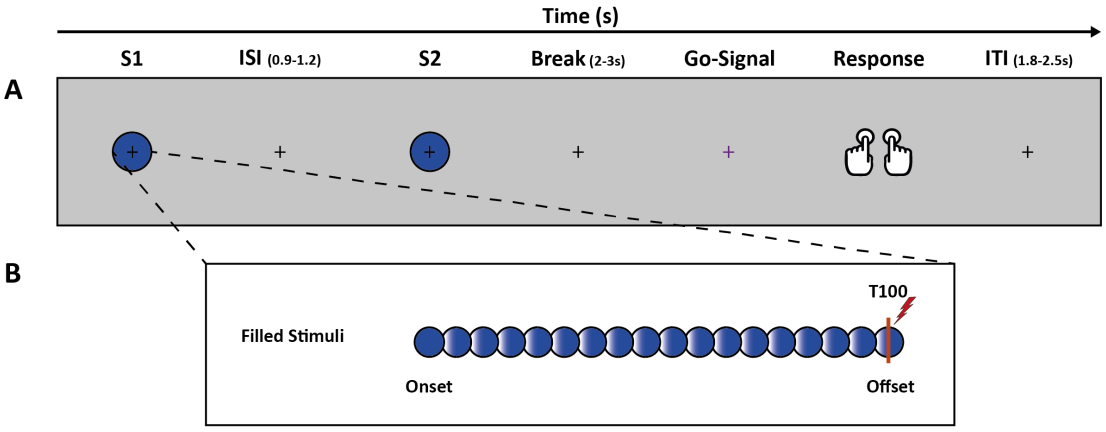

Figure 5.3. A) Schematic representation of the experimental paradigm. After a brief inter trial interval (ITI) lasting between 1.8 and 2.5 seconds, the first stimulus is presented at the centre of the screen. Paired Pulse stimulation is delivered at this stage. After the first stimulus and after a brief inter stimulus interval (ISI) lasting between 0.9 and 1.2s, the second stimulus is presented. After the end of the second stimulus, the subject waited a go signal to respond with either the left or the right hand. **B)** ppTMS was delivered at the S1 offset.

This procedure was repeated if the accuracy fell outside the range of 75-83 % or if the two obtained Weber fractions were too diverse from each other.

5.2.4 Methods of the constant stimuli

The main experiment contained three conditions: TMS stimulation over the anterior SMA, TMS stimulation over the posterior SMA, and no-stimulation condition. For those three sessions we used a constant procedure, meaning that the standard (S1) and comparison durations (S2) were fixed for each participant (Fig 5.3). Two durations of the same blue disks were presented in each trial, the first one containing one of the standard durations (0.2, 0.4, 0.75, 1.1, 1.5 s), the second one containing the comparison durations which differed for each participant according to the individual mean of their Weber fractions (S2 = S1 +/- S1*WF). Half of the comparison durations were longer, the other half shorter than the standard duration. As we were most interested in the edges of the chronomap, the shortest (0.2 s) and the longest (1.5 s) durations were presented 40 times for each condition, the other three durations 24 times, leading to a total set of 152 trials for each condition. Those 152 trials were split into four blocks of

38 trials to avoid a tiredness effect of the subjects, an overheating of the coil and to control the TMS location. The ITI, this time defined as the time between the finger response and the presentation of the next stimulus, was again a value between 1.8 – 2.5 s.

It has been shown that the stimulation of non-primary motor areas activates peripheral muscles (Teitti et al., 2008). To avoid a finger response caused by stimulating a motor area, a short break was introduced after the presentation of the comparison duration (a random value taken from a uniform distribution ranging from 2 to 3 s). This break was terminated by changing the color of the fixation cross from white to purple, asking for a response with the left hand, or to light blue, asking for a response with the right hand. Right/left responses were randomized and counterbalanced across durations. SMA is an important area for motor planning (Nachev et al., 2008). Using both hands for responding should prevent the programming of the hand response.

Subjects were given a headphone and the recorded sound of the TMS pulse was played simultaneously with the stimulation (offset of standard duration) and at the same timing (offset) for the comparison stimulus. Playing the click sound of the TMS on every trial ensures equal auditory stimulation and avoids a bias towards the first stimulus (Bueti et al., 2008a).

5.2.5 TMS parameters

TMS was delivered using a 200² BiStim stimulator and a 40 mm figure of eight coil. For this experiment we used a paired-pulse TMS protocol with an interpulse interval of 2 ms. Concerning stimulus intensities, the first pulse was 80% and the second 120% of the resting motor threshold (RMT). The coil was held tangentially to the skull and for SMA the wings of the coil were parallel to the midline with the current flowing lateral-medial rightwards. The TMS pulses were delivered at the offset of the first stimulus of the pair. We decided to stimulate the offset for two main reasons: a) because we were interested in duration representation and stimulus offset is the moment when a specific duration becomes finally available to the subjects (Protopapa

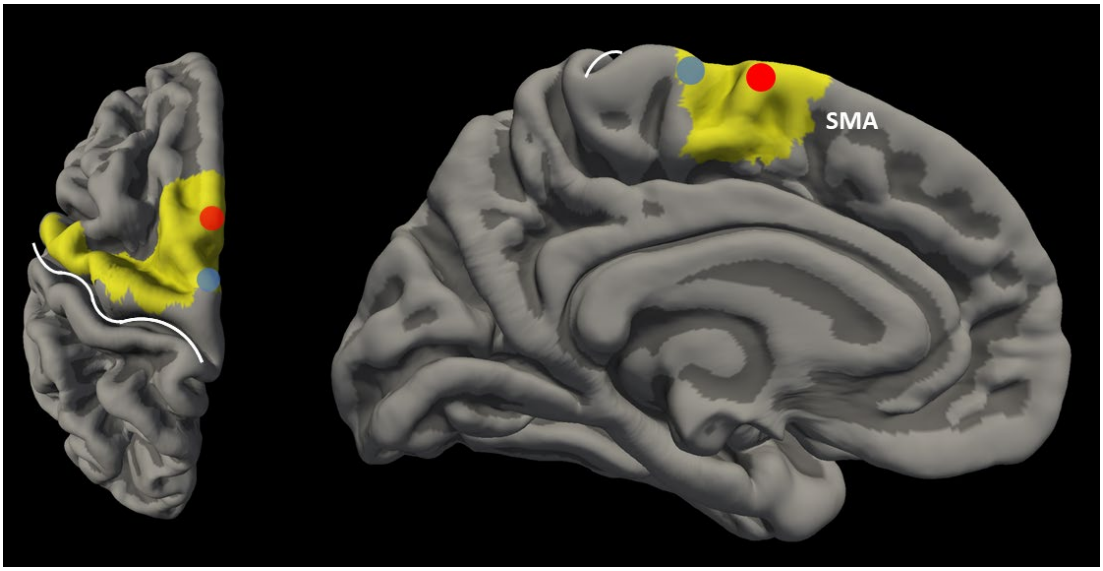

Figure 5.4. Axial (on the left) and sagittal (on the right) views of the BA6 (yellow patch) as seen with Freeview. The template displayed is the "Fsaverage" (an "average" brain constructed of MRI scans of 40 subjects). We localized the posterior part of SMA (blue dot) as the most anterior part of the prefrontal gyrus, and the for the anterior part (red dot) we moved 1.5cm anteriorly from the posterior part. In both figures the central sulcus is highlighted with a white line.

et al., 2019), and b) because this timing of stimulation has been shown to be effective in disruptive discrimination performance (see previous chapter).

5.2.6 Areas localization

As for previous experiment, we tested only participant that already participated to fMRI experiments, and of which we could therefore have a T1-weighted image of their brain. Target positions were marked for each subject individually using a Brainsight neuronavigation system (Rogue Research, Montreal, Canada). We first identified the left primary motor cortex (M1) to find the posterior border of the chronomap. In order to localize left SMA we overlaid on each individual T1-weighted image the Freesurfer label image (lh.BA6.exvivo.thresh.label) corresponding to Brodman area 6 (Figure 5.4). With the help of atlases, we chose the most anterior part of the precentral gyrus as the posterior border of left SMA. The anterior border was marked 1.5 cm anterior to the posterior landmark. Each subject's anatomical MRI scan was co-registered with visible landmarks on the subject's head using the Brainsight frameless stereotaxy

system together with the Polaris infra-red tracking camera and sensors (Northern Digital, Waterloo, Canada). The Polaris system allowed us to constantly track the coil position with respect to the target area thorough the experiment.

5.2.7 Coil

TMS pulses were delivered using two 200² units connected through a BiStim module (The Magstim Company Ltd, Whitland, Wales, UK), so that paired pulses can be delivered through one coil which was in our experiment a figure-of-eight coil. The coil produced monophasic waveforms which have been shown to elicit the greatest inhibitory effect in M1 if the current flows in a posterior-anterior direction (Davila-Pérez et al., 2018).

We used the same coil for finding the motor threshold and for the task itself. As described above we chose a figure-of-eight coil with a relatively small outer diameter of 40mm to get the best focality-depth tradeoff.

We simulated the electric field induced by the TMS with SimNIBS, a free and open source software package for the Simulation of non-invasive brain stimulation. The results revealed a more localized stimulation of the left SMA areas if the wings of the coil are parallel to the midline with the current flowing medial-lateral leftwards, in accordance with previous studies (Narayana et al., 2012; Janssen et al., 2015).

5.2.8 Resting motor threshold

Single-pulse TMS delivered over the primary motor cortex (M1) elicits a muscle response. The excitability of the stimulated area can be measured with the motor evoked potential (MEP) which are recorded with electromyography (EMG) and used to determine the resting motor threshold (RMT) of each individual participant. To elicit a SICI (short-interval intracortical inhibition) the conditioning stimulus needs to be lower than the RMT, the test stimulus higher. Thus, the stimulus intensity must be adjusted to the corticomotor excitability of each individual.

For the MEP acquisition the coil was placed over the subject's hand area at a 45° angle from the midsagittal line, perpendicular to the central sulcus (Brasil-Neto et al., 1992). Once we found a point on the scalp eliciting a MEP, the RMT was defined as the lowest stimulus intensity (given as percentage of MSO, i.e. maximal stimulator output) that is required to induce a MEP with a peak-to-peak amplitude of 50 μV in 5 out of 10 trials.

The Electromyography (EMG) was recorded using a BIOPAC MP150 system. Three electrodes were used: two Ag-AgCl surface electrodes, placed over the belly of the first dorsal interosseous (FDI) muscle of the right hand and over the head of the radius bone and one ground electrode (metallic surface electrode) placed on the right forearm.

The mean MEP was 53.18% (+/- 7.03%) of the MSO.

5.2.9 Paired-pulse protocol

During a ppTMS two pulses are delivered at the same location, separated by a certain temporal distance, the interstimulus interval (ISI). Researchers studied the effects of different stimulus intensities and ISIs to elicit a short-interval cortical inhibition (SICI) over M1 and revealed that SICI was most pronounced with an ISI of 1-6 ms (Reis et al., 2008). Ilic et al. (2002) showed that a stimulation with CS (conditioned stimulus) < RMT (Resting Motor Threshold) and TS (Test Stimulus) > RMT leads to the most pronounced SICI with an ISI of 2ms.

Only few studies tested the physiological effects of ppTMS over SMA. Vaalto et al. (2016) used ppTMS to determine the optimal paradigm for inhibiting non-primary motor areas (NPMA) which include the SMA and found the most profound inhibition of the MEP amplitude with an ISI of 2 ms, a CS of 70% or 90% and a TS of 120%. Based on those previous results (Ilić et al., 2002; Ferreri et al., 2011; Vaalto et al., 2016) we used a paired-pulse TMS paradigm using an ISI of 2 ms, a CS of 80% of the RMT and a TS of 120% of the RMT. These are the same parameters that we used to stimulate SMA in previous chapter.

5.2.10 Data Analysis

We calculated the mean proportion of correct responses per subject and condition obtaining a value of accuracy for each subject for the five different durations and three different conditions. Outlier trimming was done by searching for data points with residuals exceeding 2.5 SD and excluded a participant's whole data set. The final analysis was conducted on 17 out of 20 subjects (Figure 5.5).

Firstly, we checked that the no-TMS condition accuracy was close to the desired level (around 75% of correct answers) and that the no-TMS conditions was stable across durations.

We then grouped the data to submit them to a repeated measures ANOVA. We grouped the data relative to the short durations (0.2 and 0.4 s) and the data relative to the long durations (1.2 and 1.5 s). We therefore submitted the data to a 2x2 repeated measures analysis of variance (ANOVA) with area (SMA anterior and SMA posterior) and duration (Long or Short) as a within-subject factor.

Based on the results presented by Protopapa and colleagues (2019) we wanted to test the spatial organization of SMA in temporal computations using paired-pulse TMS. We hypothesized a double dissociation of presented duration time and the location of neuronal activation in SMA. The effect of TMS pulses over the anterior part of SMA would affect the encoding of shorter durations and we expected to see a drop of performance in those durations compared to the no-TMS condition and compared to longer durations. Similarly, stimulating the posterior SMA should lead to an impaired temporal discrimination of longer durations but not of shorter ones.

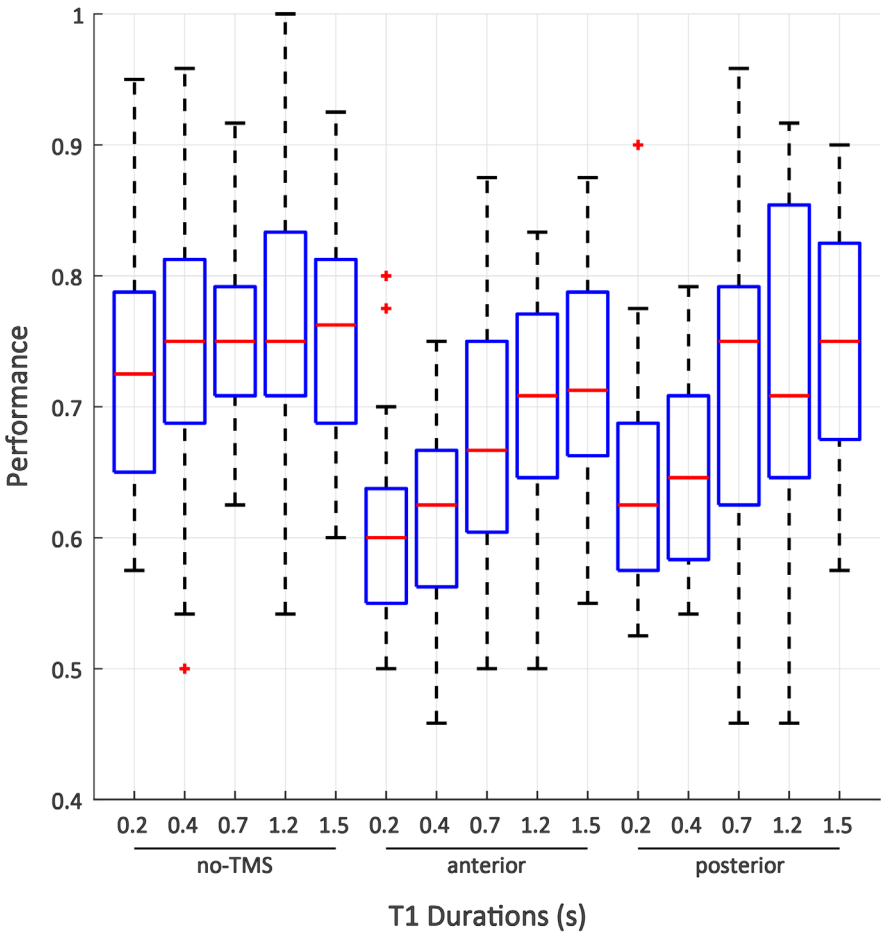

Figure 5.5. Data distribution. We excluded three subjects (Subject 3, 7 and 20).

5.3 Results

5.3.1 No-TMS condition

The no-TMS condition was used as a control to test whether the participants performed the task correctly. The overall accuracy of the control condition was 75.9% +/- 10% (mean +/- standard duration), indicating that the adaptive procedure yielded the desired effect: a stable performance in the control condition.

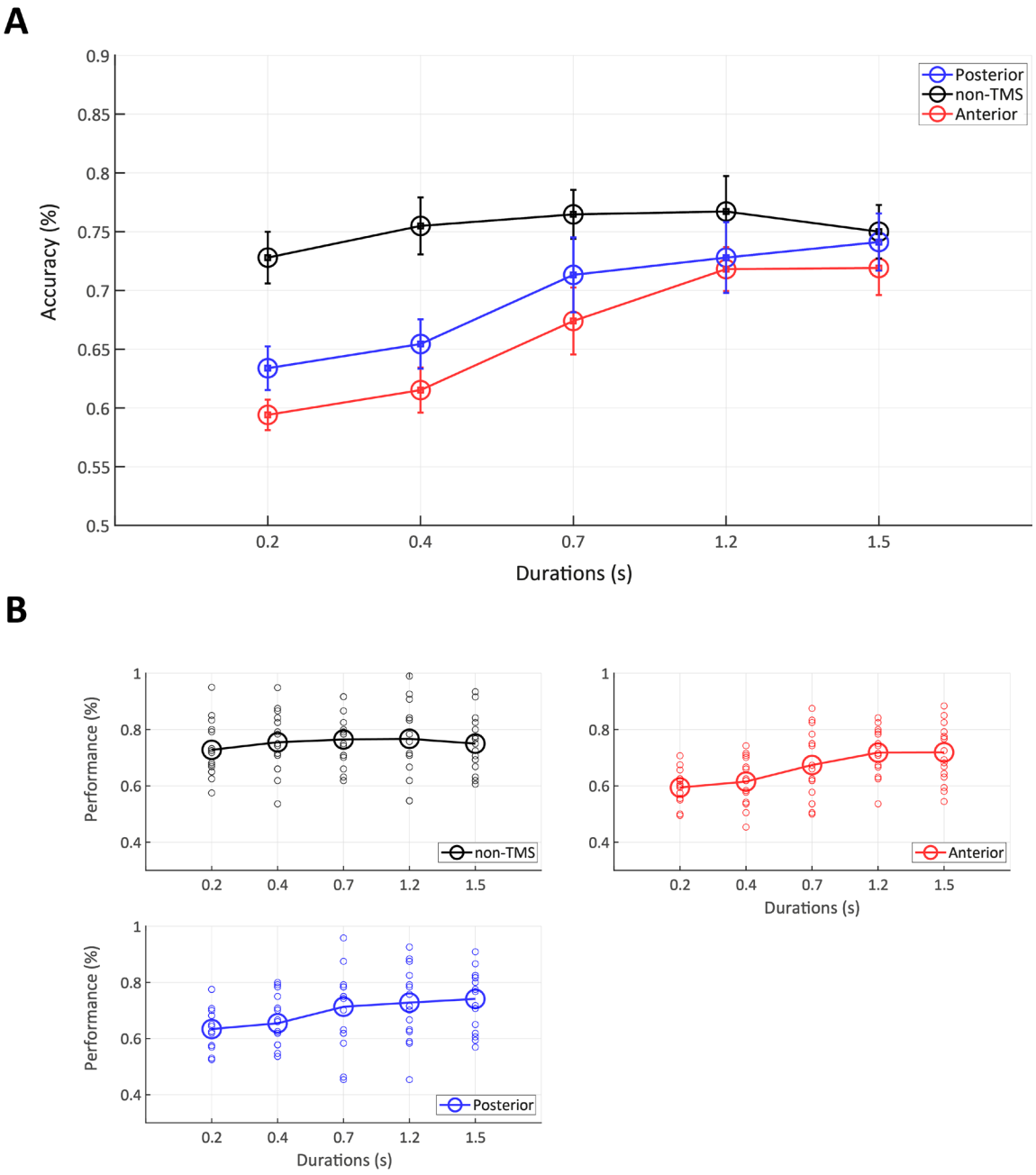

Figure 5.6. **A)** Average performance accuracy (from 0 to 1) in the different 5 durations. Performance accuracy in the non-tms condition is stable across the five durations compared to the TMS SMA conditions. After TMS on both SMA sites, performance accuracy was lower in shorter compared to longer durations. This effect was more pronounced after the anterior stimulation. **B)** Data distribution in the three experimental conditions (no-TMS, anterior and posterior ppTMS stimulation). Since some data-points were overlapping, we added a 2% of jitter.

no-TMS	0.2s	0.4s	0.7s	1.2s	1.5s
0.2s	-	0.2084	0.1297	0.1718	0.2912
0.4s	0.2084	-	0.7100	0.7094	0.8602
0.7s	0.1297	0.7100	-	0.9431	0.4463
1.2s	0.1718	0.7094	0.9431	-	0.5185
1.5s	0.2912	0.8602	0.4463	0.5185	-

Table 5.1. T values of paired-sample t test computed on the accuracy of the non-TMS condition for the different durations.

Moreover, if we compare the performance scores of the no-TMS condition at the various durations, we do not obtain any significant difference. This means that the scores of the non-tms condition, in addition to being comparable to what we expected after the adaptive procedure, are stable across durations.

5.3.2 SMA

In order to analyze the SMA data we grouped the data of the duration "0.2" and "0.4" as "Short durations" and "1.1" and "1.5" as "Long durations". We therefore conducted a repeated-measures analysis of variance (ANOVA) with area (SMA anterior and SMA posterior) and duration (Long or Short) as a within-subject factor.

The ANOVA highlighted a significant main effect of the Area ($F(1, 33) = 6{,}654$, $p=0.015$), and a significant main effect of the Duration ($F(1,33) = 55{,}361$, $p<0.001$).

Regarding the main effect of the Duration, we found significantly lower accuracy when short durations were presented (mean 0.6244, standard deviation 0.07886) compared to long durations (mean 0.7266, standard deviation 0.1014) ($t(67)= -8.0965$, $p<0.001$).

As one can appreciate by looking at Figure 5.6A, the interaction Area x Duration was not significant ($F(1,33) = 1{,}481$, $p=0.232$). since performance accuracy in posterior and anterior SMA was worse for shorter compared to longer durations ($t(67)= -8.6060$, $p<0.0001$). However, the two TMS sites show a significant difference at short durations where discrimination accuracy was worst after TMS of the anterior (Anterior: mean 0.6047, standard deviation 0.0692) compared to posterior SMA

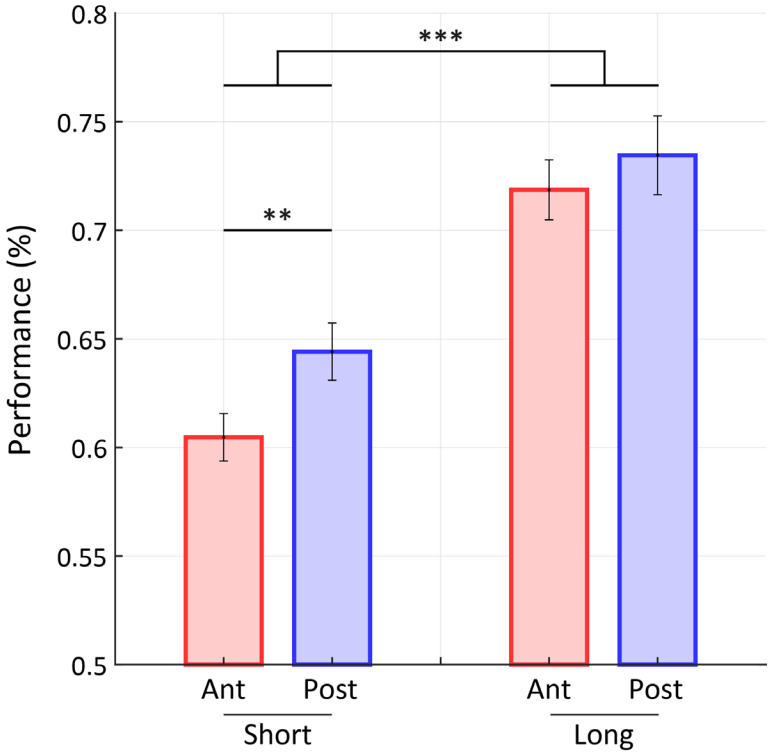

Figure 5.7. Mean performance accuracy for the two sites of stimulation (Anterior and Posterior SMA) in short or long durations. Asterisks symbols represent the results of the paired-sample *t* tests significant at * $p < 0.05$, and ** $p < 0.01$ and *** $p < 0.001$.

(Posterior: mean 0.6441, standard deviation 0.0835; t(33)= -2.7906, p= 0.0087). This difference was absent for the long durations (Anterior: mean 0.7186, standard deviation 0.0874; Posterior: mean 0.7346, standard deviation 0.1144; t(33)= -1.0802, p= 0.2879).

5.4 Discussion

With this work we tested the existence of a topographical representation of time in SMA using a causal rather than a correlational approach. A very recent study shows that visual durations ranging from a few hundreds of milliseconds to a few seconds are represented in the human supplementary motor area (SMA) and this representation is topographically organized i.e., stimuli that have similar durations engage the activity of neighboring locations on the cortical surface (Protopapa et al., 2019). Shorter durations are represented in the anterior SMA, longer durations in its posterior part.

In the present work, participants had to judge which of two subsequently presented stimuli lasted longer. We used different duration's range spanning from 0.3 to 1.5 s. while a brief ppTMS was delivered over the anterior or the posterior SMA. We predicted a double dissociation between the two stimulation sites and the duration range at hand, with the performance for short stimuli (0.2, 0.4s) more impaired after the anterior stimulation, and the performance for long stimuli (1.1, 1.5s) more impaired after posterior stimulation.

Our results are in line with the first part of the hypothesis, showing a significant drop of performance for shorter durations when stimulating SMA anterior compared to SMA posterior. This suggests that the anterior SMA is causally involved in the encoding of durations for shorter stimuli. Unfortunately, we observed no significant difference between SMA anterior and posterior for longer durations. Unexpectedly, the accuracy for short durations appeared to be overall more impaired when compared to the accuracy for long durations. I will now try to speculate on the possible reasons of the lack of a double dissociation between TMS of anterior and posterior SMA and short and long durations.

5.4.1 Duration tuning

Our data show a trend that there might be a topographical arrangement of duration-tuned neurons, as suggested by Protopapa et al., (2019). During anterior stimulation,

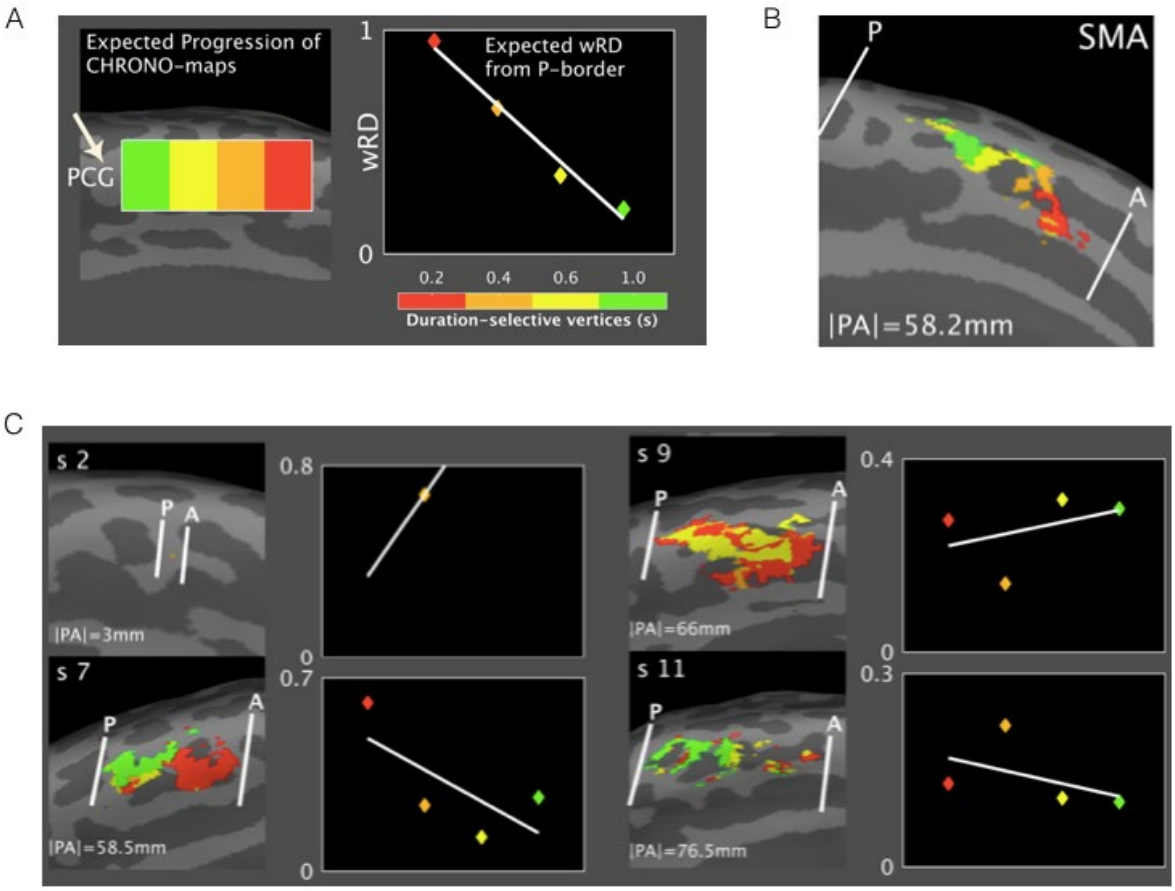

Figure 5.8. **A**-B. Expected spatial progression of duration selective voxels (A) and observed Chronomaps as shown in Protopapa et al. 2019 (Experiment 1, **B)** Group-level maps using four different standard durations (0.2 – 1 s). **C)** 4 individual maps are represented. S2 shows no progression and minimal SMA activity. S7 and S11 show the expected results. Duration-tuned voxels do not seem to follow a spatial progression in S9. Adapted from Protopapa et al., (2019). The individual maps are shown with the purpose of emphasizing the high inter-subject variability of the spatial progression in chronomaps.

we affected directly the part of SMA representing shorter durations. On the other hand, the fact that short duration seems to be impaired also after the posterior stimulation might come from an indirect stimulation. The induced electric field of TMS decreases exponentially with increasing distance from the hot spot which lies directly underneath the intersection of the two coil wings (Marg & Rudiak, 1994, Walsh & Cowey, 2000). Thus, penetrating the posterior part of SMA might have affected neural computation of short durations due to the spread of TMS to the anterior portion. This, nevertheless, do not explain why the same phenomena did not occur for longer stimuli.

5.4.2 Individual differences

Looking at the individual data of the recently published chronomap study (Protopapa et al., 2019), it shows that the presence of the map itself as well as the spatial progression of the duration selective clusters of voxels varies a lot in individual subjects (see Figure 5.8). It would be interesting to know whether the subjects who showed the expected double dissociation in our task would also show the expected spatial progression in fMRI data. Thus, in a more complex experiment one could first identify chronomaps in each subject through functional fMRI and stimulate the appropriate locations based on the functional maps.

5.4.3 Conclusions

Precise timing is critical for our everyday life activity and our brain developed to be a perfect time machine. We can sense the passage of time even without looking on our watch. However, the neural mechanism underlying this phenomenon remains largely unknown. The current study confirmed that the human supplementary motor area is a core region in the processing of temporal information. Using a paired-pulse TMS protocol we stimulated the anterior and posterior SMA. The neural activity during a temporal discrimination task was differently affected for different durations and for the different stimulation sites. Stimulating the anterior SMA decreased the participants' accuracy for shorter durations compared to longer ones. Alongside with the results of experiment 3, that revealed that the chronometry of SMA could reflect its involvement in duration encoding as a possible read-out, these findings suggest that different parts of the SMA encode different duration lengths, confirming that the functional organization within SMA reflects a high level of organization. However, we found no particular involvement of posterior SMA in the processing of longer durations. Also the fact that shorter durations appeared to be particularly affected remains unclear.

CHAPTER 6: GENERAL CONCLUSIONS

During my PhD I have tried to understand how temporal information in the millisecond range is extracted from visual inputs, how it is encoded/read-out and perceived. Specifically, I have asked "when", at which stage of temporal information processing (i.e., from sensory drive integration to duration recognition) visual and premotor areas, brain regions known to play a role in temporal computations, are engaged. Focusing of the chronometry of these areas in duration encoding, I tried to better understand the functional role of these areas and, at the same time, using stimuli with different sensory load and different durations ranges I have tried to gain insight on the mechanisms underlying duration perception.

In the first part of my work at SISSA (Experiment 1-2, chapter 2), I focused on the chronometry i.e., the engagement over time, of two visual areas, specifically V1 and V5/MT during duration encoding. Moreover I decided to check if this chronometry depends on the nature of the stimuli used i.e., stimuli with low (empty intervals) versus high (filled durations) sensory load and whether it was linked to the duration range at hand.

The results of experiments 1-2 show indeed that the effects of the TMS delivered at different timings from stimulus onset during the encoding stage of the task, depend on both, the type of stimuli involved and the duration at hand. Experiment 1 shows that with empty intervals, the stimulation of right V1 and right V5/MT is effective only if delivered from the middle to the end of the timed interval (60% and 90% of the total interval duration) and only if intervals are very short i.e., in 0.2 s range. On the other hand, experiment 2 shows that with filled durations the most effective timings of stimulation are those close to the beginning and the middle of the visual stimulus (between 30% and 60% of the whole stimulus duration).

The differences between empty intervals and filled durations seem to suggest that the mechanism through which time is computed depends on relevance of the sensory aspect of the event to be timed. During an empty interval nothing is shown on the screen, and the only available sensory input is not informative per se but only as marker of the interval. Moreover, among the two markers, the most informative one is the offset since this is the only moment when the duration becomes available. It is therefore not surprising that we were able to find significant effects only with stimulation timings closer to the interval offset (T60, T90).

Another element that seems to speak of a different mechanism at play for empty intervals compared to filled duration, is the absence of TMS effect for duration longer than 0.2 s. It might be possible that the shortest interval (0.2 s) is so brief and the two markers so close in time, to be visually relevant and consequently require the involvement of both V1 and V5/MT. With longer duration instead, the empty part of the stimulus becomes more prominent than the visual markers and if some sort of integration is taking place, this integration is not of a sensory input and does not necessarily originate in the visual areas.

The TMS effects on filled durations are independent from stimulus' duration, at least up to 0.6 s and they happen from early to middle stimulus duration. Our data are compatible with a model that sees duration perception of a sensory event as the result of the leaky integration of a sensory drive from sensory specific cortices (Toso et a., 2021). We model our data assuming that TMS affects the standard deviation of the neural noise. If this noise is applied at the sensory input level, this noise would accumulate over time. The model predicts indeed greatest TMS effects for early stimulation timings where the noise has enough time to accumulate in order to impair performance sensitivity. This prediction fits very well with the empirical findings of experiment 2 (chapter 3).

If primary visual cortex provides the input to the integrator, it remains unclear if and where in the brain a reader of the integrator's output exists.

A candidate area to be a read-out of time is the Supplementary Motor Area (SMA). SMA has been extensively associated with duration perception and production tasks

in the millisecond range (Wiener et al., 2010). Moreover both neuroimaging studies in humans (Ferrandez et al., 2003; Morillon et al., 2009; Protopapa et al., 2019) and electrophysiological recordings in monkeys (Mita et al., 2009; Merchant et al., 2013b) have shown that the role of SMA in time perception and production is independent from the sensory modality of the stimuli.

In chapter 4 we tested the hypothesis of SMA as time reader of the integrator output. In a single experiment we stimulated V1 and SMA at different timings from stimulus onset. In the leaky integrator framework, if TMS increases the variance of the neural noise and this noise is applied at the reading out stage of the integrator's output, only at later stimulation times this noise could influence performance. The predictions fitted well the experimental data. Indeed V1 TMS worsened the discrimination thresholds when delivered at T60 (half-way the duration of the stimulus) replicating my previous findings and in line with the idea that V1 provides the input to the integrator. SMA TMS instead, had an effect when delivered towards the stimulus offset (T90, T100) in line with the reading-out hypothesis. These findings are therefore indicating the existence of a functional hierarchy between V1 and SMA. Moreover, by testing alternative models of the neurophysiological effects of TMS, at the level of the variance or the mean of the neural noise, we were able to show that the models best fitting the data are those assuming an effect of TMS on the variance of the neural noise.

We then asked ourselves how we could further characterize the functional role of SMA as time read-out. To do this we were inspired by a recent fMRI study (Protopapa et al., 2019), showing the existence of a topographic representation of time in SMA. In this work the authors show that distinct portions of SMA show a preferential response to visual stimuli of different durations i.e., stimuli that have similar durations engage the activity of neighboring locations on the cortical surface (Protopapa et al., 2019). Shorter durations are represented in the anterior SMA, longer durations in its posterior part. In chapter 5 we decided to prove the existence of chronomaps with TMS. We asked volunteers to perform a temporal discrimination task of visual stimuli of different durations ranging from 0.2 to 1.5 s while TMS was applied to either the anterior or the posterior SMA. If a chronomap exists in SMA we expected a worsening of performance accuracy in the shorter durations range after stimulation of the anterior

SMA and of the longer durations after TMS of the posterior SMA. The results show that independently from the tested durations, participants' performance was worse after the stimulation of the anterior SMA compared to the posterior part. However, after TMS of the anterior SMA, the discrimination accuracy was worst for the shortest compared to the longest durations of the range. The lack of a double dissociation between durations and SMA sites could be due to the lack of a precise match between functional chronomaps and TMS sites in our subject's sample. These findings only partially support the existence of a duration map in SMA.

Taken together, my experiments have shown results that focus primarily on two different fronts.

The first is that my experiments confirmed / added some information on transcranial magnetic stimulation. In Experiment 1 and 2 we confirmed that an approach that exploits the temporal resolution of TMS is possible. In these experiments we have stimulated during the encoding of very short durations (ranging from 200ms to 600ms) and we have obtained selective effects only for certain specific timings of stimulation, despite these being extremely close in time. Moreover, despite our efforts to choose TMS parameters that could cause a suppression of the neural activity of the stimulated area - following the classical approach of the virtual lesion - the results of the model presented in chapter 3 and developed in chapter 4 showed that the best way to model the effect of the TMS to emphasize the increase in the variance of the noise, suggesting that the effects of the TMS observed at the physiologically level are due to an increase in neural noise, rather than to a general suppression of neural activity.

Secondly, my results tried to explain something more about how our visual brains encodes short durations. First, we have shown how our brain treats empty and full stimuli differently. Although my research has subsequently focused on full intervals, the pattern of results of Experiment 1 and 2 showed clearly different chronometry between empty and filled stimuli. Moreover, although we were unable to identify different chronometry between V1 and V5/MT, we found them between V1 and SMA, and the results of experiment 3 and the application of the model of Chapter 3 suggest that V1 may constitute the drive of a hypothetical accumulator, and that SMA can act as an area that integrates and reads the integrated duration. The fact that SMA plays a

high role in the perception of time is also suggested by experiment 4, which shows how - as opposed to V1 - in SMA different durations are treated differently.

Bibliography

Abrahamyan, A., Clifford, C. W. G., Ruzzoli, M., Phillips, D., Arabzadeh, E., & Harris, J. A. (2011). Accurate and rapid estimation of phosphene thresholds (REPT). *PLoS ONE*, *6*(7), 22342. https://doi.org/10.1371/journal.pone.0022342

Alexander, G. E., Crutcher, M. D., & Delong, M. R. (1991). Chapter 6 Basal ganglia-thalamocortical circuits: Parallel substrates for motor, oculomotor, "prefrontal" and "limbic" functions. *Progress in Brain Research*, *85*(C), 119–146. https://doi.org/10.1016/S0079-6123(08)62678-3

Becker, M. W., & Rasmussen, I. P. (2007). The rhythm aftereffect: Support for time sensitive neurons with broad overlapping tuning curves. *Brain and Cognition*, *64*(3), 274–281. https://doi.org/10.1016/j.bandc.2007.03.009

Benson, N. C., Butt, O. H., Datta, R., Radoeva, P. D., Brainard, D. H., & Aguirre, G. K. (2012). The retinotopic organization of striate cortex is well predicted by surface topology. *Current Biology*, *22*(21), 2081–2085. https://doi.org/10.1016/j.cub.2012.09.014

Benton, C. P., & Redfern, A. S. (2016). Perceived Duration Increases with Contrast, but Only a Little. *Frontiers in Psychology*, *7*(DEC), 1950. https://doi.org/10.3389/fpsyg.2016.01950

Bolognini, N., Miniussi, C., Savazzi, S., Bricolo, E., & Maravita, A. (2009). TMS modulation of visual and auditory processing in the posterior parietal cortex. *Experimental Brain Research*, *195*(4), 509–517. https://doi.org/10.1007/s00221-009-1820-7

Bosco, G., Carrozzo, M., & Lacquaniti, F. (2008). Contributions of the human temporoparietal junction and MT/V5+ to the timing of interception revealed by transcranial magnetic stimulation. *Journal of Neuroscience*, *28*(46), 12071–12084. https://doi.org/10.1523/JNEUROSCI.2869-08.2008

Brand, A., Behrend, O., Marquardt, T., McAlpine, D., & Grothe, B. (2002). Precise inhibition is essential for microsecond interaural time difference coding. *Nature*, *417*(6888), 543–547. https://doi.org/10.1038/417543a

Brasil-Neto, J. P., McShane, L. M., Fuhr, P., Hallett, M., & Cohen, L. G. (1992). Topographic mapping of the human motor cortex with magnetic stimulation: factors affecting accuracy and reproducibility. *Electroencephalography and Clinical Neurophysiology/ Evoked Potentials*, *85*(1), 9–16. https://doi.org/10.1016/0168-5597(92)90095-S

brown, S. W. (1995). Time, change, and motion: The effects of stimulus movement on temporal perception. *Perception & Psychophysics*, *57*(1), 105–116. https://doi.org/10.3758/BF03211853

Bueti, D. (2011). The sensory representation of time. *Frontiers in Integrative Neuroscience*, *5*. https://doi.org/10.3389/fnint.2011.00034

Bueti, D., Bahrami, B., & Walsh, V. (2008a). Sensory and Association Cortex in Time Perception. *Journal of Cognitive Neuroscience*, *20*(6), 1054–1062. https://doi.org/10.1162/jocn.2008.20060

Bueti, D., Bahrami, B., & Walsh, V. (2008b). Sensory and Association Cortex in Time Perception. *Journal of Cognitive Neuroscience*, *20*(6), 1054–1062. https://doi.org/10.1162/jocn.2008.20060

Bueti, D., Bahrami, B., & Walsh, V. (2008c). Sensory and Association Cortex in Time Perception. *Journal of Cognitive Neuroscience*, *20*(6), 1054–1062. https://doi.org/10.1162/jocn.2008.20060

Bueti, D., Bahrami, B., Walsh, V., & Rees, G. (2010). Encoding of temporal probabilities in the human brain. *Journal of Neuroscience*, *30*(12), 4343–4352. https://doi.org/10.1523/JNEUROSCI.2254-09.2010

Bueti, D., Lasaponara, S., Cercignani, M., & Macaluso, E. (2012). Learning about Time: Plastic Changes and Interindividual Brain Differences. *Neuron*, *75*(4), 725–737. https://doi.org/10.1016/j.neuron.2012.07.019

Bueti, D., & Macaluso, E. (2010). Auditory temporal expectations modulate activity

in visual cortex. *NeuroImage*, *51*(3), 1168–1183. https://doi.org/10.1016/j.neuroimage.2010.03.023

Bueti, D., van Dongen, E. V., & Walsh, V. (2008). The Role of Superior Temporal Cortex in Auditory Timing. *PLoS ONE*, *3*(6), e2481. https://doi.org/10.1371/journal.pone.0002481

Bueti, D., Walsh, V., Frith, C., & Rees, G. (2008). Different brain circuits underlie motor and perceptual representations of temporal intervals. *Journal of Cognitive Neuroscience*, *20*(2), 204–214. https://doi.org/10.1162/jocn.2008.20017

Buonomano, D. V., & Maass, W. (2009, February 15). State-dependent computations: Spatiotemporal processing in cortical networks. *Nature Reviews Neuroscience*, Vol. 10, pp. 113–125. https://doi.org/10.1038/nrn2558

Chubykin, A. A., Roach, E. B., Bear, M. F., & Shuler, M. G. H. (2013). A Cholinergic Mechanism for Reward Timing within Primary Visual Cortex. *Neuron*, *77*(4), 723–735. https://doi.org/10.1016/j.neuron.2012.12.039

Coull, J. T., Cheng, R. K., & Meck, W. H. (2011, January). Neuroanatomical and neurochemical substrates of timing. *Neuropsychopharmacology*, Vol. 36, pp. 3–25. https://doi.org/10.1038/npp.2010.113

Coull, J. T., Nazarian, B., & Vidal, F. (2008). Timing, storage, and comparison of stimulus duration engage discrete anatomical components of a perceptual timing network. *Journal of Cognitive Neuroscience*, *20*(12), 2185–2197. https://doi.org/10.1162/jocn.2008.20153

Coull, J. T., Vidal, F., Nazarian, B., & Macar, F. (2004). Functional Anatomy of the Attentional Modulation of Time Estimation. *Science*, *303*(5663), 1506–1508. https://doi.org/10.1126/science.1091573

Cowey, A., & Walsh, V. (2000). Magnetically induced phosphenes in sighted, blind and blindsighted observers. *NeuroReport*, *11*(14), 3269–3273. https://doi.org/10.1097/00001756-200009280-00044

Davila-Pérez, P., Jannati, A., Fried, P. J., Cudeiro Mazaira, J., & Pascual-Leone, A. (2018). The Effects of Waveform and Current Direction on the Efficacy and

Test–Retest Reliability of Transcranial Magnetic Stimulation. *Neuroscience*, *393*, 97–109. https://doi.org/10.1016/j.neuroscience.2018.09.044

DeCharms, R. C., & Zador, A. (2000, November 28). Neural representation and the cortical code. *Annual Review of Neuroscience*, Vol. 23, pp. 613–647. https://doi.org/10.1146/annurev.neuro.23.1.613

Del Olmo, M. F., Cheeran, B., Koch, G., & Rothwell, J. C. (2007). Role of the cerebellum in externally paced rhythmic finger movements. *Journal of Neurophysiology*, *98*(1), 145–152. https://doi.org/10.1152/jn.01088.2006

Deng, Z. De, Lisanby, S. H., & Peterchev, A. V. (2013). Electric field depth-focality tradeoff in transcranial magnetic stimulation: Simulation comparison of 50 coil designs. *Brain Stimulation*, *6*(1), 1–13. https://doi.org/10.1016/j.brs.2012.02.005

Deng, Z. De, Lisanby, S. H., & Peterchev, A. V. (2014). Coil design considerations for deep transcranial magnetic stimulation. *Clinical Neurophysiology*, *125*(6), 1202–1212. https://doi.org/10.1016/j.clinph.2013.11.038

Di Lazzaro, V., Oliviero, A., Profice, P., Saturno, E., Pilato, F., Insola, A., … Rothwell, J. C. (1998). Comparison of descending volleys evoked by transcranial magnetic and electric stimulation in conscious humans. *Electroencephalography and Clinical Neurophysiology - Electromyography and Motor Control*, *109*(5), 397–401. https://doi.org/10.1016/S0924-980X(98)00038-1

Di Lazzaro, V., Pilato, F., Oliviero, A., Dileone, M., Saturno, E., Mazzone, P., … Rothwell, J. C. (2006). Origin of facilitation of motor-evoked potentials after paired magnetic stimulation: Direct recording of epidural activity in conscious humans. *Journal of Neurophysiology*, *96*(4), 1765–1771. https://doi.org/10.1152/jn.00360.2006

Dibner, C., Schibler, U., & Albrecht, U. (2009, March 17). The mammalian circadian timing system: Organization and coordination of central and peripheral clocks. *Annual Review of Physiology*, Vol. 72, pp. 517–549. https://doi.org/10.1146/annurev-physiol-021909-135821

Diehl, R. L., Lotto, A. J., & Holt, L. L. (2004). Speech Perception. *Annual Review of Psychology*, *55*(1), 149–179. https://doi.org/10.1146/annurev.psych.55.090902.142028

Droit-Volet, S., & Izaute, M. (2005). The Effect of Feedback on Timing in Children and Adults: The Temporal Generalization Task. *The Quarterly Journal of Experimental Psychology Section A*, *58*(3), 507–520. https://doi.org/10.1080/02724980443000025

Dumoulin, S. O., Bittar, R. G., Kabani, N. J., Baker, C. L., Le Goualher, G., Pike, G. B., & Evans, A. C. (2000). A new anatomical landmark for reliable identification of human area V5/MT: A quantitative analysis of sulcal patterning. *Cerebral Cortex*, *10*(5), 454–463. https://doi.org/10.1093/cercor/10.5.454

Durstewitz, D. (2003). Self-organizing neural integrator predicts interval times through climbing activity. *Journal of Neuroscience*, *23*(12), 5342–5353. https://doi.org/10.1523/jneurosci.23-12-05342.2003

Duysens, J., Schaafsma, S. J., & Orban, G. A. (1996). Cortical off response tuning for stimulus duration. *Vision Research*, *36*(20), 3243–3251. https://doi.org/10.1016/0042-6989(96)00040-5

Eagleman, D. M. (2008, April). Human time perception and its illusions. *Current Opinion in Neurobiology*, Vol. 18, pp. 131–136. https://doi.org/10.1016/j.conb.2008.06.002

Farzan, F. (2014). Single-pulse transcranial magnetic stimulation (TMS) protocols and outcome measures. *Neuromethods*, *89*, 69–115. https://doi.org/10.1007/978-1-4939-0879-0_5

Ferrandez, A. M., Hugueville, L., Lehéricy, S., Poline, J. B., Marsault, C., & Pouthas, V. (2003). Basal ganglia and supplementary motor area subtend duration perception: An fMRI study. *NeuroImage*, *19*(4), 1532–1544. https://doi.org/10.1016/S1053-8119(03)00159-9

Ferreri, F., Pasqualetti, P., Määttä, S., Ponzo, D., Guerra, A., Bressi, F., … Rossini,

P. M. (2011). Motor cortex excitability in Alzheimer's disease: A transcranial magnetic stimulation follow-up study. *Neuroscience Letters*, *492*(2), 94–98. https://doi.org/10.1016/j.neulet.2011.01.064

Foster, K. H., Gaska, J. P., Nagler, M., & Pollen, D. A. (1985). Spatial and temporal frequency selectivity of neurones in visual cortical areas V1 and V2 of the macaque monkey. *The Journal of Physiology*, *365*(1), 331–363. https://doi.org/10.1113/jphysiol.1985.sp015776

Gerwig, M., Niehaus, L., Kastrup, O., Stude, P., & Diener, H. C. (2005). Visual Cortex Excitability in Migraine Evaluated by Single and Paired Magnetic Stimuli. *Headache: The Journal of Head and Face Pain*, *45*(10), 1394–1399. https://doi.org/10.1111/j.1526-4610.2005.00272.x

Ghose, G. M., & Maunsell, J. H. R. (2002). Attentional modulation in visual cortex depends on task timing. *Nature*, *419*(6907), 616–620. https://doi.org/10.1038/nature01057

GIBBON, J., CHURCH, R. M., & MECK, W. H. (1984). Scalar Timing in Memory. *Annals of the New York Academy of Sciences*, *423*(1), 52–77. https://doi.org/10.1111/j.1749-6632.1984.tb23417.x

Giovannelli, F., Ragazzoni, A., Battista, D., Tarantino, V., Del Sordo, E., Marzi, T., … Cincotta, M. (2014). "..the times they aren't A-Changin''." rTMS does not affect basic mechanisms of temporal discrimination: A pilot study with ERPs." *Neuroscience*, *278*(1), 302–312. https://doi.org/10.1016/j.neuroscience.2014.08.024

Grill-Spector, K., Henson, R., & Martin, A. (2006, January 1). Repetition and the brain: Neural models of stimulus-specific effects. *Trends in Cognitive Sciences*, Vol. 10, pp. 14–23. https://doi.org/10.1016/j.tics.2005.11.006

Harrington, D. L., Castillo, G. N., Fong, C. H., & Reed, J. D. (2011). Neural Underpinnings of Distortions in the Experience of Time Across Senses. *Frontiers in Integrative Neuroscience*, *5*, 32. https://doi.org/10.3389/fnint.2011.00032

Harris, J. A., Clifford, C. W. G., & Miniussi, C. (2008). The functional effect of transcranial magnetic stimulation: Signal suppression or neural noise generation? *Journal of Cognitive Neuroscience*, *20*(4), 734–740. https://doi.org/10.1162/jocn.2008.20048

Hartwigsen, G., Price, C. J., Baumgaertner, A., Geiss, G., Koehnke, M., Ulmer, S., & Siebner, H. R. (2010). The right posterior inferior frontal gyrus contributes to phonological word decisions in the healthy brain: Evidence from dual-site TMS. *Neuropsychologia*, *48*(10), 3155–3163. https://doi.org/10.1016/j.neuropsychologia.2010.06.032

Hawken, M. J., Shapley, R. M., & Grosof, D. H. (1996). Temporal-frequency selectivity in monkey visual cortex. *Visual Neuroscience*, *13*(3), 477–492. https://doi.org/10.1017/s0952523800008154

Hayashi, M. J., Ditye, T., Harada, T., Hashiguchi, M., Sadato, N., Carlson, S., … Kanai, R. (2015). Time Adaptation Shows Duration Selectivity in the Human Parietal Cortex. *PLOS Biology*, *13*(9), e1002262. https://doi.org/10.1371/journal.pbio.1002262

Hayashi, M. J., Kantele, M., Walsh, V., Carlson, S., & Kanai, R. (2014). Dissociable Neuroanatomical Correlates of Subsecond and Suprasecond Time Perception. *Journal of Cognitive Neuroscience*, *26*(8), 1685–1693. https://doi.org/10.1162/jocn_a_00580

Hubel, D. H., & Wiesel, T. N. (1962). Receptive fields, binocular interaction and functional architecture in the cat's visual cortex. *The Journal of Physiology*, *160*(1), 106–154. https://doi.org/10.1113/jphysiol.1962.sp006837

Ilić, T. V., Meintzschel, F., Cleff, U., Ruge, D., Kessler, K. R., & Ziemann, U. (2002, November 15). Short-interval paired-pulse inhibition and facilitation of human motor cortex: The dimension of stimulus intensity. *Journal of Physiology*, Vol. 545, pp. 153–167. https://doi.org/10.1113/jphysiol.2002.030122

Ivry, R. B., & Schlerf, J. E. (2008, July). Dedicated and intrinsic models of time perception. *Trends in Cognitive Sciences*, Vol. 12, pp. 273–280. https://doi.org/10.1016/j.tics.2008.04.002

Janata, P., & Grafton, S. T. (2003, July 1). Swinging in the brain: Shared neural substrates for behaviors related to sequencing and music. *Nature Neuroscience*, Vol. 6, pp. 682–687. https://doi.org/10.1038/nn1081

Janssen, A. M., Oostendorp, T. F., & Stegeman, D. F. (2015). The coil orientation dependency of the electric field induced by TMS for M1 and other brain areas. *Journal of NeuroEngineering and Rehabilitation*, *12*(1), 47. https://doi.org/10.1186/s12984-015-0036-2

Jin, D. Z., Fujii, N., & Graybiel, A. M. (2009). Neural representation of time in cortico-basal ganglia circuits. *Proceedings of the National Academy of Sciences of the United States of America*, *106*(45), 19156–19161. https://doi.org/10.1073/pnas.0909881106

Jones, C. R. G., Rosenkranz, K., Rothwell, J. C., & Jahanshahi, M. (2004). The right dorsolateral prefrontal cortex is essential in time reproduction: An investigation with repetitive transcranial magnetic stimulation. *Experimental Brain Research*, *158*(3), 366–372. https://doi.org/10.1007/s00221-004-1912-3

Kamitani, Y., & Shimojo, S. (1999). Manifestation of scotomas created by transcranial magnetic stimulation of human visual cortex. *Nature Neuroscience*, *2*(8), 767–771. https://doi.org/10.1038/11245

Kammer, T., & Baumann, L. W. (2010). Phosphene thresholds evoked with single and double TMS pulses. *Clinical Neurophysiology*, *121*(3), 376–379. https://doi.org/10.1016/j.clinph.2009.12.002

Kanai, R., Lloyd, H., Bueti, D., & Walsh, V. (2011). Modality-independent role of the primary auditory cortex in time estimation. *Experimental Brain Research*, *209*(3), 465–471. https://doi.org/10.1007/s00221-011-2577-3

Kanai, R., Paffen, C. L. E., Hogendoorn, H., & Verstraten, F. A. J. (2006). Time dilation in dynamic visual display. *Journal of Vision*, *6*(12), 1421–1430. https://doi.org/10.1167/6.12.8

Karmarkar, U. R., & Buonomano, D. V. (2007). Timing in the Absence of Clocks: Encoding Time in Neural Network States. *Neuron*, *53*(3), 427–438.

https://doi.org/10.1016/j.neuron.2007.01.006

Klomjai, W., Katz, R., & Lackmy-Vallée, A. (2015, September 1). Basic principles of transcranial magnetic stimulation (TMS) and repetitive TMS (rTMS). *Annals of Physical and Rehabilitation Medicine*, Vol. 58, pp. 208–213. https://doi.org/10.1016/j.rehab.2015.05.005

Koch, G., Oliveri, M., Brusa, L., Stanzione, P., Torriero, S., & Caltagirone, C. (2004). High-frequency rTMS improves time perception in Parkinson disease. *Neurology*, *63*(12), 2405–2406. https://doi.org/10.1212/01.WNL.0000147336.19972.82

Koch, G., Oliveri, M., Torriero, S., Salerno, S., Gerfo, E. Lo, & Caltagirone, C. (2007). Repetitive TMS of cerebellum interferes with millisecond time processing. *Experimental Brain Research*, *179*(2), 291–299. https://doi.org/10.1007/s00221-006-0791-1

Krekelberg, B., Boynton, G. M., & van Wezel, R. J. A. (2006, May 1). Adaptation: from single cells to BOLD signals. *Trends in Neurosciences*, Vol. 29, pp. 250–256. https://doi.org/10.1016/j.tins.2006.02.008

Kujirai, T., Caramia, M. D., Rothwell, J. C., Day, B. L., Thompson, P. D., Ferbert, A., … Marsden, C. D. (1993). Corticocortical inhibition in human motor cortex. *The Journal of Physiology*, *471*(1), 501–519. https://doi.org/10.1113/jphysiol.1993.sp019912

Lapid, E., Ulrich, R., & Rammsayer, T. (2008). On estimating the difference limen in duration discrimination tasks: A comparison of the 2 AFC and the reminder task. *Perception and Psychophysics*, *70*(2), 291–305. https://doi.org/10.3758/PP.70.2.291

Levitt, H. (1971). Transformed Up-Down Methods in Psychoacoustics. *The Journal of the Acoustical Society of America*, *49*(2B), 467–477. https://doi.org/10.1121/1.1912375

Lewis, P. A., & Miall, R. C. (2003). Brain activation patterns during measurement of sub- and supra-second intervals. *Neuropsychologia*, *41*(12), 1583–1592.

https://doi.org/10.1016/S0028-3932(03)00118-0

Macar, F., Lejeune, H., Bonnet, M., Ferrara, A., Pouthas, V., Vidal, F., & Maquet, P. (2002). Activation of the supplementary motor area and of attentional networks during temporal processing. *Experimental Brain Research*, *142*(4), 475–485. https://doi.org/10.1007/s00221-001-0953-0

Macar, Françoise, Coull, J., & Vidal, F. (2006). The supplementary motor area in motor and perceptual time processing: fMRI studies. *Cognitive Processing*, *7*(2), 89–94. https://doi.org/10.1007/s10339-005-0025-7

Malach, R. (2012, August 15). Targeting the functional properties of cortical neurons using fMR-adaptation. *NeuroImage*, Vol. 62, pp. 1163–1169. https://doi.org/10.1016/j.neuroimage.2012.01.002

Marg, E., & Rudiak, D. (1994). Phosphenes induced by magnetic stimulation over the occipital brain: Description and probable site of stimulation. *Optometry and Vision Science*, *71*(5), 301–311. https://doi.org/10.1097/00006324-199405000-00001

McConnell, K. A., Nahas, Z., Shastri, A., Lorberbaum, J. P., Kozel, F. A., Bohning, D. E., & George, M. S. (2001). The transcranial magnetic stimulation motor threshold depends on the distance from coil to underlying cortex: A replication in healthy adults comparing two methods of assessing the distance to cortex. *Biological Psychiatry*, *49*(5), 454–459. https://doi.org/10.1016/S0006-3223(00)01039-8

Meck, W. H., Penney, T. B., & Pouthas, V. (2008, April 1). Cortico-striatal representation of time in animals and humans. *Current Opinion in Neurobiology*, Vol. 18, pp. 145–152. https://doi.org/10.1016/j.conb.2008.08.002

Meister, I. G., Weidemann, J., Dambeck, N., Foltys, H., Sparing, R., Krings, T., … Boroojerdi, B. (2003). Chapter 31 Neural correlates of phosphene perception. *Supplements to Clinical Neurophysiology*, *56*(C), 305–311. https://doi.org/10.1016/S1567-424X(09)70234-X

Méndez, J. C., Rocchi, L., Jahanshahi, M., Rothwell, J., & Merchant, H. (2017).

Probing the timing network: A continuous theta burst stimulation study of temporal categorization. *Neuroscience*, *356*, 167–175. https://doi.org/10.1016/j.neuroscience.2017.05.023

Merchant, H., & Georgopoulos, A. P. (2006). Neurophysiology of Perceptual and Motor Aspects of Interception. *Journal of Neurophysiology*, *95*(1), 1–13. https://doi.org/10.1152/jn.00422.2005

Merchant, H., Harrington, D. L., & Meck, W. H. (2013a). Neural Basis of the Perception and Estimation of Time. *Annual Review Neuroscience*, *36*, 313–336. https://doi.org/10.1146/annurev-neuro-062012-170349

Merchant, H., Harrington, D. L., & Meck, W. H. (2013b). Neural Basis of the Perception and Estimation of Time. *Annual Review Neuroscience*, *36*(May), 313–336. https://doi.org/10.1146/annurev-neuro-062012-170349

Merchant, H., Harrington, D. L., & Meck, W. H. (2013c, July). Neural basis of the perception and estimation of time. *Annual Review of Neuroscience*, Vol. 36, pp. 313–336. https://doi.org/10.1146/annurev-neuro-062012-170349

Merchant, H., Pérez, O., Zarco, W., & Gámez, J. (2013). Interval tuning in the primate medial premotor cortex as a general timing mechanism. *Journal of Neuroscience*, *33*(21), 9082–9096. https://doi.org/10.1523/JNEUROSCI.5513-12.2013

Miller, P., & Wang, X. J. (2006). Inhibitory control by an integral feedback signal in prefrontal cortex: A model of discrimination between sequential stimuli. *Proceedings of the National Academy of Sciences of the United States of America*, *103*(1), 201–206. https://doi.org/10.1073/pnas.0508072103

Miniussi, C., Bortoletto, M., Thut, G., & Veniero, D. (2012). Accessing cortical connectivity using TMS: EEG Co-registration TMS and connectivity. In *Cortical Connectivity: Brain Stimulation for Assessing and Modulating Cortical Connectivity and Function* (pp. 93–110). https://doi.org/10.1007/978-3-642-32767-4_5

Mita, A., Mushiake, H., Shima, K., Matsuzaka, Y., & Tanji, J. (2009). Interval time

coding by neurons in the presupplementary and supplementary motor areas. *Nature Neuroscience*, *12*(4), 502–507. https://doi.org/10.1038/nn.2272

Moliadze, V., Giannikopoulos, D., Eysel, U. T., & Funke, K. (2005). Paired-pulse transcranial magnetic stimulation protocol applied to visual cortex of anaesthetized cat: Effects on visually evoked single-unit activity. *Journal of Physiology*, *566*(3), 955–965. https://doi.org/10.1113/jphysiol.2005.086090

Moliadze, V., Zhao, Y., Eysel, U., & Funke, K. (2003, December 1). Effect of transcranial magnetic stimulation on single-unit activity in the cat primary visual cortex. *Journal of Physiology*, Vol. 553, pp. 665–679. https://doi.org/10.1113/jphysiol.2003.050153

Morillon, B., Kell, C. A., & Giraud, A. L. (2009). Three stages and four neural systems in time estimation. *Journal of Neuroscience*, *29*(47), 14803–14811. https://doi.org/10.1523/JNEUROSCI.3222-09.2009

Morrone, M. C., Ross, J., & Burr, D. (2005). Saccadic eye movements cause compression of time as well as space. *Nature Neuroscience*, *8*(7), 950–954. https://doi.org/10.1038/nn1488

Nachev, P., Kennard, C., & Husain, M. (2008, November 9). Functional role of the supplementary and pre-supplementary motor areas. *Nature Reviews Neuroscience*, Vol. 9, pp. 856–869. https://doi.org/10.1038/nrn2478

Narayana, S., Laird, A. R., Tandon, N., Franklin, C., Lancaster, J. L., & Fox, P. T. (2012). Electrophysiological and functional connectivity of the human supplementary motor area. *NeuroImage*, *62*(1), 250–265. https://doi.org/10.1016/j.neuroimage.2012.04.060

Pascual-Leone, A., & Walsh, V. (2001). Fast backprojections from the motion to the primary visual area necessary for visual awareness. *Science*, *292*(5516), 510–512. https://doi.org/10.1126/science.1057099

Pascual-Leone, Alvaro, Bartres-Faz, D., & Keenan, J. P. (1999). Transcranial magnetic stimulation: Studying the brain-behaviour relationship by induction of "virtual lesions." *Philosophical Transactions of the Royal Society B: Biological*

Sciences, *354*(1387), 1229–1238. https://doi.org/10.1098/rstb.1999.0476

Pascual-Leone, Alvaro, Walsh, V., & Rothwell, J. (2000, April 1). Transcranial magnetic stimulation in cognitive neuroscience - Virtual lesion, chronometry, and functional connectivity. *Current Opinion in Neurobiology*, Vol. 10, pp. 232–237. https://doi.org/10.1016/S0959-4388(00)00081-7

Pastor, M. A., Day, B. L., Macaluso, E., Friston, K. J., & Frackowiak, R. S. J. (2004). The Functional Neuroanatomy of Temporal Discrimination. *Journal of Neuroscience*, *24*(10), 2585–2591. https://doi.org/10.1523/JNEUROSCI.4210-03.2004

Paton, J. J., & Buonomano, D. V. (2018, May 16). The Neural Basis of Timing: Distributed Mechanisms for Diverse Functions. *Neuron*, Vol. 98, pp. 687–705. https://doi.org/10.1016/j.neuron.2018.03.045

Paus, T. (2005). Inferring causality in brain images: A perturbation approach. *Philosophical Transactions of the Royal Society B: Biological Sciences*, Vol. 360, pp. 1109–1114. https://doi.org/10.1098/rstb.2005.1652

Protopapa, F., Hayashi, M. J., Kulashekhar, S., van der Zwaag, W., Battistella, G., Murray, M. M., … Bueti, D. (2019). Chronotopic maps in human supplementary motor area. *PLOS Biology*, *17*(3), e3000026. https://doi.org/10.1371/journal.pbio.3000026

Rao, S. M. (1997). Distributed neural systems underlying the timing of movements. *Journal of Neuroscience*, *17*(14), 5528–5535. https://doi.org/10.1523/jneurosci.17-14-05528.1997

Ray, P. G., Meador, K. J., Epstein, C. M., Loring, D. W., & Day, L. J. (1998). Magnetic stimulation of visual cortex: Factors influencing the perception of phosphenes. *Journal of Clinical Neurophysiology*, *15*(4), 351–357. https://doi.org/10.1097/00004691-199807000-00007

Reis, J., Swayne, O. B., Vandermeeren, Y., Camus, M., Dimyan, M. A., Harris-Love, M., … Cohen, L. G. (2008, January 15). Contribution of transcranial magnetic stimulation to the understanding of cortical mechanisms involved in motor

control. *Journal of Physiology*, Vol. 586, pp. 325–351. https://doi.org/10.1113/jphysiol.2007.144824

Repp, B. H., & Su, Y. H. (2013). Sensorimotor synchronization: A review of recent research (2006-2012). *Psychonomic Bulletin and Review*, *20*(3), 403–452. https://doi.org/10.3758/s13423-012-0371-2

Reutimann, J., Yakovlev, V., Fusi, S., & Senn, W. (2004). Climbing Neuronal Activity as an Event-Based Cortical Representation of Time. *Journal of Neuroscience*, *24*(13), 3295–3303. https://doi.org/10.1523/JNEUROSCI.4098-03.2004

Ridding, M. C., & Rothwell, J. C. (2007, July). Is there a future for therapeutic use of transcranial magnetic stimulation? *Nature Reviews Neuroscience*, Vol. 8, pp. 559–567. https://doi.org/10.1038/nrn2169

Roach, N. W., Heron, J., Whitaker, D., & McGraw, P. V. (2011). Asynchrony adaptation reveals neural population code for audio-visual timing. *Proceedings of the Royal Society B: Biological Sciences*, *278*(1710), 1314–1322. https://doi.org/10.1098/rspb.2010.1737

Romei, V., Thut, G., & Silvanto, J. (2016, November 1). Information-Based Approaches of Noninvasive Transcranial Brain Stimulation. *Trends in Neurosciences*, Vol. 39, pp. 782–795. https://doi.org/10.1016/j.tins.2016.09.001

Rossi, S., Hallett, M., Rossini, P. M., Pascual-Leone, A., Avanzini, G., Bestmann, S., … Ziemann, U. (2009, December). Safety, ethical considerations, and application guidelines for the use of transcranial magnetic stimulation in clinical practice and research. *Clinical Neurophysiology*, Vol. 120, pp. 2008–2039. https://doi.org/10.1016/j.clinph.2009.08.016

Sack, A. T., Kohler, A., Linden, D. E. J., Goebel, R., & Muckli, L. (2006). The temporal characteristics of motion processing in hMT/V5+: Combining fMRI and neuronavigated TMS. *NeuroImage*, *29*(4), 1326–1335. https://doi.org/10.1016/j.neuroimage.2005.08.027

Salvioni, P., Murray, M. M., Kalmbach, L., & Bueti, D. (2013a). How the Visual

Brain Encodes and Keeps Track of Time. *Journal of Neuroscience*, *33*(30), 12423–12429. https://doi.org/10.1523/JNEUROSCI.5146-12.2013

Salvioni, P., Murray, M. M., Kalmbach, L., & Bueti, D. (2013b). How the Visual Brain Encodes and Keeps Track of Time. *Journal of Neuroscience*, *33*(30), 12423–12429. https://doi.org/10.1523/JNEUROSCI.5146-12.2013

Schluter, N. D., Rushworth, M. F. S., Passingham, R. E., & Mills, K. R. (1998). Temporary interference in human lateral premotor cortex suggests dominance for the selection of movements A study using transcranial magnetic stimulation. In *Brain* (Vol. 121).

Shuler, M. G., & Bear, M. F. (2006). Reward timing in the primary visual cortex. *American Journal of Ophthalmology*, *142*(1), 202. https://doi.org/10.1016/j.ajo.2006.05.013

Silvanto, J., Lavie, N., & Walsh, V. (2005). Double dissociation of V1 and V5/MT activity in visual awareness. *Cerebral Cortex*, *15*(11), 1736–1741. https://doi.org/10.1093/cercor/bhi050

Silvanto, J., Muggleton, N. G., Cowey, A., & Walsh, V. (2007). Neural adaptation reveals state-dependent effects of transcranial magnetic stimulation. *European Journal of Neuroscience*, *25*(6), 1874–1881. https://doi.org/10.1111/j.1460-9568.2007.05440.x

Silvanto, J., Muggleton, N., & Walsh, V. (2008). State-dependency in brain stimulation studies of perception and cognition. *Trends in Cognitive Sciences*, *12*(12), 447–454. https://doi.org/10.1016/j.tics.2008.09.004

Spencer, R. M. C., Zelaznik, H. N., Diedrichsen, J., & Ivry, R. B. (2003). Disrupted timing of discontinuous but not continuous movements by cerebellar lesions. *Science*, *300*(5624), 1437–1439. https://doi.org/10.1126/science.1083661

Teitti, S., Määttä, S., Säisänen, L., Könönen, M., Vanninen, R., Hannula, H., … Karhu, J. (2008). Non-primary motor areas in the human frontal lobe are connected directly to hand muscles. *NeuroImage*, *40*(3), 1243–1250. https://doi.org/10.1016/j.neuroimage.2007.12.065

Théoret, H., Haque, J., & Pascual-Leone, A. (2001). Increased variability of paced finger tapping accuracy following repetitive magnetic stimulation of the cerebellum in humans. *Neuroscience Letters*, *306*(1–2), 29–32. https://doi.org/10.1016/S0304-3940(01)01860-2

Thielscher, A., & Kammer, T. (2004). Electric field properties of two commercial figure-8 coils in TMS: Calculation of focality and efficiency. *Clinical Neurophysiology*, *115*(7), 1697–1708. https://doi.org/10.1016/j.clinph.2004.02.019

Töpper, R., Mottaghy, F., Brügmann, M., Noth Huber, J. W., Noth, J., & Huber, W. (1998). Facilitation of picture naming by focal transcranial magnetic stimulation of Wernickes area. In *Exp Brain Res* (Vol. 121). Springer-Verlag.

Toso, A., Fassihi, A., Paz, L., Pulecchi, F., & Diamond, M. E. (2020, August 2). A sensory integration account for time perception. *BioRxiv*, p. 2020.08.02.232801. https://doi.org/10.1101/2020.08.02.232801

Treisman, M. (1963). Temporal discrimination and the indifference interval. Implications for a model of the "internal clock". *Psychological Monographs*, *77*(13), 1–31. https://doi.org/10.1037/h0093864

Treisman, M., Faulkner, A., Naish, P. L., & Brogan, D. (1990). The internal clock: evidence for a temporal oscillator underlying time perception with some estimates of its characteristic frequency. *Perception*, *19*(6), 705–743. https://doi.org/10.1068/p190705

Ueno, S., Tashiro, T., & Harada, K. (1988). Localized stimulation of neural tissues in the brain by means of a paired configuration of time-varying magnetic fields. *Journal of Applied Physics*, *64*(10), 5862–5864. https://doi.org/10.1063/1.342181

Usher, M., & McClelland, J. L. (2001). The time course of perceptual choice: The leaky, competing accumulator model. *Psychological Review*, *108*(3), 550–592. https://doi.org/10.1037/0033-295X.108.3.550

Vaalto, S., Julkunen, P., Säïsänen, L., Könönen, M., Määttä, S., & Karhu, J. (2016).

Increased Inhibition in Non-Primary Motor Areas of String-Instrument Players: A Preliminary Study with Paired-Pulse Transcranial Magnetic Stimulation. *Brain Plasticity*, *1*(2), 223–234. https://doi.org/10.3233/bpl-150015

Walsh, V., Ellison, A., Battelli, L., & Cowey, A. (1998). Task-specific impairments and enhancements induced by magnetic stimulation of human visual area V5. *Proceedings of the Royal Society B: Biological Sciences*, *265*(1395), 537–543. https://doi.org/10.1098/rspb.1998.0328

Walsh, Vincent, & Cowey, A. (1998, March 1). Magnetic stimulation studies of visual cognition. *Trends in Cognitive Sciences*, Vol. 2, pp. 103–110. https://doi.org/10.1016/S1364-6613(98)01134-6

Walsh, Vincent, & Cowey, A. (2000). Transcranial magnetic stimulation and cognitive neuroscience. *Nature Reviews Neuroscience*, *1*(1), 73–80. https://doi.org/10.1038/35036239

Walsh, Vincent, & Rushworth, M. (1998, November 1). A primer of magnetic stimulation as a tool for neuropsychology. *Neuropsychologia*, Vol. 37, pp. 125–135. https://doi.org/10.1016/S0028-3932(98)00087-6

Wiener, M. (2014). Transcranial Magnetic Stimulation Studies of Human Time Perception: A Primer. *Timing & Time Perception*, *2*(3), 233–260. https://doi.org/10.1163/22134468-00002022

Wiener, M., Kliot, D., Turkeltaub, P. E., Hamilton, R. H., Wolk, D. A., & Coslett, H. B. (2012). Parietal influence on temporal encoding indexed by simultaneous transcranial magnetic stimulation and electroencephalography. *Journal of Neuroscience*, *32*(35), 12258–12267. https://doi.org/10.1523/JNEUROSCI.2511-12.2012

Wiener, M., Matell, M. S., & Coslett, H. B. (2011). Multiple Mechanisms for Temporal Processing. *Frontiers in Integrative Neuroscience*, *5*, 31. https://doi.org/10.3389/fnint.2011.00031

Wiener, M., Turkeltaub, P., & Coslett, H. B. (2010). The image of time: A voxel-wise meta-analysis. *NeuroImage*, *49*(2), 1728–1740.

https://doi.org/10.1016/j.neuroimage.2009.09.064

Ziemann, U., Corwell, B., & Cohen, L. G. (1998). Modulation of plasticity in human motor cortex after forearm ischemic nerve block. *Journal of Neuroscience*, *18*(3), 1115–1123. https://doi.org/10.1523/jneurosci.18-03-01115.1998

Zwislocki, J., & Feldman, R. S. (1956). Just Noticeable Differences in Dichotic Phase. *Journal of the Acoustical Society of America*, *28*(5), 860–864. https://doi.org/10.1121/1.1908495